DOE/NASA/0300-1
NASA CR-168255
FMI NAS-8273

NASA-CR-168255
19840025233

Steam Bottoming Cycle for an Adiabatic Diesel Engine

E. Poulin, R. Demler,
I. Krepchin, and D. Walker
Foster-Miller, Inc.

March 1984

Prepared for
NATIONAL AERONAUTICS AND SPACE ADMINISTRATION
Lewis Research Center
Cleveland, Ohio
Under Contract DEN-3-300

for
U.S. DEPARTMENT OF ENERGY
Conservation and Renewable Energy
Office of Vehicle and Engine R&D

DISCLAIMER

Printed in the United States of America

Available from
National Technical Information Service
U.S. Department of Commerce
5285 Port Royal Road
Springfield, VA 22161

NTIS price codes[1]
Printed copy: A07
Microfiche copy: A01

[1]Codes are used for pricing all publications. The code is determined by the number of pages in the publication. Information pertaining to the pricing codes can be found in the current issues of the following publications, which are generally available in most libraries: *Energy Research Abstracts (ERA); Government Reports Announcements* and Index (*GRA* and I); *Scientific and Technical Abstract Reports (STAR);* and publication, NTIS-PR-360 available from NTIS at the above address.

DOE/NASA/0300-1
NASA CR-168255
FMI NAS-8273

Steam Bottoming Cycle for an Adiabatic Diesel Engine

E. Poulin, R. Demler,
I. Krepchin, and D. Walker
Foster-Miller, Inc.
Waltham, Massachusetts 02254

March 1984

Prepared for
NATIONAL AERONAUTICS AND SPACE ADMINISTRATION
Lewis Research Center
Cleveland, Ohio 44135
Under Contract DEN 3-300

for
U.S. DEPARTMENT OF ENERGY
Conservation and Renewable Energy
Wind Energy Technology Division
Under Interagency Agreement DE-AI01-80CS50194

FOREWORD

Foster-Miller, Inc. would like to acknowledge the exceptional cooperation and technical assistance provided by both Modine Manufacturing Co. and Voss Finned Tube Products during the execution of this contract.

CONTENTS

	Page
SUMMARY	1
INTRODUCTION	3
PARAMETRIC ANALYSIS	5
Baseline Boiler Design Analysis	5
Rankine Cycle Analysis	23
Expander Design Analysis	28
Condenser Design Analysis	40
Performance of Combined Diesel Engine/Steam Bottoming System	41
PRELIMINARY BOTTOMING SYSTEM DESIGN	45
System Configuration	45
Boiler Design	48
Expander Design	54
Cooling Assembly Design	60
Feedwater Pump Design	60
Miscellaneous Bottoming Cycle System Components	63
Advantages of the Steam Bottoming Cycle System	66
FREEZE PROTECTION RESEARCH	69
Boiler Freeze Protection	69
Expander Freeze Protection	72
Condenser Freeze Protection	72
Boiler Feed Pump Freeze Protection	78
TECHNOLOGY REQUIREMENTS	81
Expander Piston Ring Limitations	81

Page

Compact Boiler Limitations 89

Condenser Drying for Freeze Protection 90

Short Term Technology Development Needs. 91

STEAM RANKINE BOTTOMING SYSTEM ECONOMICS 93

Equipment Costs. 93

Maintenance Costs. 95

Performance and Cost Summary 97

Economic Analyses. 97

Simple Payback Period. 99

Net Present Value (NPV). 99

Return on Investment (ROI) 104

ADVANCED STEAM BOTTOMING CYCLES. 109

Improved Cycle for 944^{o}K (1240^{o}F) Diesel Exhaust . 109

Advanced Cycle for 1144^{o}K (1600^{o}F) Diesel Exhaust. 110

Performance and Economic Comparisons 111

SUMMARY OF RESULTS 115

Bottoming System Analysis. 115

Preliminary Design 116

Economics. 118

REFERENCES 121

APPENDIX A - FREEZE PROTECTION TEST RESULTS. 122

APPENDIX B - LIST OF SYMBOLS 126

SUMMARY

The objective of this DOE/NASA sponsored study of a steam Rankine bottoming system was to develop information required for an objective evaluation of the feasibility and economics of applying bottoming cycle concepts to heavy duty transport adiabatic diesels. The program conducted by Foster-Miller, Inc. included: a parametric review of component and system performance versus configuration and steam cycle variables; preliminary design of system components and overall layout; a review and experimental investigation of factors related to freeze protection of the system; the evaluation of technology developments which would increase system reliability and performance; an economic assessment of the preliminary steam bottoming system design; and a brief analysis of the impact of advanced steam cycles on steam bottoming system cost and performance.

A state-of-the-art steam bottoming system for a NASA specified adiabatic turbocharged diesel was ultimately selected for preliminary design. While the preliminary analysis indicated that a somewhat different expander configuration and cycle conditions would result in a greater output, the 811°K/6.90 MPa (1000°F/1000 psia) simple cycle incorporated by the design represents the combined operational experience of perhaps 10,000 steam engine hours at these conditions accumulated by several research and development firms in this field. System components include: a compact monotube boiler with a 52 kg (114 lb) tube bundle of stainless steel tubes with clad carbon steel fins; an oil lubricated V-twin expander with bore and stroke equal to 0.089m (3.5 in.) which runs at the same speed as the diesel; a typical radiator core condenser with shutters, fan, subcooler and oil cooler which is ram air cooled above 64.4 km/hr (40 mph); a two-cylinder piston type boiler feedwater pump with solenoids on the intake valves for flow control; microprocessor-based control system; and sensors and plumbing as required. The steam expander power transfer is through a clutch and then by high velocity chain to the diesel output shaft.

The system economic evaluation was made relative to a NASA specified adiabatic turbocharged aftercooled diesel with a turbocompound exhaust energy recovery system. NASA supplied capital cost figures for the adiabatic diesels while the steam bottoming system cost was derived from OEM component costs provided by major manufacturers of identical or similar equipment based on preliminary drawings and specifications. The ultimate selling price of the bottoming system to the truck owner was estimated at $6,070.

The preliminary design evaluation projected substantial performance and economic benefits for long haul trucks. The turbocharged diesel with bottoming system (TC/B) showed a 9 percent lower brake specific fuel consumption than the turbocompound diesel with aftercooling (TCPD/A). This implies an annual fuel savings of $1719 for the TC/B system above the TCPD/A system. Combined with the added capital cost of $2610 and added annual maintenance of $580 for the TC/B system, a payback period of 2.3 years is projected.

A major attraction of a steam Rankine cycle, as opposed to a cycle using organic working fluids that decompose if overheated, is the ability to clean the boiler by running it dry. On the road run dry cleaning might eliminate the 35 percent bottoming cycle power loss experienced after an average of 100 hr due to boiler fouling.

Cold chamber testing of an air-cooled condenser showed that intake shutters and typical radiator tube sizes are sufficient to prevent damage due to water freezing.

INTRODUCTION

The work documented in this report is part of the DOE Heavy Duty Transport Technology (HDTT) Project and was performed under the supervision of NASA Lewis Research Center (LeRC) Energy Technology Division.

The objective of the HDTT Project is to provide a technology base for industry's use in developing advanced fuel-efficient heavy duty transport engines. This effort is motivated by projected increases in fuel usage by trucks and buses coupled with uncertain availability of limited petroleum resources. Significant gains in heavy duty diesel fuel economy can be realized by advanced engine design. The Army Tank Automotive Command projects that 40 percent fuel savings are possible by reducing engine heat loss and friction loss (1). The energy conservation effort of the HDTT Project has, therefore, been focused primarily on adiabatic diesel technology development.

In addition to improved fuel efficiency, advanced adiabatic engines will have higher exhaust temperatures and energy than current diesels. As a result even greater fuel economy for adiabatic engines is possible through the application of waste heat recovery technology. As part of the HDTT Project LeRC initiated several parallel waste heat utilization studies. The purpose of these studies is to develop information required for an objective evaluation of the feasibility and economics of applying bottoming cycle concepts to heavy duty transport adiabatic diesels. The concepts being investigated include Brayton cycle, steam and organic Rankine cycle, Stirling cycle and fluidized bed heat recovery.

This report describes the analysis and preliminary design of a steam Rankine bottoming cycle system for a generic adiabatic diesel engine. This investigation was conducted by Foster-Miller, Inc. (FMI) between November 1982 and October 1983. The program scope of work included:

- A parametric review of performance versus size, weight and configuration of boiler, condenser, expander, and overall system for a range of temperatures and pressures.
- The selection of a system configuration based on the above analyses, and design of the system components and overall layout.

- Analysis and experimental investigation of several techniques for freeze protection of the system.

- The evaluation of the advancement in state-of-the-art required to produce reliable hardware for selected components and evaluation of associated technology development program.

- The evaluation of capital cost, maintenance costs, and return on investment associated with the selected steam bottoming cycle design.

The parametric review, system design and economic analysis tasks were more or less sequential while the freeze protection and technology development tasks were carried out in parallel efforts.

The practical and technical basis for the steam Rankine system evaluation is Foster-Miller's 12-year $12,000,000 dedication to small steam engines, extensive experience in compact boiler design and thermal system analysis, and expertise in specialty equipment design. The experience gained by Foster-Miller in the design, fabrication and operation of a 97 kW (130 hp), four-cylinder, automotive steam engine and a 30 kW (40 hp), single cylinder steam expander, for a program sponsored by EPA/ERDA, was directly applicable to the bottoming cycle system design. The results of these previous investigations also provided a documented baseline performance level for the economic evaluation conducted as a part of this program.

Steam Rankine bottoming systems for large stationary diesel engines (over 2000 kW) are currently available commercially. These systems convert the energy of generated steam to shaft power by means of large steam turbines. The use of steam turbines in bottoming cycles at lower power levels is impractical because of low turbine efficiencies and the complexity of turbine manufacture for low steam flow rates. The results of this analysis, preliminary design and economic evaluation indicate that a reciprocating steam expander is a more practical prime mover in Steam Rankine systems applied to lower power diesel engines. The Steam Rankine bottoming system is suitable for mobile diesels due to its responsiveness to severe load variations as demonstrated in the light duty vehicle Federal Driving Cycles.

Fuel savings similar to those projected for heavy duty transport diesels are also possible with steam bottoming cycles for spark ignition engines burning a wide range of high octane fuels, such as natural gas, alcohols and gasoline.

PARAMETRIC ANALYSIS

The first step in evaluating the appropriateness of a steam bottoming cycle for thermal energy recovery from transport diesel engine exhaust was to determine the output potential of a Rankine system. A schedule of adiabatic diesel engine data versus engine speed for four diesel configurations was provided by NASA LeRC for input to the performance analysis. Exhaust temperature, flow rate, and engine power from the schedule are listed in Table 1. This data assumed wide open throttle conditions. These conditions and a minimum exhaust gas temperature constraint of 422°K (300°F) established the maximum energy extractable from the exhaust stream. The maximum recoverable power as a function of engine type and speed is illustrated in Figure 1. This ideal bottoming cycle output was calculated using the specific heat of air, the major component of the diesel exhaust, at the mean exhaust temperature.

The actual power recovered by a bottoming system will be significantly lower than the ideal due to limitations of the system components and thermodynamic considerations. In a steam Rankine bottoming system the steam generator heat transfer and prime mover energy conversion inefficiencies reduce gross cycle output. In addition the requirements of power consuming auxiliaries, such as the feedwater pump and condenser cooling fan, are charged against the system in deriving the net bottoming system output. Optimum Rankine bottoming system design therefore requires a critical review of design variables versus performance for the major system components: the boiler, prime mover and condenser.

Baseline Boiler Design Analysis

In general the boiler analysis was guided by typical design goals: high effectiveness, low cost and minimum practical size and weight. Boiler application to the Rankine bottoming system required that more specific design constraints be established prior to conducting a detailed parametric analysis. In order to minimize bottoming system interference with the diesel engine performance, a maximum gas side pressure drop of 0.0015 MPa (6 in. of water) was fixed. On the steam side, experience recommended a pressure drop limit of 15 percent of supply pressure to avoid flow instability. And, as specified by NASA design criteria, a minimum outlet gas temperature of 422°K (300°F) was established to avoid condensation of highly corrosive components (e.g., sulfuric acid). Also, finned tube geometry and materials were limited to those

TABLE 1. - NASA REFERENCE DIESEL ENGINE DATA (PART 1)

Adiabatic diesel configuration	Engine speed		Exhaust temperature		Exhaust flow rate		Engine power	
	(rad/sec)	(rpm)	(^{o}K)	(^{o}F)	(kg/hr)	(lb/min)	(kW)	(hp)
Turbocharged non-aftercooled (TC)	136	1300	1022	1380	884	32.5	184	247
	168	1600	966	1280	1135	41.7	213	286
	199	1900	944	1240	1309	48.1	236	317
Turbocharged aftercooled (TC/A)	136	1300	955	1260	906	33.3	187	251
	168	1600	905	1170	1137	41.8	216	290
	199	1900	878	1120	1295	47.6	239	320
Turbocharged turbocompound non-aftercooled (TCPD)	136	1300	933	1220	879	32.3	198	265
	168	1600	900	1160	1127	41.4	231	310
	199	1900	889	1140	1301	47.8	250	335
Turbocharged turbocompound aftercooled (TCPD/A)	136	1300	900	1160	887	32.6	201	269
	168	1600	850	1070	1137	41.8	231	310
	199	1900	844	1060	1317	48.4	254	340

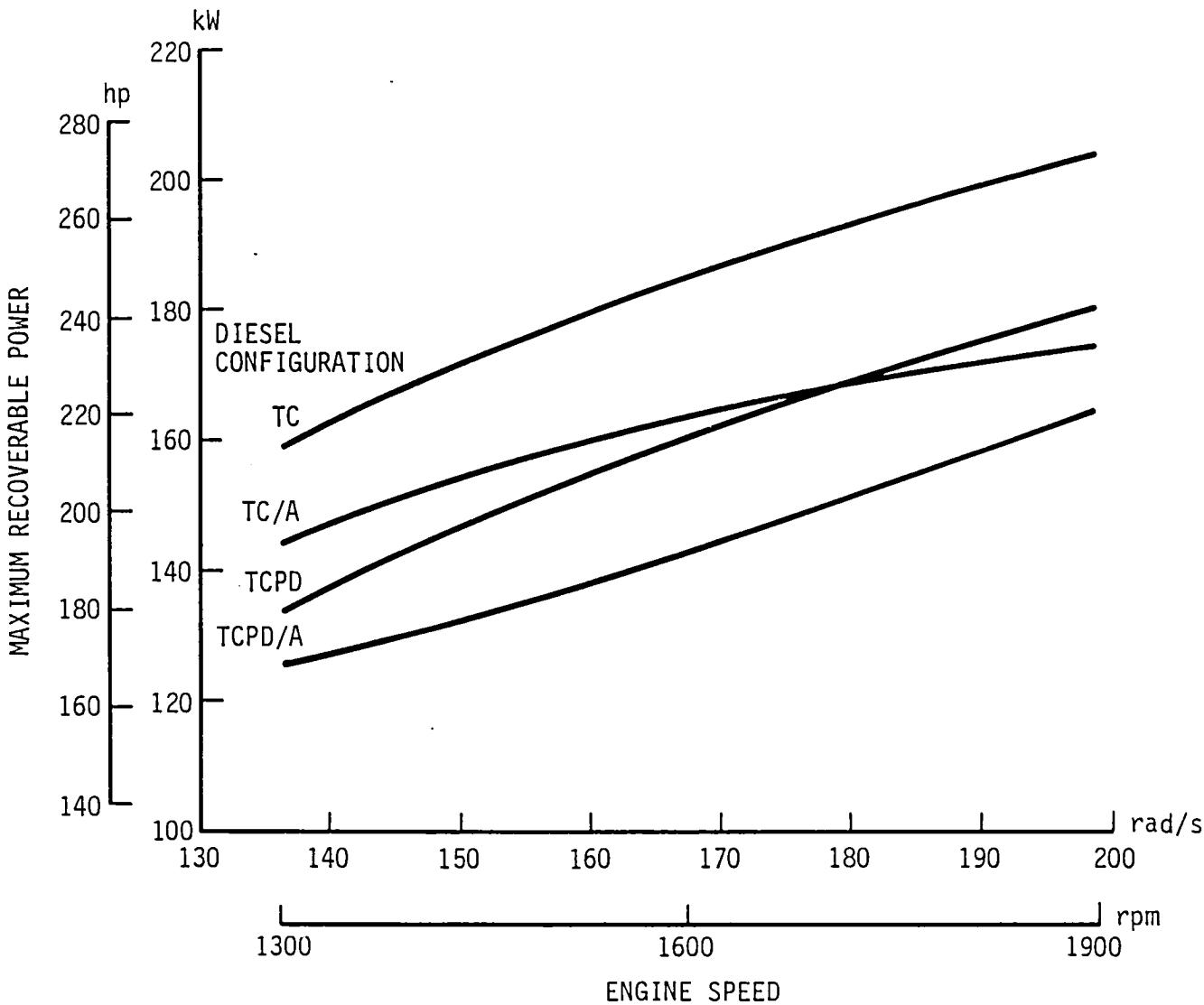

Figure 1. - Ideal bottoming cycle output for four diesel configurations.

currently available commercially in order to simplify boiler fabrication. ASME boiler code stress limits were also assumed.

Boiler configuration. - The boiler configuration selected for the steam Rankine bottoming system is illustrated in Figure 2. It is a patented compact structure consisting of spiral wound finned-tube cones nested together in a close packed arrangement. Consecutive tube spirals are connected so that a monotube coil is formed. The conical structure allows for simple mandril wound fabrication and the close packing provides maximum gas-metal contact for high heat transfer. The boiler configuration also features diminishing gas flow area which insures high gas side velocities, and thus high heat transfer coefficients, as the gas cools and its specific volume decreases.

Boiler design variables. - For given steam and gas conditions there are a number of design variables which can be adjusted to accommodate the design factors summarized in Table 2. Tube diameter will affect steamside pressure drop, heat transfer coefficients and surface-to-volume ratio. Generally the preheater section of the boiler will have smaller tubes than the boiling or superheating sections.

Also, since the gas side heat transfer coefficients are significantly less than those on the steam side, an extended surface (i.e., fins) on the gas side is desirable.

The overall diameter of the configuration will affect both the frontal area and total heat transfer area. The former determines the gas side pressure drop, while the latter determines the total duty.

Increasing the number of tube passes improves heat exchanger performance by making it more like an ideal counterflow exchanger, but gas side pressure drop is also increased.

Finally, materials of construction affect both performance and system life. Based on past experience, stainless steel tubes (type 316) with carbon steel fins and nickel chromium cladding have been selected. Stainless steel on the steam side provides greater oxidation and corrosion resistance. Carbon steel fins provide better thermal performance, at lower cost, than stainless. The thermal conductivity of carbon steel is on the order of 43 $W/(m \cdot {}^{o}K)$ or 25 $Btu/(hr \cdot ft \cdot {}^{o}F)$, compared to 17 $W/(m \cdot {}^{o}K)$ or 10 $Btu/(hr \cdot ft \cdot {}^{o}F)$ for stainless. Recent price quotes show the relative cost of the two to be as much as 7:1.

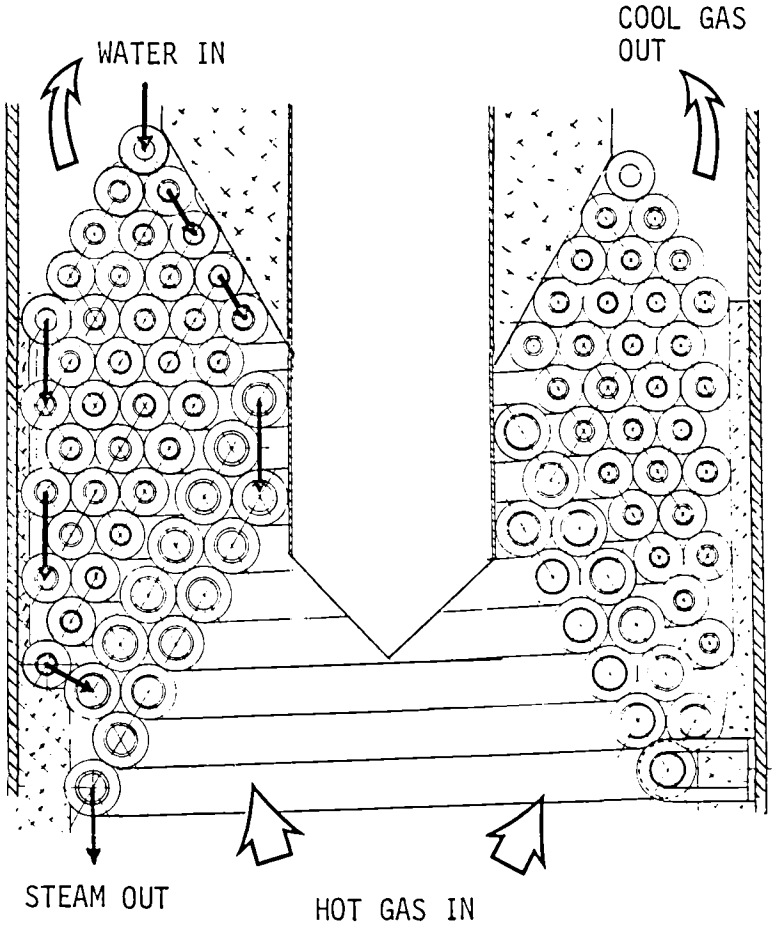

Figure 2. - Steam Rankine system boiler configuration.

TABLE 2. - BOILER DESIGN FACTORS

Goals	• Good thermal performance • Low cost • Minimum practical size and weight
Constraints	• Maximum pressure drops - Gas side = 0.0015 MPa (6 in. H_2O) - Steam side = 15 percent of supply pressure • Minimum gas outlet temperature = 422°K (300°F) • ASME boiler code
Limitations	• Readily available finned tubing • Thermodynamic pinch point

The nickel-chromium cladding is a feature gained at little extra effort when fins are attached to tubes by a brazing process similar to the one used by FMI in previous projects. The brazing method leaves a smooth fillet at the fin/tube joint, giving a larger heat flow path and eliminating a crevice which exists in some welding attachment processes. This adds to the cost of the tubing, but provides the same high thermal performance as the untreated carbon steel and improves corrosion and oxidation resistance up to temperatures of 1089°K (1500°F). Thus, running the boiler dry, as a result of process control failure or intentionally for boiler cleaning as will be discussed later in this report, will not damage tubes or fins.

Boiler analysis program. - A detailed thermal analysis of the boiler design was accomplished through the use of a proprietary computer model, Boiler Analysis Program. Input data required to run the program includes:

- Water-side conditions - inlet water temperature, outlet steam temperature, saturation pressure.
- Inlet gas conditions - temperature, flow rate.
- Tube geometry - tube and fin dimensions, fin density.
- Boiler geometry - number of tube passes (i.e., nested spirals), tube pitch, maximum and minimum coil diameters for each pass.
- Materials of construction - tube and fin material properties.

The program output consists of a general performance summary and a detailed account of node by node results. More specifically, the output listing reports input parameter values followed by a matrix of steam temperatures, steam enthalpies, gas temperatures, outer tube wall temperatures, and fin tip temperatures, as well as efficiencies, flow rates, pressure drops (steam and gas sides), metal energy contents, metal weights and a variety of secondary parameters.

The analysis program begins by determining heat transfer surface areas, flow areas, volumes, etc. Each boiler pass is then divided into ten equally sized elements as shown in the flow schematic of Figure 3. An initial guess of water flow rate serves as the basis for estimates of gas conditions and heat transfer effectiveness for successive boiler passes. Each element is evaluated as an individual heat exchanger with inlet steam temperature, inlet gas temperature, and an effectiveness yielding outlet steam condition and outlet gas condition. The outlet steam condition now becomes the inlet condition to the next element in the same pass, while the outlet gas temperature becomes the inlet to the corresponding element in the next pass. Iteration of water flow rate around a fixed gas flow rate is done until the pass connection errors are reduced below an allowable tolerance.

Boiler Analysis Program has been validated by experimental data and by several successful boiler designs. Figure 4 presents a comparison of Boiler Analysis Program predictions and actual test data for the previously developed Model 5 Vapor Generator (2). As is demonstrated by the graph, the performance prediction stays within 3 percent. Other successful applications of the program have included steam car (2) and RAMCAR (3) boiler designs, and the analysis of operational problems on an existing shipboard waste heat boiler (4).

Boiler performance tradeoffs. - The first step in the boiler sizing study was to determine the effect of various process variables on boiler weight and efficiency. Boiler efficiency is defined as the ratio of energy absorbed by the water stream to the energy available in the gas stream. If thermal losses are assumed to be negligible then heat gained by the water is equivalent to heat extracted from the gas so that

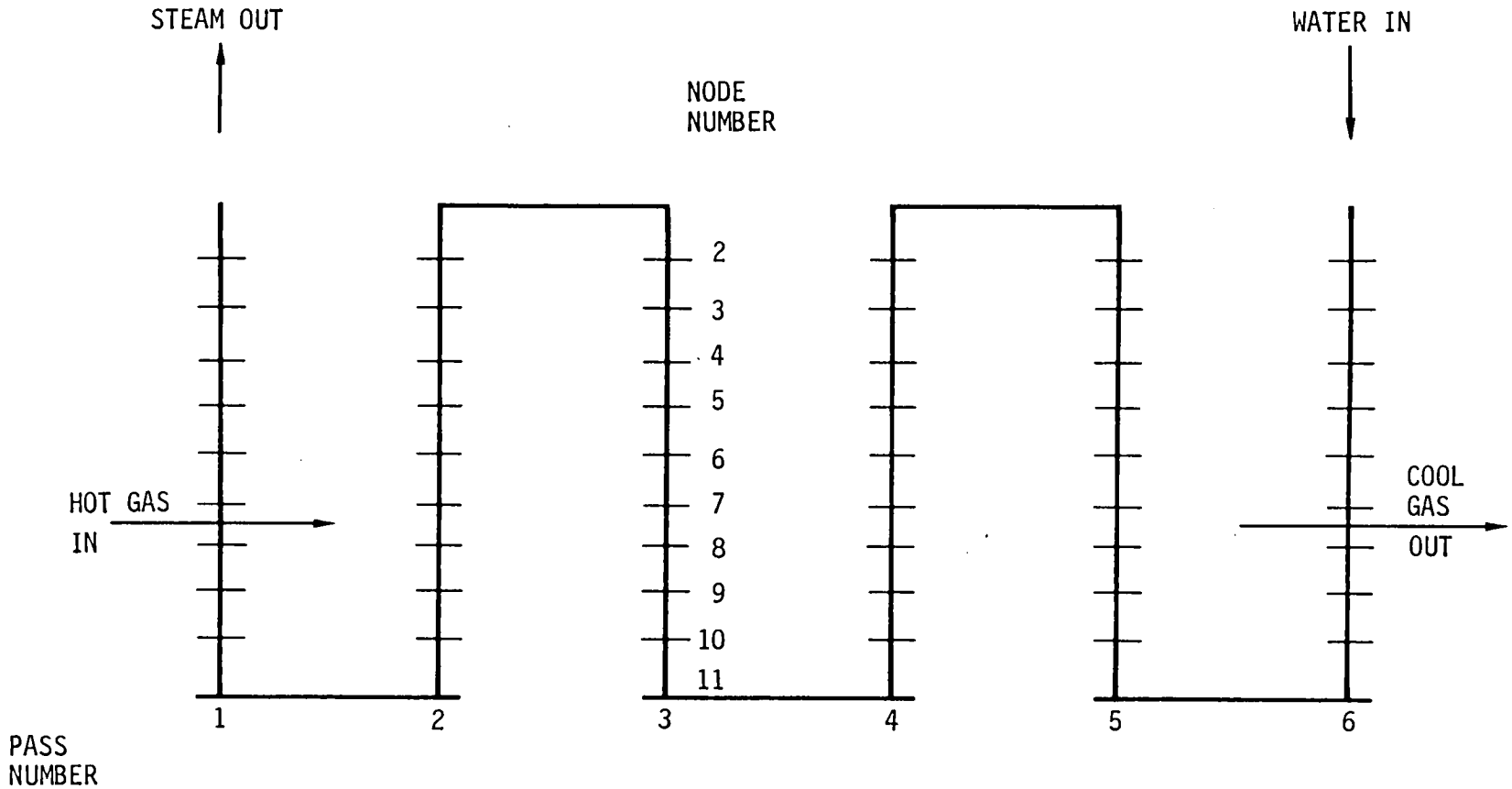

Figure 3. - Typical flow schematic for monotube boiler analysis.

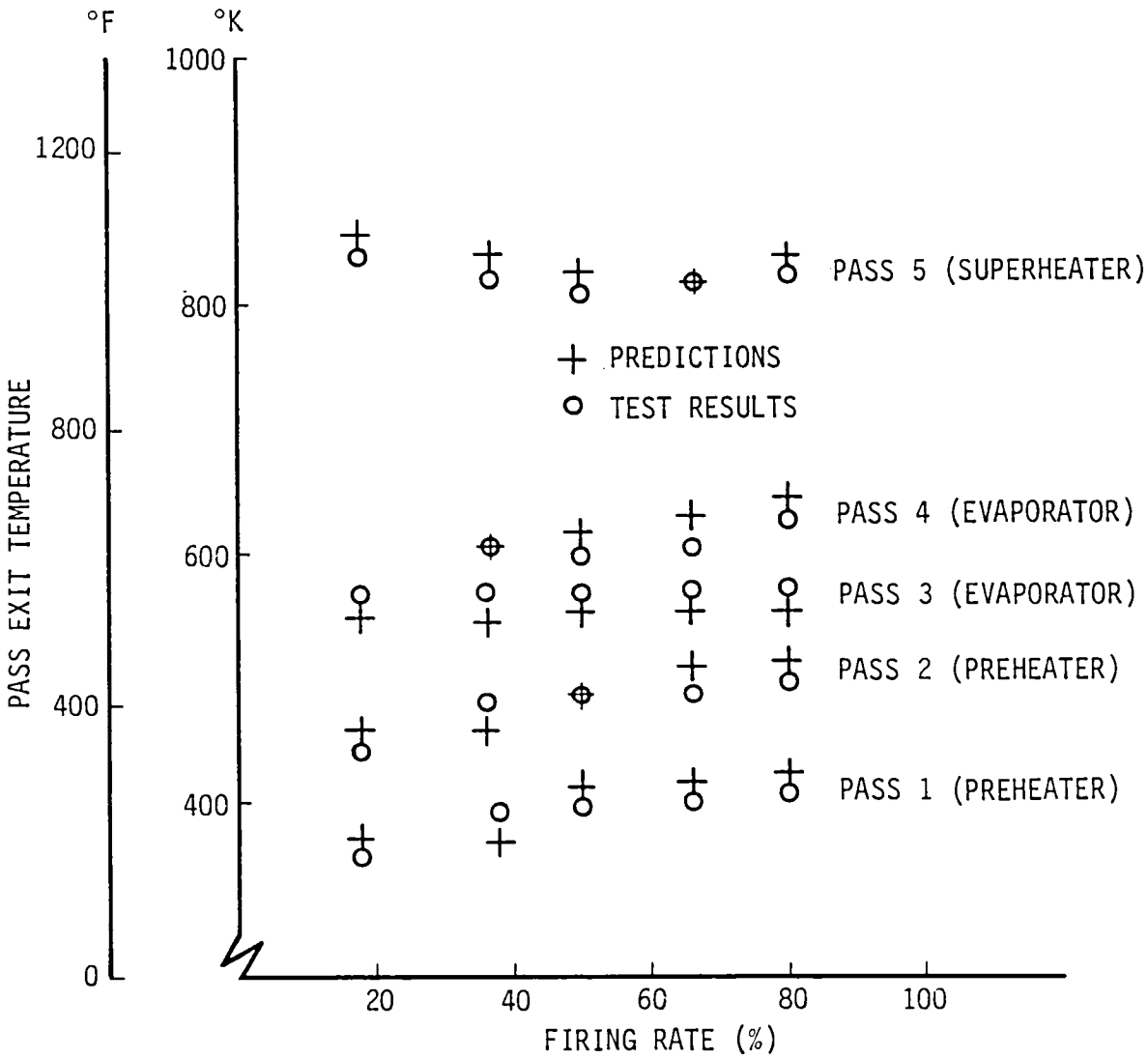

Figure 4. - Comparison of test results and Boiler Analysis Program predictions, Model 5 Vapor Generator.

boiler efficiency is inversely related to the gas exiting or stack temperature. A stack temperature of 422°K (300°F) corresponds to 100 percent boiler efficiency due to the assumed stack temperature limit and the definition of maximum energy extractable from the gas stream. Figure 5 shows the boiler core weight required to recover exhaust energy down to the indicated stack temperatures. The process variables are steam pressure, steam outlet temperature and diesel exhaust gas temperature. While the particular boiler designs represented by the data points in Figure 5 were generated to match the exhaust conditions of the TC/A diesel configuration at full speed, full throttle and reference and elevated temperatures, the qualitative conclusions drawn from the curves are equally applicable to the other adiabatic engine configurations which have different exhaust flow rates.

One significant result illustrated in Figure 5 is that at the higher steam pressure the dominant factor in maximizing boiler performance per unit weight is the diesel exhaust gas temperature. A 110°K (200°F) increase in gas temperature can produce a 30° to 40°K (60° to 75°F) decrease in stack temperature for the same boiler weight when 6.9 MPa (1000 psia) steam is generated. This translates into 10 percent higher boiler efficiency, η_B, and a 40 percent increase in total energy absorbed by the steam since the temperature drop in the exhaust gas increases about 150°K (270°F) for steam between 700° and 811°K (800° and 1000°F). This effect is considerably diminished at the lower steam pressure evaluated.

The data of Figure 5 also indicates that for the higher gas temperature the steam pressure and temperature have little effect on the boiler weight required to recover a given energy from the diesel exhaust. For the range of steam conditions considered and 989°K (1320°F) exhaust gas a 93 percent efficient boiler will weigh 41 to 49 kg (~90 to 108 lb) and 98 percent efficiency will require a 63 to 74 kg (140 to 160 lb) boiler. As is illustrated by the data 100 percent boiler efficiency can be obtained with approximately 80 kg (176 lb) of boiler finned tubing for 989°K (1320°F) diesel exhaust gas.

For the lower reference gas temperature the steam pressure and temperature selected have a significant impact on the boiler weight for a given boiler efficiency and the weight variation increases with increasing boiler efficiency. This occurs because the lower gas temperature implies smaller temperature differences between the heat exchange fluids so that the pinch point is beginning to dominate the heat transfer area requirements. In fact for specific combinations of diesel exhaust and desired steam conditions, the pinch point effect

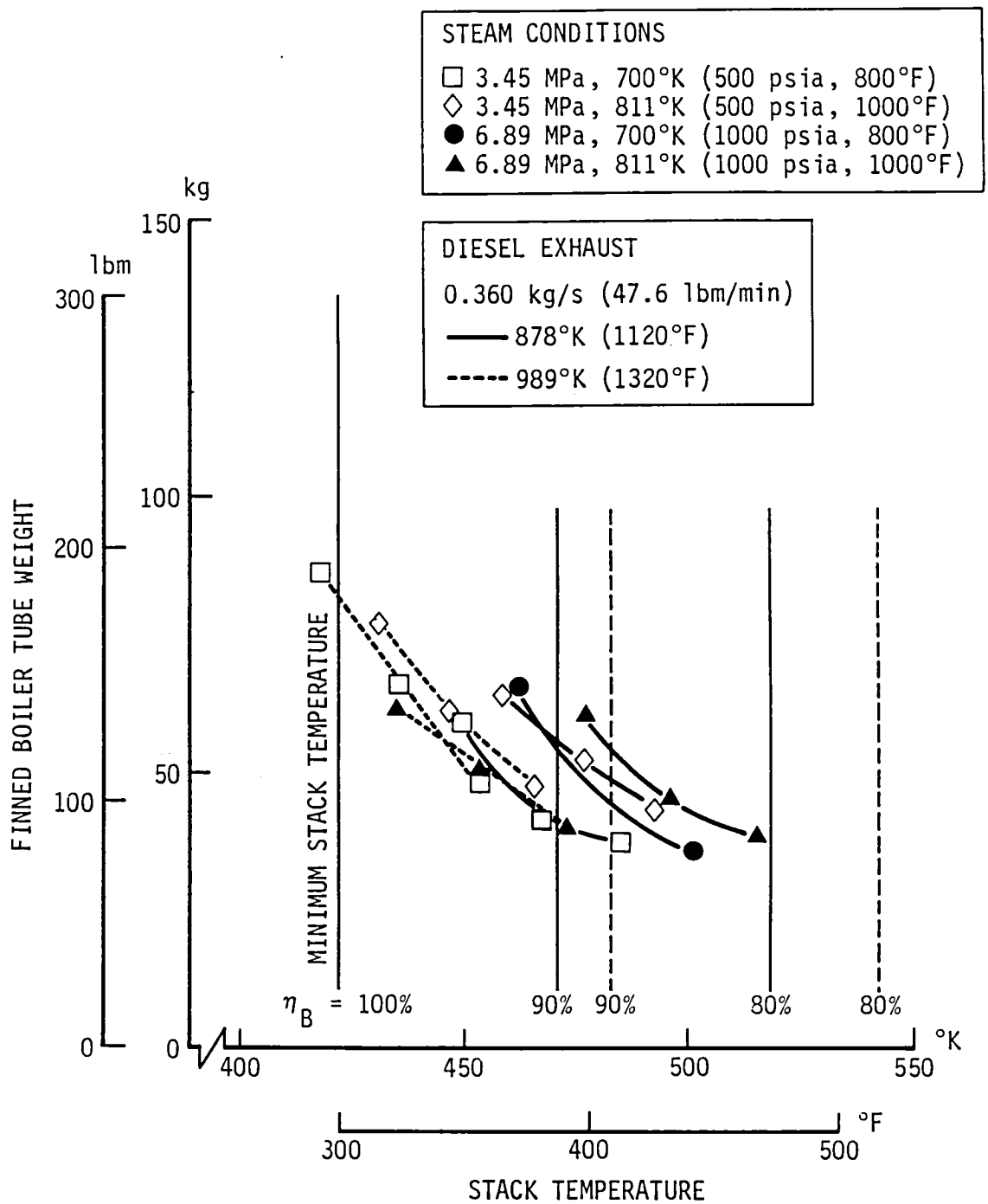

Figure 5. - Effect of diesel exhaust and steam conditions on boiler weight and performance.

imposes a minimum achievable stack temperature and therefore, a maximum boiler efficiency. This effect is elaborated in the following discussion.

Pinch point effect on boiler performance and size. - Pinch point is defined as the heat transfer temperature difference at the saturated liquid point in the boiler. This boiler characteristic is identified in Figure 6 which illustrates the typical variation of fluid temperatures through a monotube boiler.

Due to the phase change occurring on the water side, heat transfer analysis of a superheating boiler is most easily accomplished by separating the boiler into three parts: the preheater, vaporizer, and superheater sections. The heat transfer rate for each section, as well as for the overall boiler, can be determined by

$$q = \dot{m}_G \, c_{p,G} \, \Delta T_G \tag{1}$$

$$q = \dot{m}_w \, \Delta h \tag{2}$$

$$q = (FUA) \, LMTD \tag{3}$$

where

q = heat transfer rate

$\dot{m}_G$ = mass flow rate of the diesel exhaust gas

$c_{p,G}$ = specific heat of the diesel exhaust gas

ΔT_G = change in temperature of the diesel exhaust gas

$\dot{m}_w$ = mass flow rate of water/steam

Δh = change in enthalpy of water/steam

F = correction factor which depends upon heat exchanger type

U = overall heat-transfer coefficient

A = surface area for heat transfer, consistent with definition of U

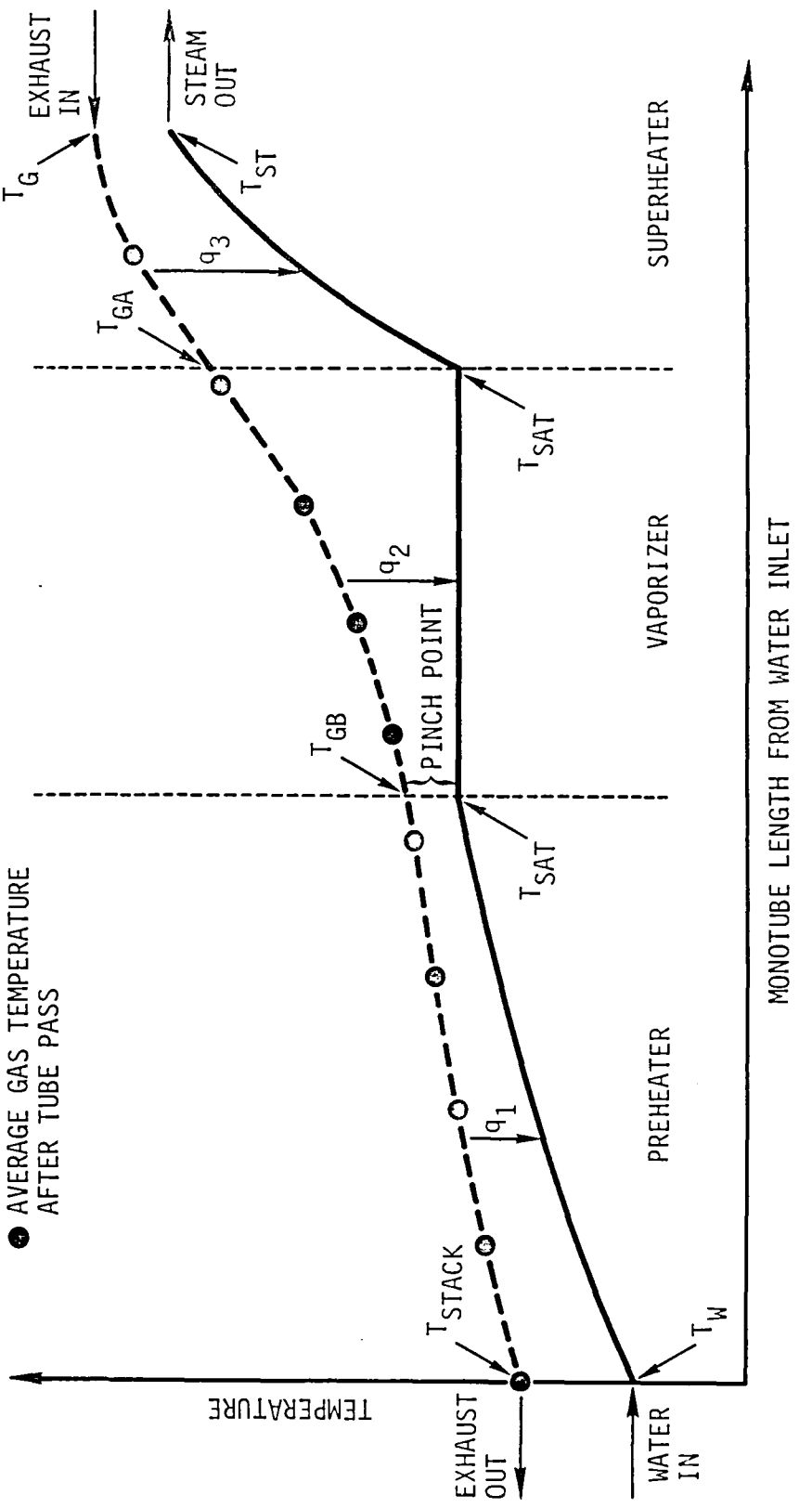

Figure 6. - Typical fluid temperature profile through monotube boiler.

LMTD = log-mean temperature difference

$= (\Delta T_2 - \Delta T_1)/\ln(\Delta T_2/\Delta T_1)$

ΔT_1 = temperature difference at one end of the heat exchanger

ΔT_2 = temperature difference at the other end of the heat exchanger

The relationship between the stack temperature and the pinch point (PP) can be determined from an analysis of the preheater heat transfer rate.

Since, with reference to Figure 6,

$$PP = T_{GB} - T_{SAT} \tag{4}$$

$$T_{GB} = T_{SAT} + PP \tag{5}$$

Equation (1) for the preheater section (identified by subscript 1) becomes

$$q_1 = \dot{m}_G \, c_{p,G1}(T_{GB} - T_{STACK}) \tag{6}$$

$$= \dot{m}_G \, c_{p,G1}(T_{SAT} + PP - T_{STACK}) \tag{7}$$

so that

$$T_{STACK} = T_{SAT} + PP - \frac{q_1}{\dot{m}_G \, c_{p,G1}} \tag{8}$$

According to equation (2) the heat transfer rate in the preheater is also represented by

$$q_1 = \dot{m}_w(h_f - h_w) \tag{9}$$

where

h_f = enthalpy of saturated water

h_w = enthalpy of compressed water entering the boiler

Combining equations (8) and (9) the following expression is derived:

$$T_{STACK} = T_{SAT} + PP - \frac{\dot{m}_w(h_f - h_w)}{\dot{m}_G\, c_{p,G1}} \tag{10}$$

The water flow rate is also a function of the boiler pinch point. Considering the combined heat transfer rate for the vaporizer and superheater sections (subscript 23),

$$q_{23} = \dot{m}_G\, c_{p,G23}(T_G - T_{GB}) \tag{11}$$

$$= \dot{m}_G\, c_{p,G23}(T_G - T_{SAT} - PP) \tag{12}$$

and

$$q_{23} = \dot{m}_w(h_{ST} - h_f) \tag{13}$$

yield

$$\dot{m}_w = \frac{\dot{m}_G\, c_{p,G23}(T_G - T_{SAT} - PP)}{(h_{ST} - h_f)} \tag{14}$$

where

h_{ST} = enthalpy of superheated steam.

Finally, equations (10) and (14) are combined to produce:

$$T_{STACK} = T_{SAT} + PP - \frac{c_{p,G23}(T_G - T_{SAT} - PP)(h_f - h_w)}{c_{p,Gl}(h_{ST} - h_f)} \qquad (15)$$

or

$$T_{STACK} = \alpha + \beta(PP) \qquad (16)$$

where

$$\alpha = T_{SAT} - \frac{c_{p,G23}(h_f - h_w)(T_G - T_{SAT})}{c_{p,Gl}(h_{ST} - h_f)} \qquad (17)$$

and

$$\beta = 1 + \frac{c_{p,G23}(h_f - h_w)}{c_{p,Gl}(h_{ST} - h_f)} \qquad (18)$$

The above expression demonstrates that for a given inlet water temperature and diesel exhaust gas temperature and for specified steam outlet conditions, stack temperature is linearly related to the boiler pinch point. Since the pinch point is always greater than zero the stack gas temperature will always be greater than the minimum value determined by setting PP = O, that is,

$$T_{STACK} \geq \alpha \qquad (19)$$

As an example, given diesel exhaust from a TC/A adiabatic engine running at full speed and full throttle, consider that 811°K/6.90 MPa (1000°F/1000 psia) steam is desired. Assume that the pressure throughout the boiler is constant and that water enters the boiler at T_W equal to 375°K (215°F).

Thus,

$$T_G = 878^{\circ}K \ (1120^{\circ}F)$$

$$T_{ST} = 811^{\circ}K \ (1000^{\circ}F)$$

$$P_{ST} = 6.90 \text{ MPa } (1000 \text{ psia})$$

$$T_{SAT} = 558^{\circ}K \ (544.8^{\circ}F)$$

$$T_w = 375^{\circ}K \ (215^{\circ}F)$$

$$h_w = 431.3 \text{ kJ/kg } (185.4 \text{ Btu/lbm})$$

$$h_f = 1262.2 \text{ kJ/kg } (542.6 \text{ Btu/lbm})$$

$$h_{ST} = 3502.0 \text{ kJ/kg } (1505.4 \text{ Btu/lbm})$$

$$c_{p,G1} \simeq 1050 \text{ J/kg}^{\circ}K \ (\sim 0.25 \text{ Btu/lbm}^{\circ}F)$$

$$c_{p,G23} \simeq 1090 \text{ J/kg}^{\circ}K \ (\sim 0.26 \text{ Btu/lbm}^{\circ}F)$$

yields

$$T_{STACK}(^{\circ}K) = 468 + 1.28 \ PP(^{\circ}K) \qquad (20a)$$

$$T_{STACK}(^{\circ}F) = 383 + 1,28 \ PP(^{\circ}F) \qquad (20b)$$

and

$$T_{STACK} \_ 468^{\circ}K \ (383^{\circ}F)$$

A zero pinch point and therefore the minimum stack temperature determined from equation (15) is actually never achieved but is approached asymptotically as the preheater heat transfer area approaches infinity and PP approaches zero. A mathematical demonstration of this characteristic can be derived from the application of equation (3) to the preheater boiler section:

$$q_1 = F_1 U_1 A_1 \ LMTD_1 \qquad (21)$$

or

$$A_1 = \frac{q_1}{F_1 U_1 \ LMTD_1} \tag{22}$$

$$= \frac{q_1[\ln(T_{STACK} - T_w) - \ln(PP)]}{F_1 U_1 (T_{STACK} - T_w - PP)} \tag{23}$$

Combining equations (23), (16) and (7) results in the following relationship between preheater area and boiler pinch point:

$$A_1 = a \left[\frac{b - \gamma(PP)}{c + \gamma(PP)}\right] \ln \left[(1 + \gamma) + \frac{c}{PP}\right] \tag{24}$$

with

$$a = \frac{\dot{m}_G \ c_{p,G1}}{F_1 U_1} \tag{25}$$

$$b = \gamma(T_G - T_{SAT}) \tag{26}$$

$$c = (T_{SAT} - T_w) - \gamma(T_G - T_{SAT}) \tag{27}$$

$$\gamma = \beta - 1 \tag{28}$$

$$= \frac{c_{p,G23}(h_f - h_w)}{c_{p,G1}(h_{ST} - h_f)} \tag{29}$$

If the water inlet, steam outlet and diesel exhaust conditions are fixed and assuming that F_1U_1, which is primarily a function of heat exchanger geometry, is constant then according to equation (24) with a, b, c, and γ constant, as PP approaches zero the area A_1 approaches infinity. This conclusion is consistent with the curves of Figure 5 which illustrates boiler weight as a function of stack temperature.

Summary of boiler analysis results. - As illustrated by the previous example and by the curves of Figure 5, a 422°K (300°F) stack temperature is theoretically impossible to achieve for some combinations of exhaust gas temperature, inlet water temperature and outlet steam conditions and is impractical due to extreme boiler weight requirements for other combinations of conditions. The constraints on achievable stack temperature diminish as the gas stream temperature increases and as the feedwater temperature, steam outlet temperature and steam outlet pressure decrease. Thus the TC engine configuration with its higher exhaust temperature combined with low pressure and temperature steam production would result in the best boiler efficiency for a given boiler core weight. This conclusion is supported by the design data presented in Figure 5.

Optimum boiler efficiency, however, does not necessarily correspond with optimum overall system efficiency since both the ideal Rankine cycle and steam expander efficiencies decrease as steam outlet temperature and pressure decrease. The selection of steam conditions and boiler weight is further confused because the lower the desired steam temperature and the smaller the pinch point the more steam is produced and the larger the prime mover must be. The various influences on rate of steam production are illustrated in Figure 7. The symbols from left to right on the chart mark 27.8, 41.7 and 55.6°K (50, 75, and 100°F) boiler pinch points for each steam condition.

Rankine Cycle Analysis

The Rankine cycle is the ideal cycle for a steam power plant. Rankine cycle efficiency, h_R, is defined as the ratio of the net cycle power, P_{net} to the rate of heat transfer to the working fluid in the boiler, q_H:

$$\eta_R = \frac{P_{net}}{q_H} \tag{30}$$

The Rankine cycle net power is equal to the output of the prime mover, P_{PM} less the power consumed by the boiler feedwater pump, P_{pump}.

$$P_{net} = P_{PM} - P_{pump} \tag{31}$$

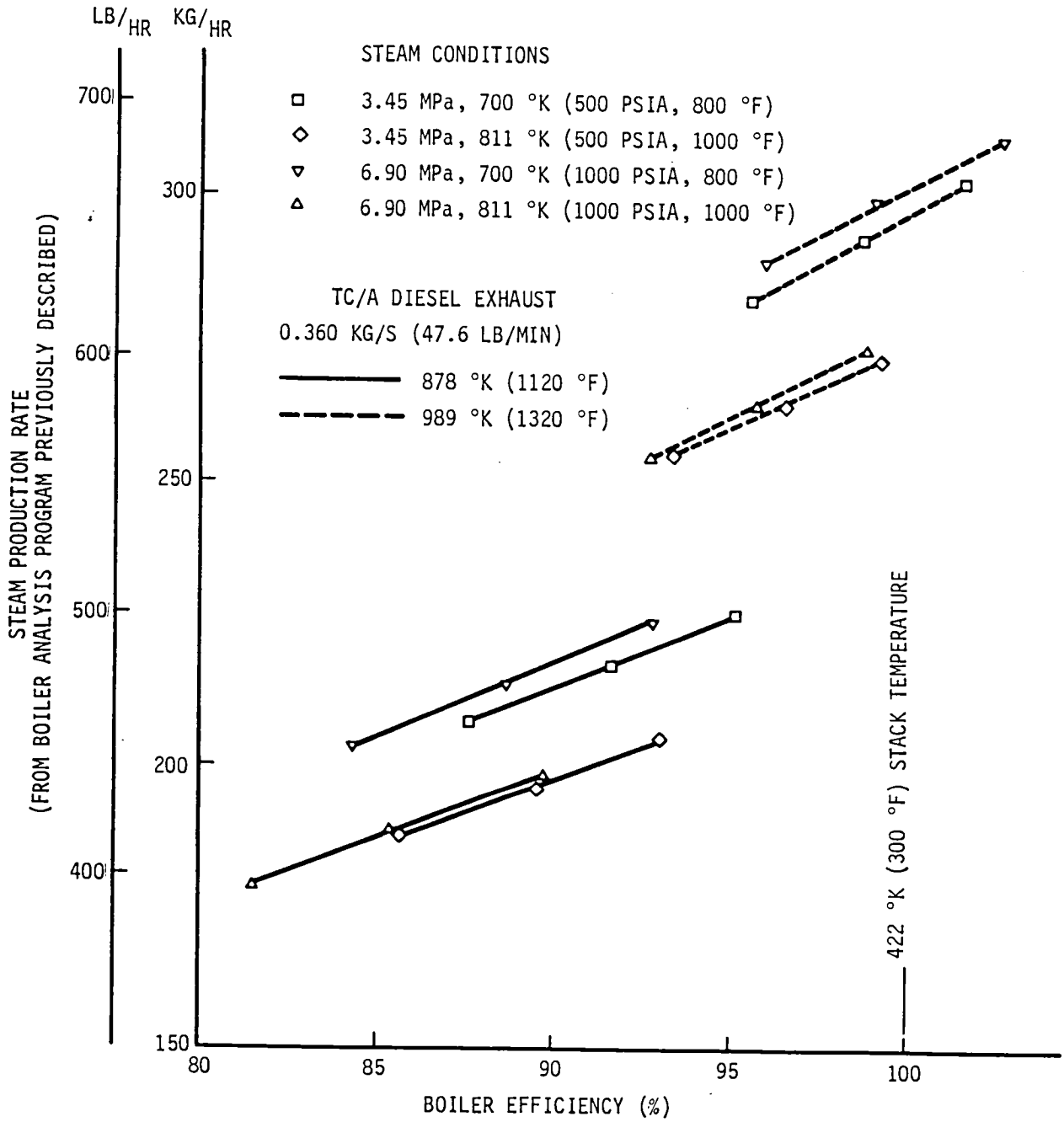

Figure 7. - Effect of steam and gas conditions and boiler efficiency on steam production rate.

According to the first law of thermodynamics, the net power from the cycle is equal to the net rate of heat transfer, or

$$P_{net} = q_H - q_L \tag{32}$$

where

q_L = rate of heat rejection in the condenser.

Neglecting changes in kinetic and potential energy from one point in the cycle to the other (a reasonable assumption for actual cycles) the net cycle output may be represented by the area inside the cycle plot on a temperature entropy diagram as illustrated in Figure 8. The reference superheated Rankine cycle is an ideal cycle which assumes isentropic pumping from A to B, constant pressure heat transfer in the boiler from B to C, isentropic expansion in the prime mover from C to D, and constant pressure heat transfer in the condenser from D to A to complete the cycle.

As indicated by the associated changes in area identified in Figure 8, increasing the steam outlet temperature or decreasing the condensing temperature (i.e., pressure) will increase the net work output with relatively little or no increase in heat transfer to the steam so that the cycle efficiency increases. A greater cycle efficiency can also be obtained by increasing the maximum cycle pressure. In this case the net work tends to remain the same, but relative heat rejection decreases for a net improvement in cycle efficiency.

In an actual steam Rankine cycle, pressure losses occur in the boiler and condenser and various losses and irreversabilities associated with fluid flow cause the pump compression and prime mover expansion to be non-isentropic. Taking pump and prime mover efficiencies into account, the actual Rankine cycle efficiency is

$$\eta_{R,actual} = \frac{\eta_{PM} P_{PM,ideal} - P_{pump,ideal}/\eta_{pump}}{q_H} \tag{33}$$

This equation can be expressed in terms of the enthalpy, h, of the water/steam at the state points as labeled in Figure 8 as follows:

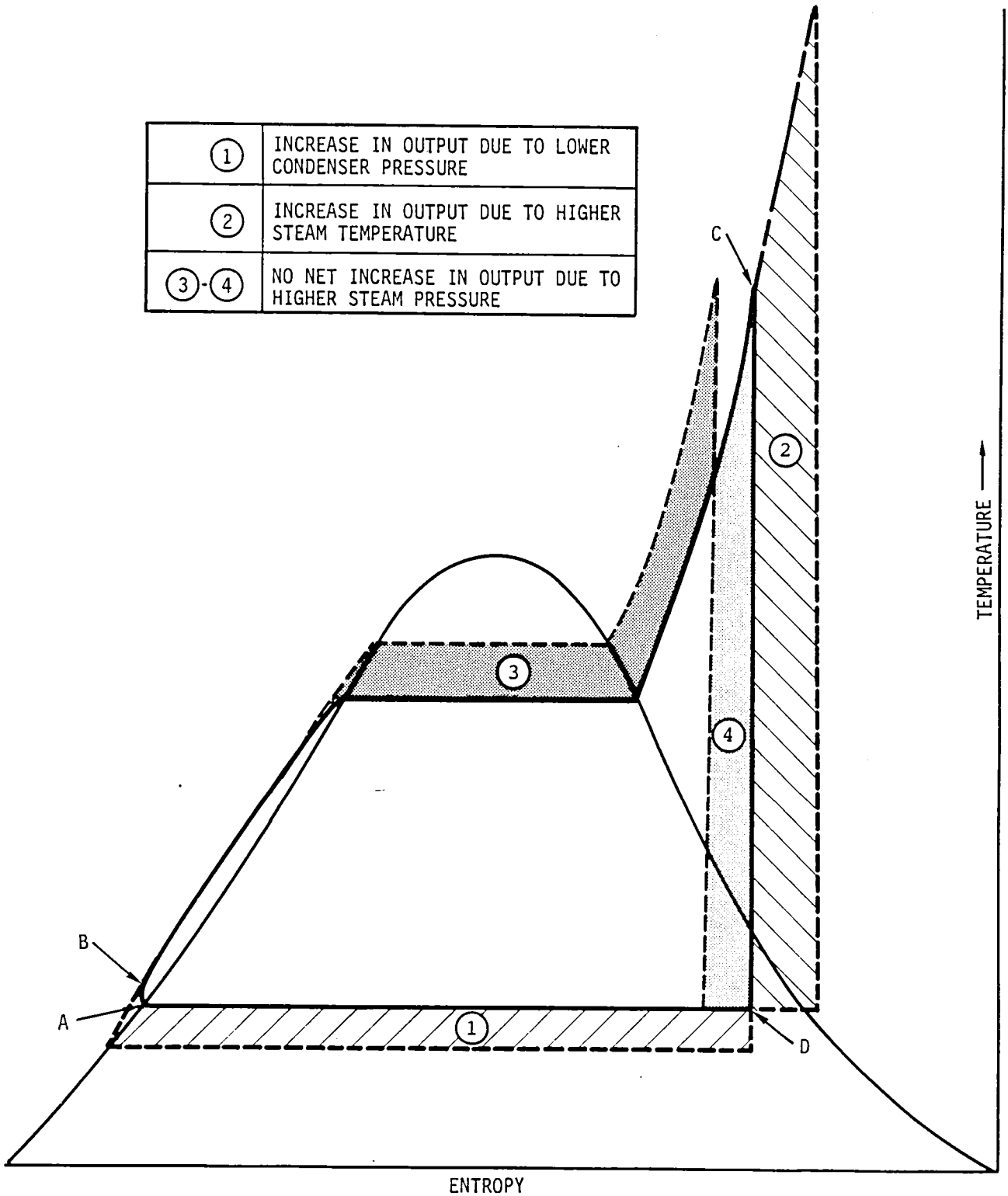

Figure 8. - Temperature-entropy diagram for ideal steam Rankine cycle.

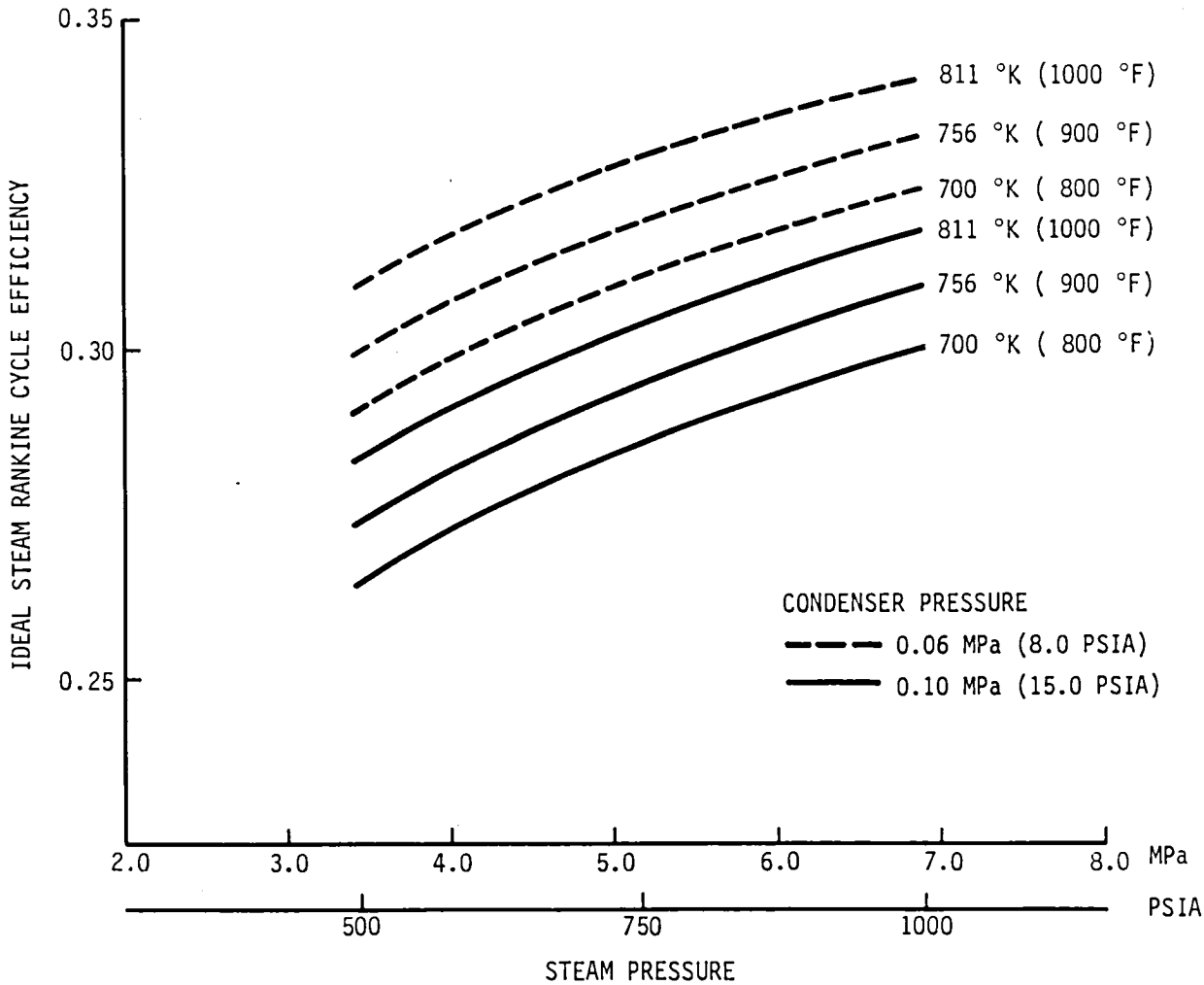

Figure 9. - Effect of steam cycle variables on ideal Rankine cycle efficiency.

$$\eta_{R,actual} = \frac{\eta_{PM}(h_C - h_D) - (h_B - h_A)/\eta_{pump}}{(h_C - h_B)} \qquad (34)$$

Since the change in enthalpy associated with boiler feedwater pumping is relatively small, Equation 34 demonstrates that the actual Rankine cycle efficiency, and therefore bottoming system output, is almost directly proportional to the prime mover

efficiency and to the ratio of ideal prime mover output to boiler heat transfer.

A reciprocating piston steam expander has been selected as the bottoming system prime mover due to its demonstrated performance under the cycle conditions being considered and its design which allows fabrication and maintenance according to techniques well established in the diesel engine industry.

Expander Design Analysis

The expander analysis was guided by the same general goals as specified for the boiler: high effectiveness, low cost and minimum practical size and weight. Other specific design constraints adopted prior to conducting the analysis were:

- Expander shaft speed equal to diesel shaft speed, i.e. 199 rad/s (1900 rpm) at full speed.
- Piston speed approximately equal to 4.06 m/s (800 fpm).
- Steam temperatures and pressures not to exceed current experience with standard expander materials.
- Uniflow expander configuration.
- Simple steam cycle.

The expander shaft speed was selected to simplify power transmission from the expander to the engine output shaft. The low piston speed was aimed at reducing piston ring and cylinder wear and minimizing power losses due to friction. A conservative design strategy with respect to steam conditions was selected to insure low cost fabrication with standard materials.

The uniflow expander configuration, with steam admission at the top of the cylinder, and steam exhaust through a port at the bottom of the cylinder, was specified because it also is consistent with current practice in steam engine design. While a counterflow configuration (both admission and exhaust ports in cylinder head) has potential for significant improvement in performance over that historically reported, a low technology risk approach was adhered to in order to emphasize that steam bottoming cycle benefits are attainable in the near term.

Finally, the design analysis was restricted to the simple steam cycle since reheat or compound cycle systems would each require one small primary expansion cylinder for high pressure

steam and a large volume secondary cylinder for efficient expansion of the low pressure steam. These cycles would thus require two separate cylinder manufacturing set-ups. In addition, the reheat cycle system design would require considerable additional development and analysis of a reheat boiler.

Expander design variables. - Expander design variables include geometry and valve timing parameters as well as steam supply conditions, steam flow rate and condenser back pressure. For a given gas stream and selected steam supply conditions and condenser back pressure, a particular steam mass flow rate implies a particular boiler design (pinch point). Expander geometry specifications required are cylinder bore (inside diameter) and clearance (volume occupied by the fluid when piston is at top dead center). By defining specific expander and piston speeds as design constraints, the expander stroke was determined according to

$$\text{stroke} = \frac{\text{piston speed}}{\frac{2}{2\pi} \times \text{expander shaft speed}}$$

$$= \frac{4.06 \text{ m/s}}{\frac{2}{2\pi} \times 199 \text{ rad/s}}$$

$$= 0.064\text{m} \qquad (35)$$

The valve timing parameters which influence the expander analysis results are steam admission timing or cut-off (CO) and steam blowdown timing or exhaust (E). In a uniflow expander, the exhaust valve timing is symmetric about bottom dead center (BDC), while the admission valve is opened on the piston return stroke after top dead center (TDC). These variables are usually expressed in fractions of a stroke.

Given supply steam conditions, steam flow rate, cut-off and piston speed, the appropriate cylinder bore is determined from

$$\text{bore} = \left(\frac{4 \times \dot{m}_{ST}}{\pi \times SP \times CO \times \rho_{ST}} \right)^{1/2} \qquad (36)$$

where

SP = piston speed

ρ_{ST} = supply steam density

and all variables are in appropriate units.

For each set of expander variables, the cylinder clearance (expressed as a fraction of the swept cylinder volume which is equivalent to a fraction of the stroke) was specified so that 100 percent recompression would occur. This means that the gas remaining in the cylinder after the exhaust port closes would be compressed to the supply steam pressure during the piston return stroke. This eliminates expander inefficiencies associated with either overcompression, in which some steam blows back out of the cylinder for part of the cut-off, or undercompression, in which excess steam is admitted during cut-off to bring the cylinder pressure up to supply pressure.

Once steam, geometry and valve timing parameters have been established, expander efficiency and finally gross expander output are calculated using formulations developed from thermodynamics, heat transfer and dynamics principles and adjusted to reflect empirical data.

Expander performance analysis. - The plot of cylinder pressure versus cylinder volume presented in Figure 10 illustrates a uniflow expander cycle with 100 percent recompression. This type of plot is known as an indicator diagram and is a very convenient method of analyzing the performance of a reciprocating device since the power output is proportional to the net area enclosed by the cycle curve.

The diagram of Figure 10 is termed ideal in that isentropic expansion and compression are represented, no pressure loss occurs during steam admission, and the cylinder pressure immediately drops to back pressure when the exhaust valve is opened. The cycle of Figure 10 does not however deliver maximum expander output. Maximum expander power results when the steam flow is expanded isentropically from the supply steam state to the condenser back pressure. The isentropic expansion illustrated in the figure only occurs to a pressure greater than the back pressure so that the expansion is incomplete with respect to the available pressure ratio.

Thus expander cycle thermodynamics as represented by the ideal indicator diagram reduce expander output. Thermal effects resulting from the temperature differences between the

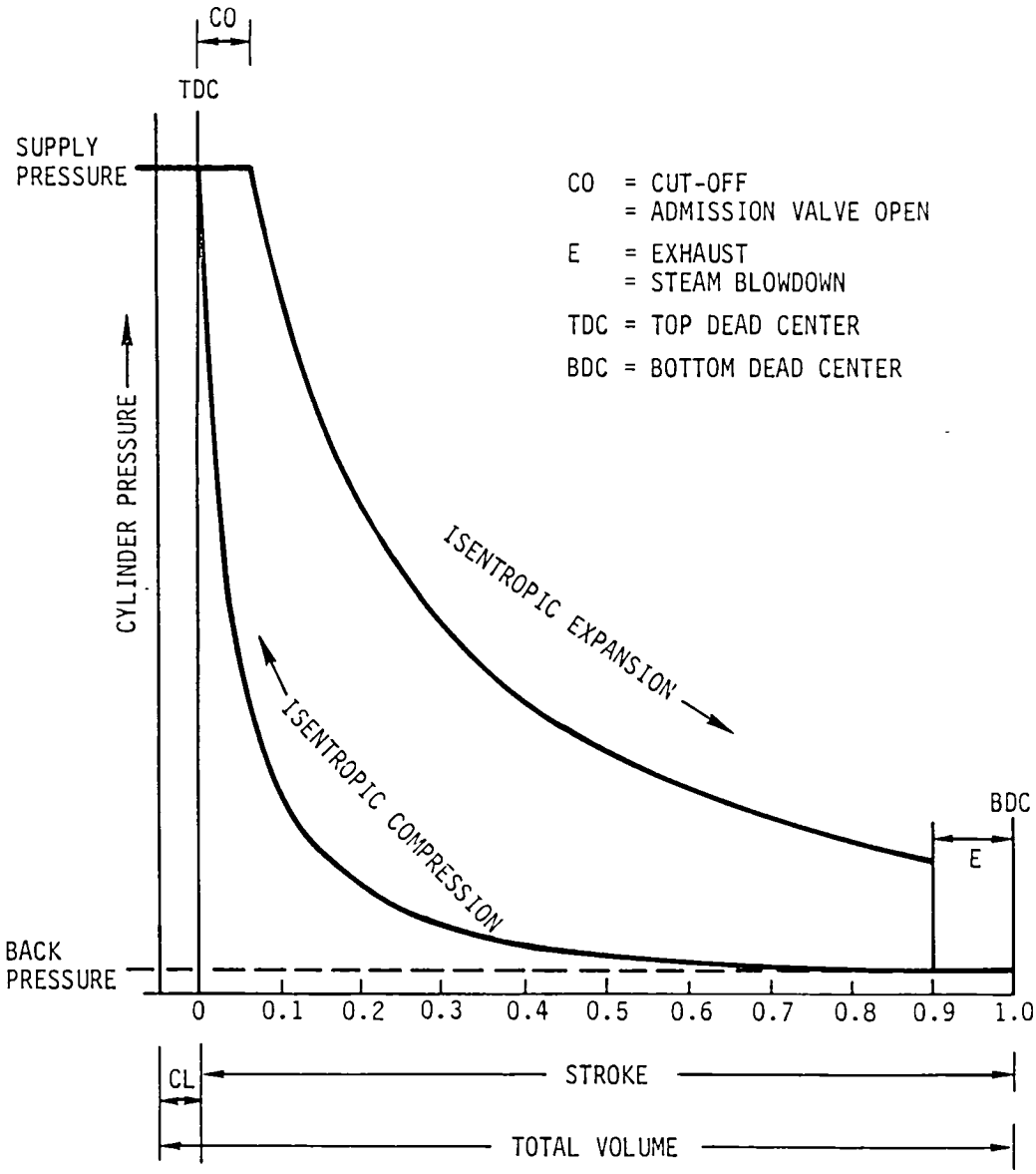

Figure 10. - Ideal indicator diagram for 100 percent recompression, uniflow expander.

steam, cylinder walls and ambient environment reduce expander performance as does the reduction in actual pressure ratio in the cylinder due to pressure losses which occur when the steam flows through the admission and exhaust ports.

All of the above expander inefficiencies are reflected in pressure versus volume traces of actual reciprocating steam expanders. In addition, losses are incurred due to friction between moving parts (e.g., piston rings moving against the

cylinder wall) and transmission inefficiency between the expander shaft and the diesel shaft. The overall expander efficiency, or the ratio of actual to ideal expander output, may be expressed as the product of several components:

$$\eta_{EX} = \eta_D \times \eta_B \times \eta_T \times \eta_M \qquad (37)$$

where

η_{EX} = overall expander efficiency

η_D = diagram efficiency

η_B = breathing efficiency

η_T = thermal efficiency

and

η_M = mechanical efficiency

The above mechanisms which influence reciprocating steam expander performance have been considered in some detail. The derivations of expressions that can be used to calculate each efficiency component are described in reference (5) and summarized below.

As previously noted, the diagram efficiency, η_D, is a measure of the completeness of the expansion. The smaller the cut-off, the more complete the expansion and therefore the greater is η_D. Diagram efficiency was determined strictly by a thermodynamic analysis of the expander cycle, that is, on a specific work basis:

$$\eta_D = \frac{\text{diagram output}}{\text{ideal output}} \qquad (38a)$$

$$= \frac{W_{AD} + W_{EX} - W_{CMP}}{h_{ST} - h_B} \qquad (38b)$$

where

W_{AD} = admission work per unit mass

W_{EX} = isentropic expansion work per unit mass

W_{CMP} = isentropic compression work per unit mass

h_{ST} = enthalpy of supply steam

h_B = enthalpy of steam at back pressure after isentropic expansion

The breathing efficiency is a measure of the adequacy of the valves. Good valve design minimizes pressure losses so that the cylinder pressure ratio remains close to the available ratio. Experience has shown that a 5-percent valve pressure loss is reasonable and results in a breathing efficiency of better than 98 percent for an available pressure ratio of 50:1.

The thermal efficiency is a measure of both internal cyclical heat transfer effects and steady state heat loss to the environment. Cyclical heat losses result from the alternate cooling and heating of the steam by the cylinder walls during the expander cycle. During the steam admission process the steam is typically at a higher temperature than the cylinder walls exposed near the top of the stroke. Thus, heat energy which would otherwise contribute to the expander work is transfered into the cylinder material. If the wall temperature is less than the saturation temperature of the incoming steam then condensation, with its significantly greater heat transfer rate, may occur. As the piston proceeds to the bottom of the cylinder, the steam is expanded and the average wall temperature in the cylinder becomes greater than the steam temperature. Some of the thermal energy extracted earlier in the stroke is then transferred back to the steam just before it is exhausted.

The steady state heat loss includes conduction losses through the head, piston, and cylinder. The heat transfer losses can obviously be reduced by minimizing heat exchanger effectiveness (more cylinder insulation) and area (higher cut-off).

A gross approximation of the influence of heat transfer on expander efficiency was made by assuming that all heat transfer takes place during the cut-off process. The following inlet charge cooling formulation was then derived by analogy to heat loss correlations, by reference to condensing heat transfer equations and by empirical approximation of the coefficients:

$$\Delta T_c = 0.065(T_s - T_{ex}) \left(\frac{b}{\dot{m}_{ST}} \right)^{1/4}$$

$$+ 0.23(T_{sat} - T_{ex}) \left(\frac{b^2}{\dot{m}_{ST}} \right) \quad (39)$$

with,

ΔT_c = inlet charge cooling, ^oK

T_s = supply temperature, ^oK

T_{ex} = exhaust temperature, ^oK

T_{sat} = saturation temperature of supply steam, ^oK

b = bore, cms

$\dot{m}_{ST}$ = steam flow rate, kg/hr.

The consequences of heat transfer loss on expander performance is then estimated by

$$\eta_T = 1 - \frac{\Delta T_c}{T_s} \quad (40)$$

Finally, expander power loss due to friction between moving parts from the piston to the expander shaft is determined from

$$P_{friction} = \left[35 + 0.017 \left(\frac{P_I + 2P_{CMP}}{A_p} \right) + 6.9 \times SP \right]$$

$$\times A_p \times \frac{SP}{2} \quad (41)$$

with

A_p = piston area, m^2

SP = piston speed, m/s

P_I = total indicator power, kW

P_{CMP} = indicated compression power, kW

$P_{friction}$ = friction power, kW

The above formulation was derived from the results of an experiment reported in reference (6) in which reciprocating engine friction was measured as a function of piston speed while a range of steady gas pressure was applied to the piston.

Neglecting transmission losses, the mechanical efficiency of the expander is then determined by

$$\eta_M = 1 - \frac{P_{friction}}{P_I} \qquad (42)$$

Typical relative magnitudes of each of the expander efficiency components as well as their variation with steam admission timing are presented in Figure 11. Note that the influence of breathing efficiency is minimal and that the opposing trends of the diagram versus the mechanical and thermal efficiencies with increasing cut-off produces a maximum expander efficiency at approximately a 10-percent cut-off.

Summary of expander analysis results. - For the combinations of steam supply conditions and steam flow rates generated during the boiler design analysis, expander geometry and efficiency were calculated for a range of cut-offs and exhaust valve timings and for two condenser pressures.

The optimum expander performance conditions were then identified. Figure 12 illustrates how the optimum overall expander efficiency varies with steam conditions and condenser back pressure for a TC/A diesel with a 42°K (75°F) pinch point boiler. As expected, like the Rankine cycle efficiency, the expander efficiency improves with steam temperature. The expander performance on the other hand appears to decrease slightly with increasing pressure. Also, whereas the Rankine cycle efficiency showed a significant increase with decreasing

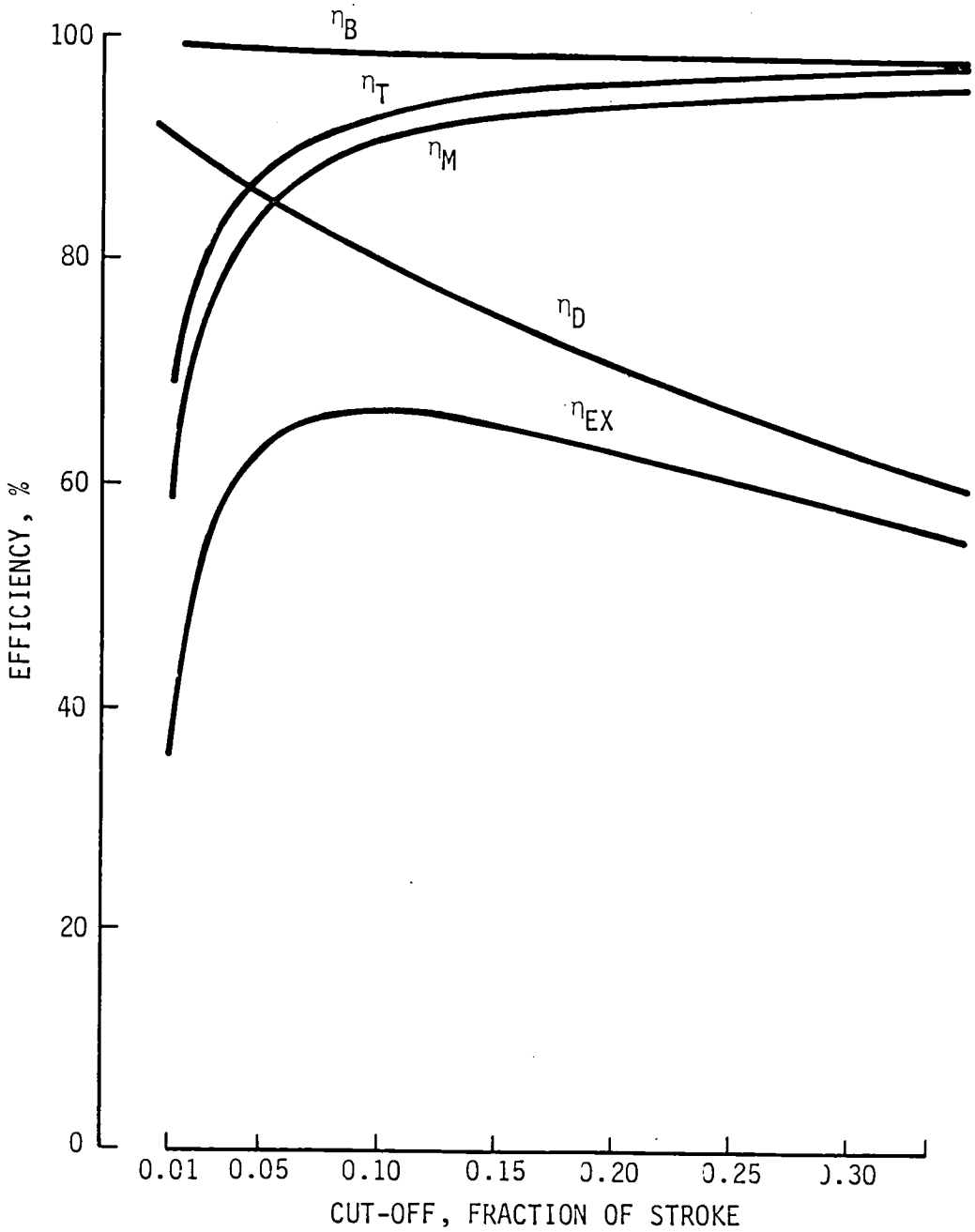

Figure 11. - Typical variation of expander component efficiencies with cut-off.

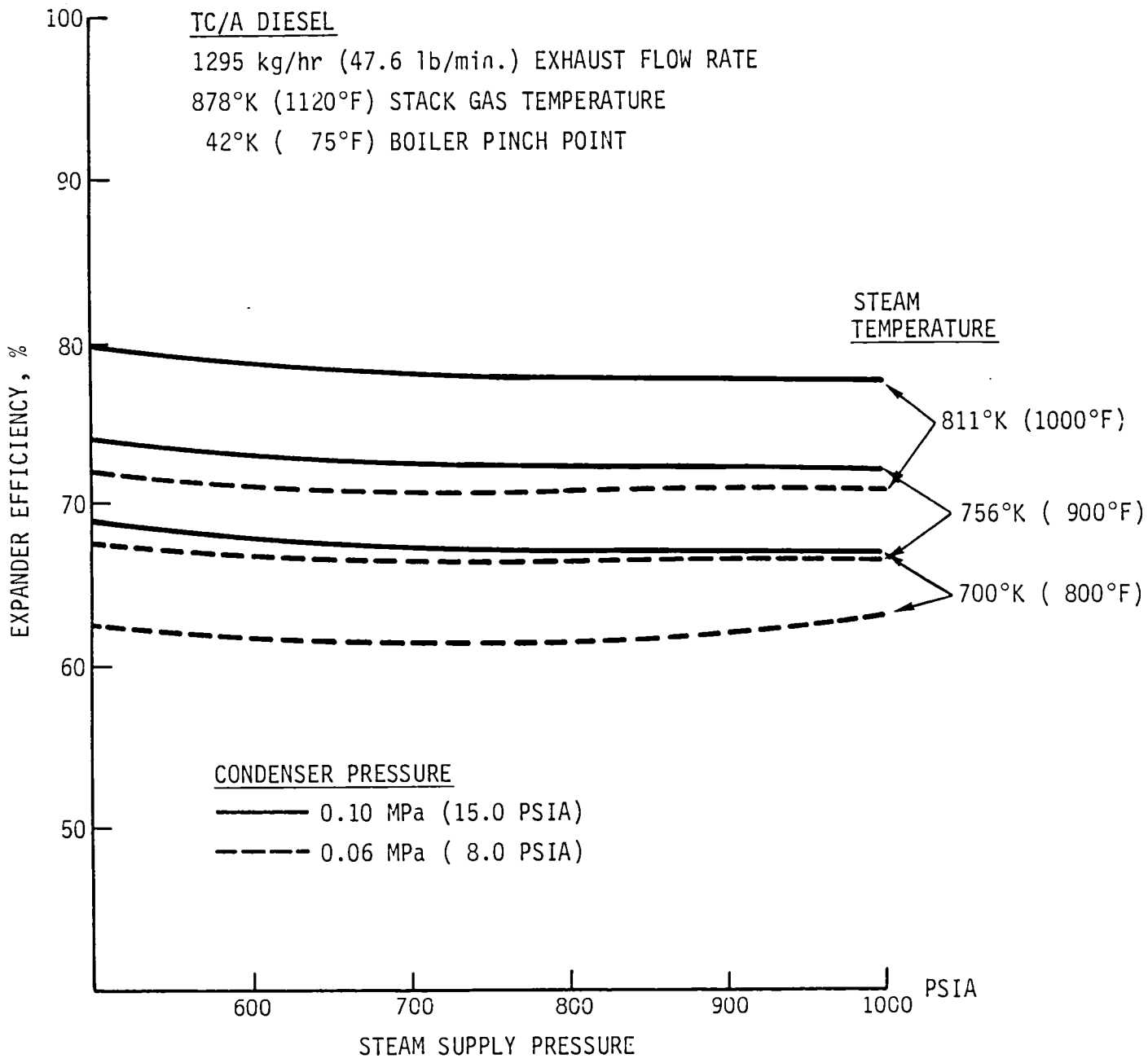

Figure 12. - Variation of overall expander efficiency with steam cycle variables.

condenser pressure, the opposite is true with respect to the expander efficiency. Expander exhaust pressure below about 0.10 MPa (15 psia) incurred increased expander losses due to higher friction and thermal losses associated with the greater piston displacement needed to produce the higher expansion ratios.

The net effect of expander efficiency variation with expander cycle conditions is presented in Figure 13. The ideal power charted at the top of the graph represents the expander shaft output for an TC/A diesel with a 42°K (75°F) pinch point boiler and a 100-percent efficient expander. The actual expander shaft power plotted at the bottom of the graph reflects the impact of expander losses on net output.

Due to higher Rankine cycle efficiencies, high steam temperature and pressure combined with the lower condenser pressure produce the greatest potential for expander output. The advantage of lower back pressure is minimized, however, by the expander while the gain in output with higher steam temperature is accentuated. Although some improvement in output with the lower back pressure is still evident, it is not sufficient to justify the added system complexity of a sub-atmospheric condenser, especially at the elevated steam conditions which produce the best system performance.

The expander specifications for optimum performance given a TC/A diesel with a 42°K (75°) pinch point boiler generating 811°K/6.90 MPa (1,000°F/1,000 psia) steam are listed in Table 3.

The net system output for a system as specified above, assuming a feedwater pump efficiency of 75 percent, is

$$\text{Bottoming system output power} = P_{EX} - P_{pump,ideal}/\eta_{pump}$$

$$= 39.9 \text{ kW} - 0.38/0.75$$

$$= 39.4 \text{ kW (52.8 hp)} \qquad (43)$$

with

P_{EX} = gross expander shaft output power

P_{pump} = power consumed by pump

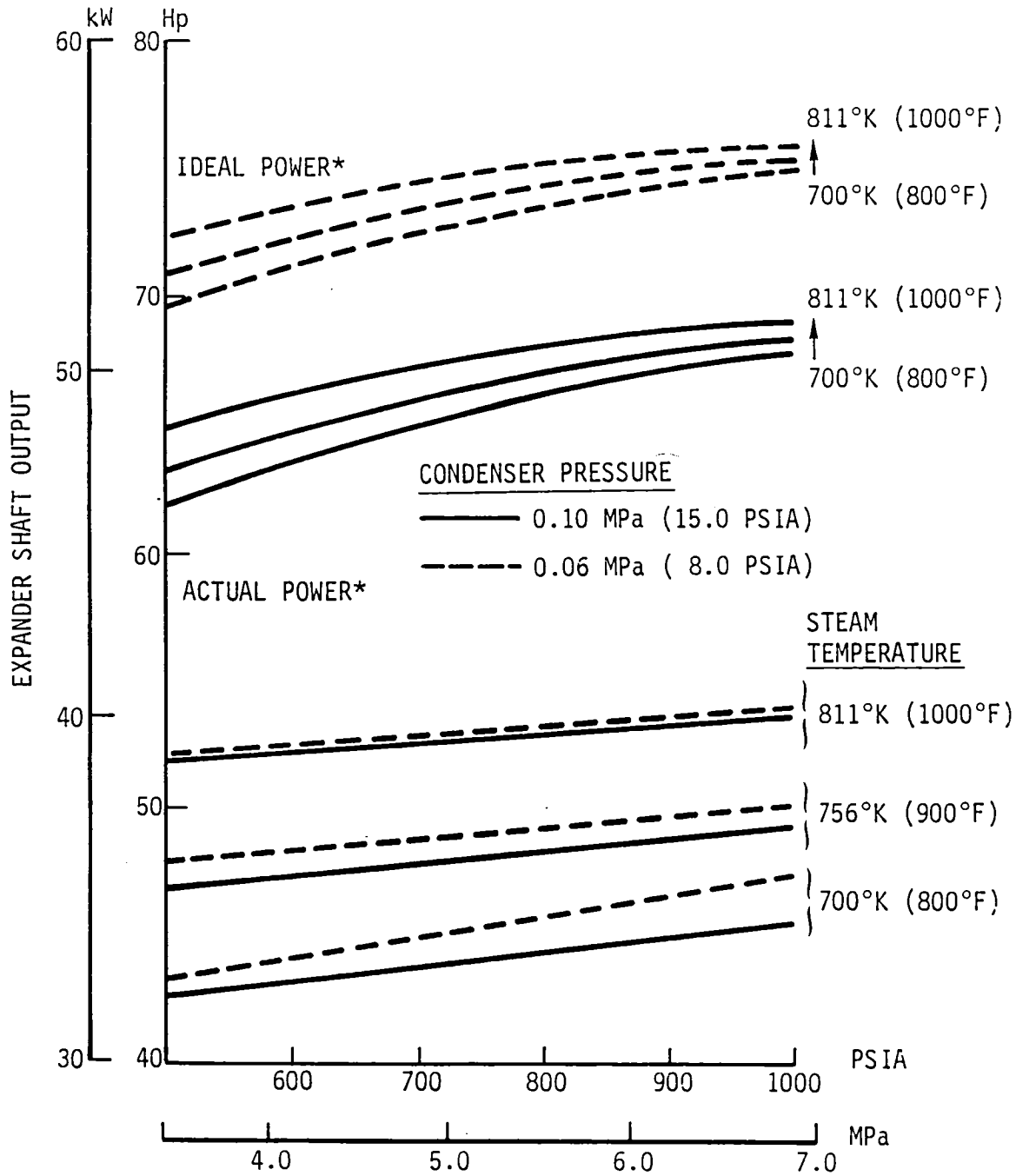

* TC/A DIESEL, 1295 kg/hr (47.6 lb/min) EXHAUST FLOW RATE, 878°K (1120°F) STACK GAS, 42°K (75°F) BOILER PINCH POINT

Figure 13. - Variation of expander shaft output with steam cycle variables.

TABLE 3. - OPTIMUM[a] SINGLE CYLINDER UNIFLOW EXPANDER SPECIFICATIONS

Bore = 0.131m (5.15 in.) Stroke = 0.064m (2.50 in.) Clearance = 0.031, fraction of stroke Cut-off = 0.094, fraction of stroke Exhaust = 0.100, fraction of stroke
Diagram efficiency = η_D = 95.1% Breathing efficiency = η_B = 99.0% Thermal efficiency = η_T = 89.4% Mechanical efficiency = η_M = 92.0%
Expander shaft output = 39.9 kW (53.5 hp)
[a]For TC/A diesel with 42°K (75°F) pinch point boiler generating 811°K/6.90 MPa (1,000°F/1,000 psia) steam.

The sensitivity of the optimized steam bottoming system performance to diesel exhaust temperature is shown in Table 4. Obviously higher temperatures give better system performance, all else being equal.

Condenser Design Analysis

The basic condenser configuration assumes standard automobile radiator construction, that is, flattened tubes with plate fins. This insures a durable, inexpensive and time tested design. For the purposes of the parametric investigation, performance data for a typical core from Kays and London (7) was used.

In the design of a condenser, constraints include space and air side pressure drop as well as freeze protection considerations. Design variables include core geometry (tubes, fins, etc.) and operating pressure.

Space limitations are obviously a function of vehicle design. For this exercise, a frontal area limit of approximately 0.42 m^2 (4.5 ft^2) was chosen.

One goal of the current design was that the condenser operate without a fan under "most" conditions. This implied a limit on the air side pressure drop through the condenser. In this case, a limit of 0.001 MPa (4 in. H_2O), which

TABLE 4. - SENSITIVITY OF BOTTOMING SYSTEM PERFORMANCE TO DIESEL EXHAUST TEMPERATURE

Diesel exhaust temperature		Net bottoming system output[a]		Brake specific fuel consumption		BSFC improvement
°K	°F	kW	hp	kg/(kW·h)	lb/(Bhp·hr)	%
878	1120	39.4	52.8	0.162	0.266	14.2
922	1200	43.8	58.7	0.160	0.262	15.5
1033	1400	59.1	79.3	0.151	0.248	20.0
1144	1600	74.0	99.3	0.144	0.237	23.5

[a]Based on: TC/A Diesel Configuration
42°K (75°F) pinch point boiler design
811°K/6.90 MPa (1,000°F/1,000 psia) steam
0.10 MPa (15.0 psia) condenser pressure

corresponds to 50 percent of ram air pressure at 64.4 km/hr (40 mph) was chosen.

In addition, condensing pressure affects condenser size and complexity as well as expander performance (as discussed in the previous section). A subatmospheric condenser will increase expander performance, but will also have a higher duty and consequently higher weight, as shown in Figure 14. In addition, a subatmospheric condenser requires extra precaution to keep out noncondensables (air).

Performance of Combined Diesel Engine/Steam Bottoming System

Table 5 lists the performance of the optimized bottoming cycle system as it varies with adiabatic diesel configuration. The same boiler/expander/condenser system, as previously described, is assumed for each. The difference in performance are due to the differences in exhaust gas flow rates and temperatures. The brake specific fuel consumption (BSFC) of the combined diesel/bottomer systems are shown in Table 6. On a percentage basis, the turbocharged (TC) diesel shows the greatest improvement through the use of a bottoming cycle. On an absolute basis, the turbocompound/steam bottomer (TCPD/S) system has the best BSFC but the improvement over the TC/S system is quite small (3 percent).

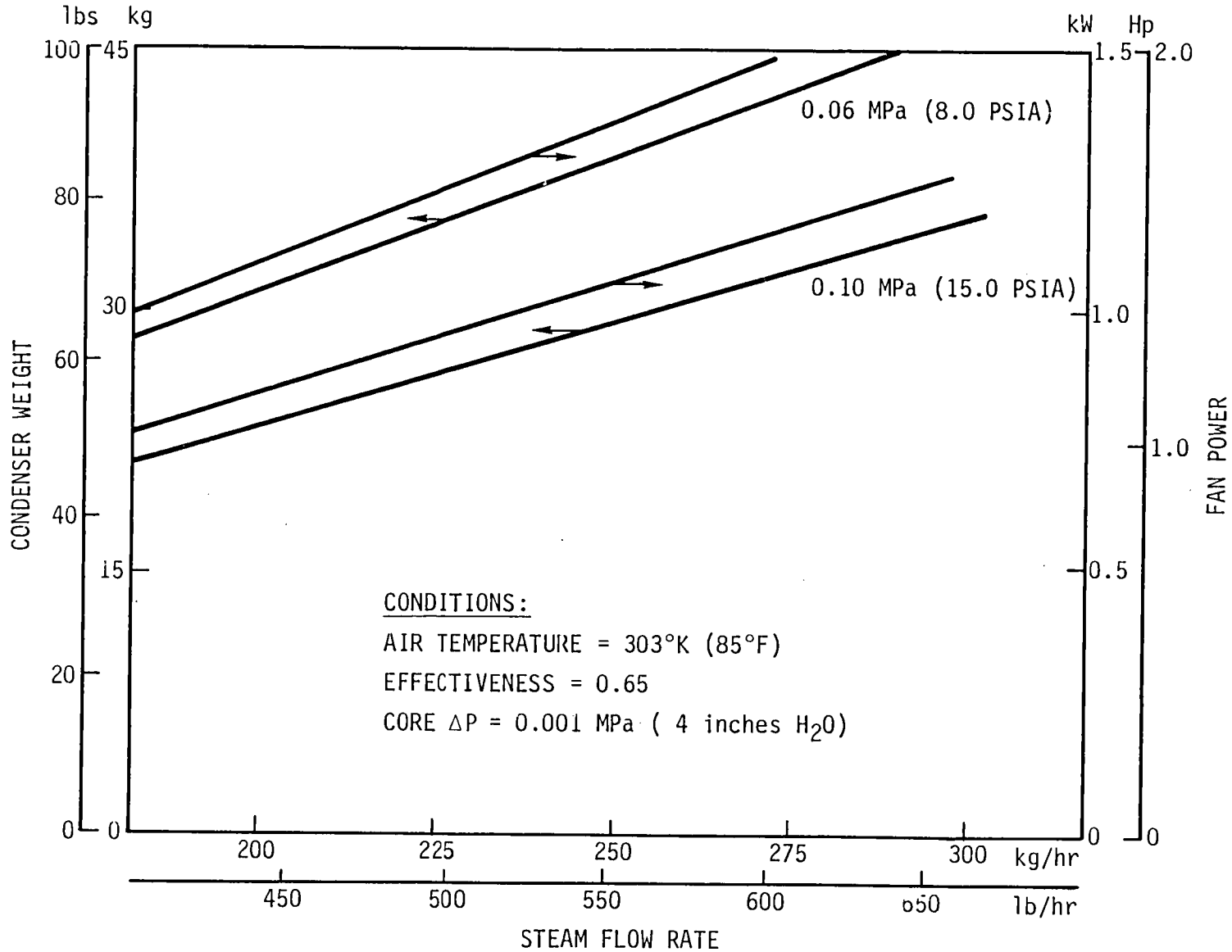

Figure 14. - Effect of pressure and steam flow on condenser weight and fan power.

TABLE 5. - VARIATION OF STEAM BOTTOMING SYSTEM PERFORMANCE WITH DIESEL CONFIGURATION

Diesel configuration	Expander efficiency	Bottoming system efficiency[a]	Net power output		Stack temperature	
	%	%	kW	hp	^{o}K	^{o}F
TC	0.775	0.245	45.6	61.2	503	445
TC/A	0.775	0.244	39.4	52.8	496	432
TCPD	0.775	0.244	39.9	53.5	502	444
TCPD/A	0.775	0.243	30.3	40.6	550	530

[a]Full speed, full throttle.

TABLE 6. - COMBINED DIESEL ENGINE/BOTTOMING SYSTEM PERFORMANCE

Diesel exhaust configuration	Net bottoming system output[a]		Brake specific fuel consumption		BSFC improvement[b]
	kW	hp	kg/(kW·h)	lb/(Bhp·hr)	%
TC	282.0	378.2	0.161	0.264	16.2
TC/A	278.0	372.8	0.162	0.266	14.2
TCPD	289.7	388.5	0.156	0.156	13.8
TCDP/A	283.8	380.6	0.160	0.262	10.6

[a]Full speed, full throttle.
[b]BSFC for adiabatic diesels alone are listed in Table 17.

PRELIMINARY BOTTOMING SYSTEM DESIGN

Based on the parametric analysis documented in this report FMI has generated a preliminary baseline design of a steam bottoming cycle system for an adiabatic diesel engine. The baseline design strategy was to develop a minimum risk system to show that impressive benefits were readily obtainable using state-of-the-art steam power technology.

Characteristics of the preliminary system design are therefore:

- Documented performance.
- Every part like a currently mass-produced part.
- Independent and fail-safe operation.
- Component design and cost reviewed with established manufacturers.

The preliminary design effort included detailed heat transfer design of the heat exchanger-boiler and the condenser, preliminary mechanical design of the expander, the transmission for power transfer to the prime mover, the controls, the freeze protection system and overall design layout of the system and all components required for its operation. The size, weight, and cost of all components required for system operation were also evaluated. This section of the report presents an overall system description, discusses the major system components, and points out the advantages of the steam bottoming cycle over competing configurations.

System Configuration

The adiabatic diesel selected for bottoming cycle application was the turbocharged version without aftercooling. This configuration derives the greatest percent improvement in specific fuel consumption with the added bottoming system. The full speed, full throttle exhaust gas conditions assumed for the preliminary design were therefore, 944^{o}K and 1309 kg/hr (1240^{o}F, 48.1 lbm/min).

A 6.90 MPa, 811^{o}K (1000 psia, 1000^{o}F) simple steam cycle was selected for the preliminary design. This represents current proven durability and experimentally verified performance. FMI's background, through acquisition of Scientific Energy Systems, Inc., in 1977 and through continued boiler and

advanced expander research, includes over 5000 steam engine hours at the above steam conditions. Overall, perhaps 10,000 steam engine hours at these conditions have been accumulated by several research and development firms.

A conservative 20 psia condenser back pressure was selected so that noncondensable gases could be simply vented by a steam trap without a vacuum pump.

A detailed heat transfer design analysis of the boiler for the given diesel exhaust conditions and water/steam conditions yielded an 88 percent boiler efficiency for a 50°K (91°F) boiler pinch point. The rate of steam production for such a boiler was determined to be 239 kg/hr (526 lbm/hr).

The optimum dimensions for a single cylinder expander for the given steam conditions, piston speed limit of 4.06 m/s (800 fpm) and 199 rad/s (1900 rpm) engine speed are a 0.147m (5.77 in) bore and a 0.064m (2.5 in) stroke. This is an oversquare cylinder configuration with a bore to stroke ratio of more than 2:1. FMI's experience and documented steam expander performance data, however, have been obtained with square cylinder configurations, i.e., bore equal to stroke. While the trends in efficiency resulting from this difference in geometry can be estimated, the results cannot be confirmed by available experimental data.

In order to maintain our conservative approach to the preliminary design and evaluation of the steam Rankine bottoming system, a dual cylinder expander was adopted. In this configuration the steam flow from the boiler is divided between two identical expander cylinders, each with a bore and stroke equal to 0.089m (3.5 in). The major dimensions of these cylinders are then identical to those of the single cylinder expander extensively tested by FMI for an EPA/ERDA program.

Since the stroke assumed for the preliminary design expander is greater than that required for the previously assumed piston speed limit, a somewhat higher piston speed of 5.64m/s (1110 ft/min) at 199 rad/s (1900 rpm) will result. This is well within the range of acceptable practice. While the expander performance model projects a significant reduction in overall expander efficiency with the change from a single to dual cylinders, the dual expander performance predicted using the efficiency models previously described corresponds fairly well to actual documented performance of the EPA/ERDA test cylinder as illustrated by Figure 15.

The discrepancies between the actual data points and predicted performance curves appear to be related to speed.

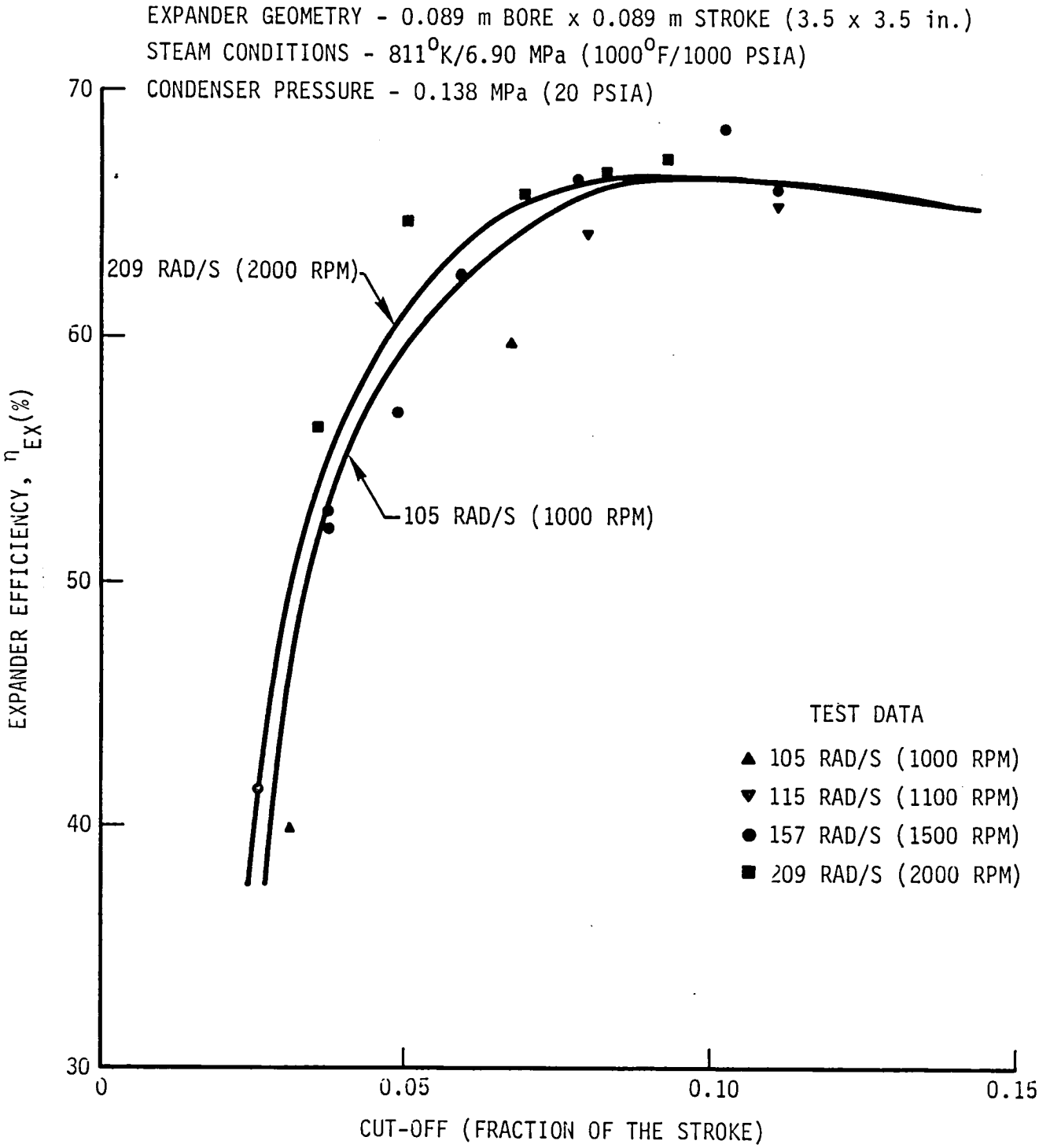

Figure 15. - Actual expander performance compared to expander performance model predictions.

The performance is overestimated at the low end and is underestimated at the high end of the expander speed range. Thus the actual expander efficiency for dual cylinders is expected to be somewhat higher than the model predicts at the full speed of 199 rad/s (1900 rpm).

In addition, the steam flow admitted to the cylinders at full speed and full throttle requires a 0.10 cut-off which is consistent with achieving optimum performance as demonstrated by the experimental data. Thus the expander design proposed is conservative by analysis and well supported by actual data.

Since steam expander performance at these conditions is well documented, the overly conservative expander model efficiency of 65 percent was rejected in favor of the 68 percent efficiency projected from the actual measured output as illustrated in Figure 15.

The baseline steam bottoming cycle is represented in the temperature-entropy diagram of Figure 16. The difference between the actual and ideal cycles is due to expander inefficiencies as previously discussed and pressure losses in the boiler and condenser.

The net bottoming cycle output for the preliminary design system is 42 kW (56.0 hp) assuming ram air cooling and the condenser fan declutched. Given the TC diesel's 236 kW (317 hp) a total combined output of 278 kW (373 hp) results. This represents a 17.7 percent increase in power which is equivalent to a 15 percent reduction in specific fuel consumption.

Figure 17 is the schematic and process flowsheet for the design system. The system components with brief descriptions are listed in Table 7. More detailed component descriptions are presented in following report sections.

Figure 18 is an overall scale layout of the system wherein the expander output is coupled to the diesel with a chain drive into the end of the transmission. A simpler arrangement, if chassis space is available, would have the expander coupled to the crank nose.

Total installed weight is estimated at 254 kg or 6.0 kg/kW (560 lb or 10 lb/hp). The boiler would replace the normal muffler function for some additional installed weight reduction.

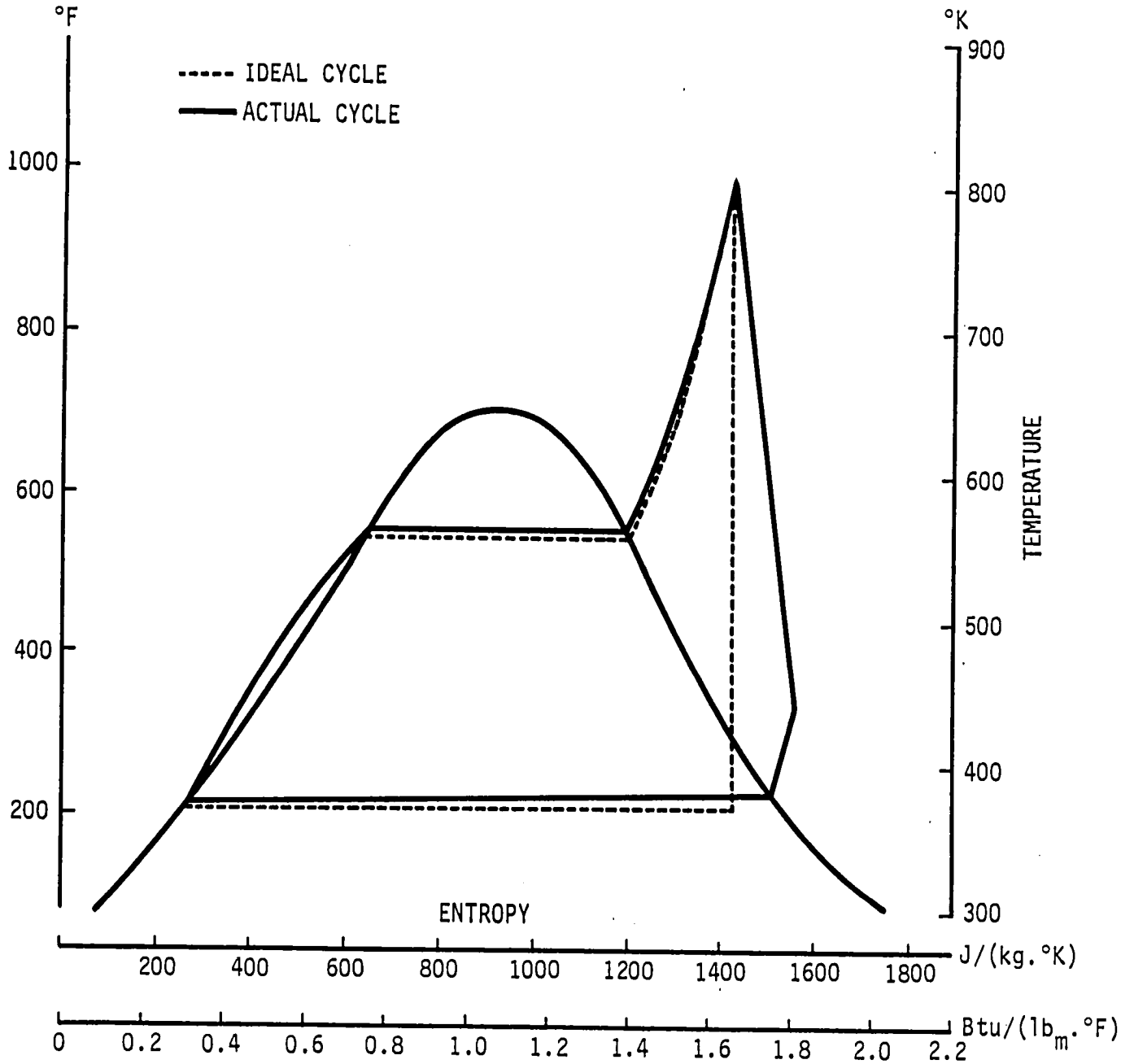

Figure 16. - Temperature-entropy diagram for baseline steam bottoming cycle.

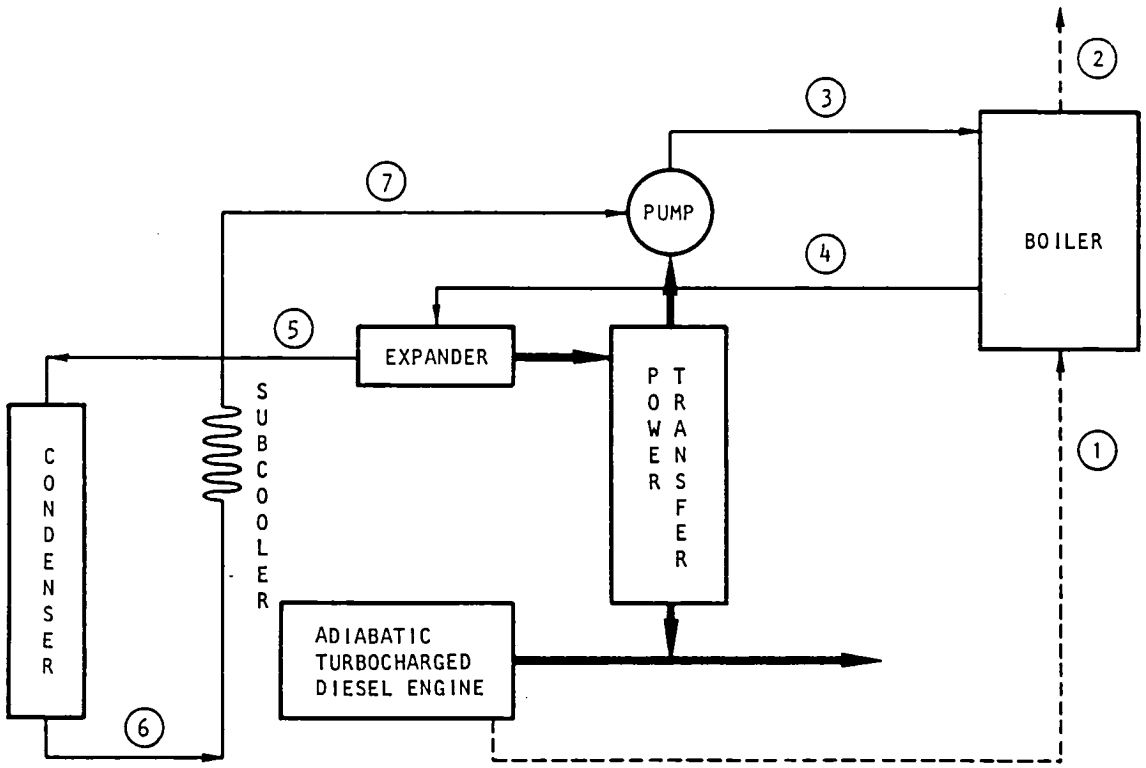

	Diesel Exhaust Gas		Water/Steam				
Point Number	(1)	(2)	(3)	(4)	(5)	(6)	(7)
SI Units							
Flow rate, kg/hr	1306.	1306.	239.	239.	239.	239.	239.
Pressure, MPa	0.102	0.101	7.41	6.90	0.138	0.138	0.103
Temperature, ^{o}K	944.	485.	371.	811.	442.	382.	371.
Standard Units							
Flow rate, lb/hr	2880.	2880.	526.	526.	526.	526.	526.
Pressure, psia (in. H_2O, abs)	(411.)	(407.)	1075.	1000.	20.0	20.0	15.0
Temperature, ^{o}F	1240.	413.	209.	1000.	336.	228.	208.

Figure 17. - Steam bottoming system schematic and process flowsheet.

TABLE 7. - SYSTEM COMPONENTS

Component	Description
Expander	V-twin, 89 mm (3-1/2 in.) bore and stroke, 199 rad/s (1900 rpm), oil lubricated.
Feedwater Pump	Two cylinder, solenoids on intake valves for flow control.
Boiler	Clad fins on stainless tubes, 52 kg (114 lb) tube bundle, 0.001 MPa (4 in. H_2O) gas side loss.
Condenser	0.79 m^2 (8.5 ft^2) frontal area, typical truck core, ram cooled above 64.4 km/hr (40 mph), with shutters, fan, subcooler and oil cooler.
Other	Sensors, controls.

Boiler Design

The boiler analysis previously described has resulted in a compact, efficient unit which is easy to fabricate and maintain. A detailed drawing of the baseline system boiler is shown in Figure 19. The flow arrangement is "cross" - counterflow with warm water entering at the top of the boiler and following a spiral path as it moves from pass to pass. Pass connections are made with unfinned loops, as shown in view A-A of the drawing. The darkened arrows show the water flow path. Steam exits at the bottom of the boiler and moves on to the expander.

The hot gas flows in the direction opposite that of the water. It follows a path of decreasing flow area, maintaining high velocities as it cools.

A key feature of the boiler design is the conical structure which allows simple, mandril-wound fabrication, and provides a diminishing gas flow area. The latter means that high gas-side velocities are maintained, even as the gas cools, thus enhancing heat transfer characteristics. The design also features close-packing wherein adjacent coils (passes) are nested together for maximum gas-metal contact, which again enhances heat transfer and minimizes surface area requirements.

The tube passes are mechanically fastened at the inner core to a series of slotted roll formed channels. These hold the

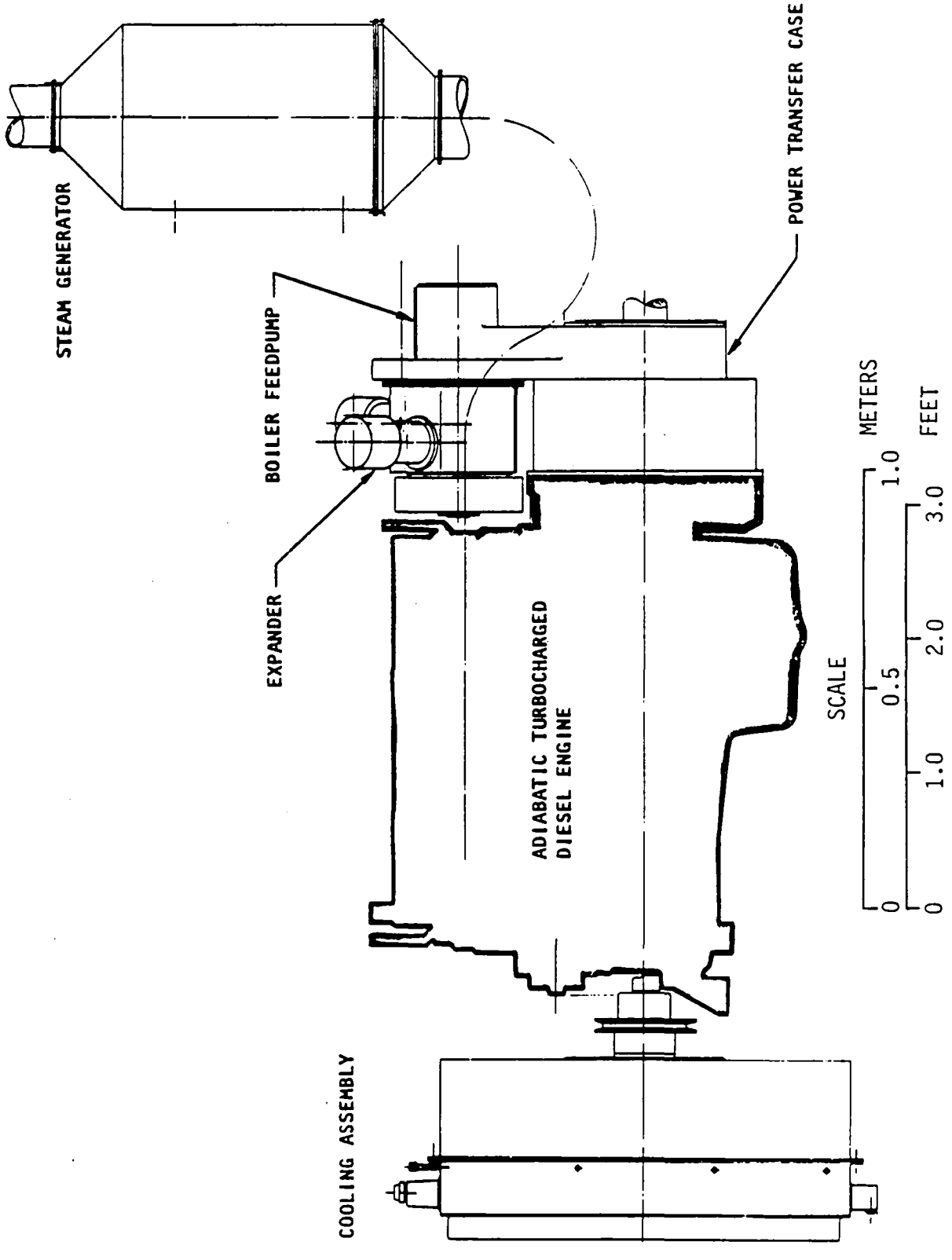

Figure 18. - Baseline steam bottoming system layout.

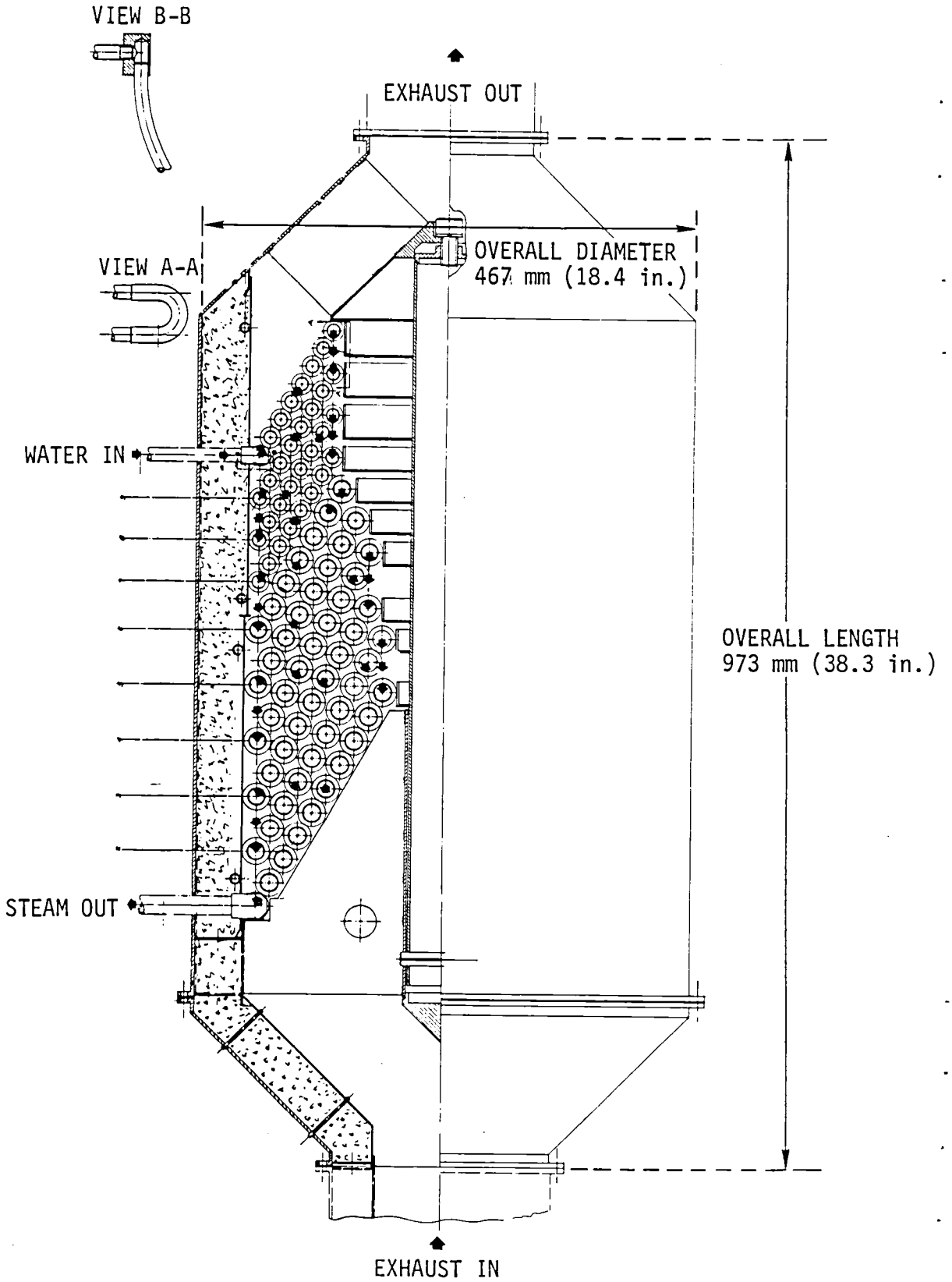

Figure 19. - Baseline boiler configuration.

tubes in place, yet are flexible enough to accommodate expected thermal expansions and contractions.

The tube bundle is then wrapped with a sheet metal cylinder that is split and overlapped to accommodate thermal expansion. This cylinder is held in place by a series of garter springs, wrapped in high temperature insulation, and encased in wire mesh. The entire assembly is then housed in a metal shell.

When assembled the boiler is a relatively monolithic structure. Because of the distributed nature of the many attachment points, the assembly is resistant to shock and vibration. There are no lumped masses connected by long members which can excite destructive oscillations. The housing is arranged so that the tube assembly can be easily removed for repair or replacement. All that is required is the removal of the bolts attaching the tube assembly inner support cylinder to the main assembly and unthreading of the water and steam connections detailed in view B-B. The bottom housing piece can then be disconnected at the flange and removed, and the tube assembly will slide out.

The ten conical passes of stainless steel tubes are finned with carbon steel ribbon brazed/coated with nickel-chromium alloy. Stainless steel tubes provide good oxidation and corrosion resistance, and thus can accommodate variations in water quality. Carbon steel fins with their higher conductivity provide better thermal performance at lower cost, than stainless steel. The nickel-chromium cladding is a brazing process that will provide improved gas side corrosion and oxidation resistance at temperatures up to 1089^{o}K (1500^{o}F). Thus the fins will not be damaged when the boiler is run dry for self-cleaning. This boiler feature will be discussed in more detail later in this report. The cladding also ensures good fin/tube contact for improved heat transfer and a smooth fin/tube interface.

A summary of the boiler design characteristics is presented in Table 8.

Expander Design

The baseline steam expander illustrated in Figures 20a and 20b is a single expansion piston type with two cylinders. The twin cylinders are arranged in a 90^{o}-V for optimum utilization of space and have a bore and stroke of 89 mm (3-1/2 in.). The overall expander volume is approximately 533 mm high by 610 mm wide by 406 mm deep (21 x 24 x 16 in.).

TABLE 8. - BASELINE BOILER SPECIFICATIONS

10 passes
Stainless steel tubes
Carbon steel fins
Nickel chromium cladding
Overall diameter - 467 mm (18.4 in.)
Overall length - 973 mm (38.3 in.)
Tubing weight - 52 kg (114 lb)
Total weight - 75 kg (165 lb)
Heat transfer area - 18.6 m^2 (200 ft^2)
ΔP_{GAS} - 0.001 MPa (4 in. H_2O)
ΔP_{steam} - 0.517 MPa (75 psi)
Gas flow - 1306 kg/hr (2880 lb/hr)
Steam flow - 239 kg/hr (526 lb/hr)
Stack temperature - 485°K (413°F)
Steam temperature - 811°K (1000°F)
Heat transfer rate - 204 kW

The expander has a uniflow configuration in which steam is admitted near top dead center (TDC) of the stroke and is exhausted through ports in the liner at the bottom of the cylinder. This configuration has better demonstrated performance than a counterflow configuration which has both admission and exhaust ports in the cylinder head. A cam and poppet valve train with one fixed cutoff poppet intake valve per cylinder is used to control steam admission to the cylinders. Oil lubricated plain bearings and hard coated piston rings follow prior practice and were selected here due to low cost and good durability characteristics.

Power transfer between the expander and the diesel is through a clutch and then by high velocity chain to the diesel output shaft as illustrated by Figure 21. The hydraulic clutch would be used for startup and as a disconnect should the bottoming cycle fail. A one-to-one match between the expander and diesel shaft speeds results in a modest piston speed of 5.6 m/s (1100 fpm).

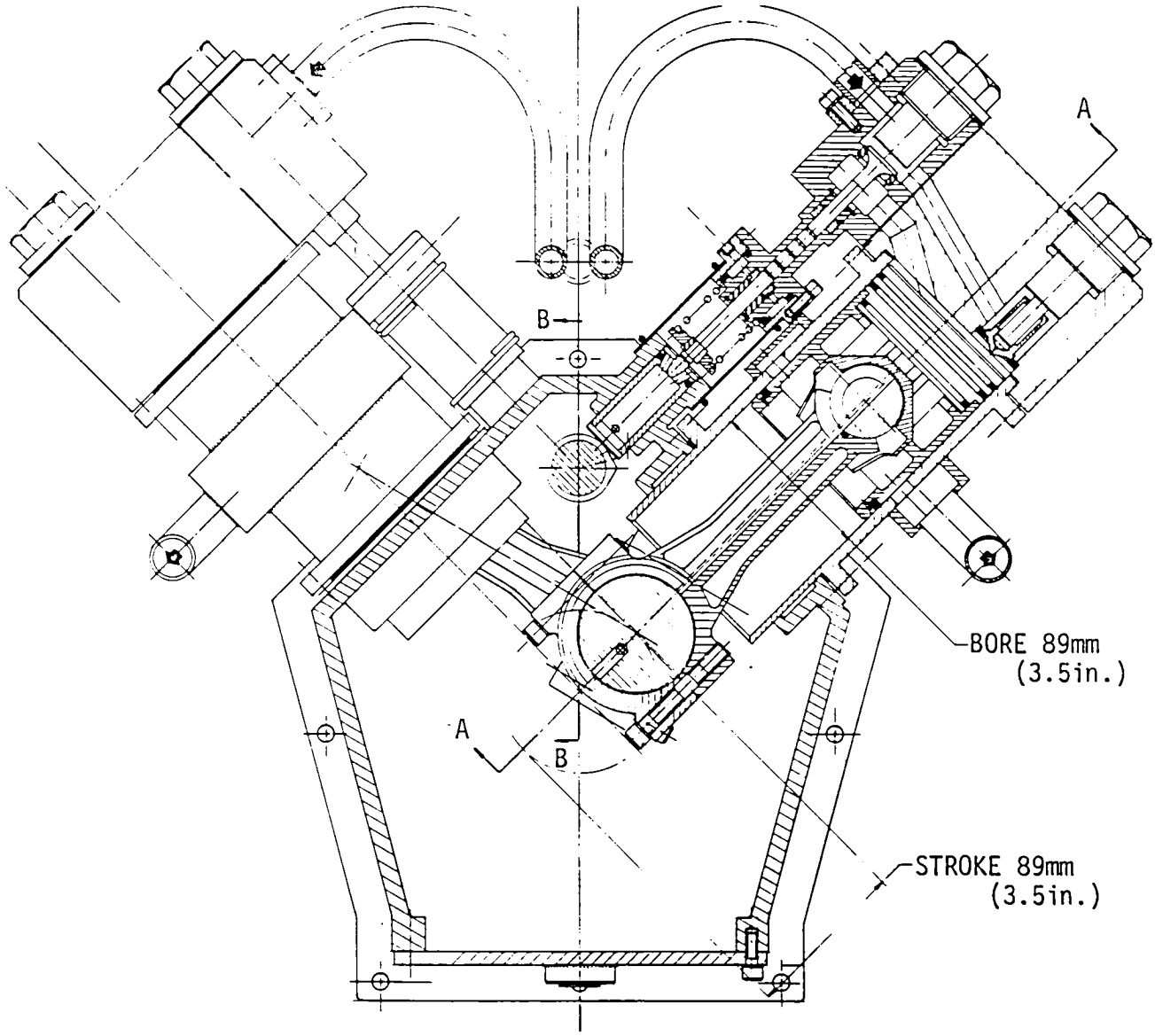

Figure 20a. - Baseline steam expander configuration.

The following materials selections for the expander components were dictated by prior experience and are compatible with current fabrication technology:

- Cast iron crankshaft and crankcase.
- Cast stainless steel or perhaps cast high alloy iron head.
- Stellite-faced valve and seat.
- High alloy iron piston and liner.
- Triballoy ring and cylinder coating.

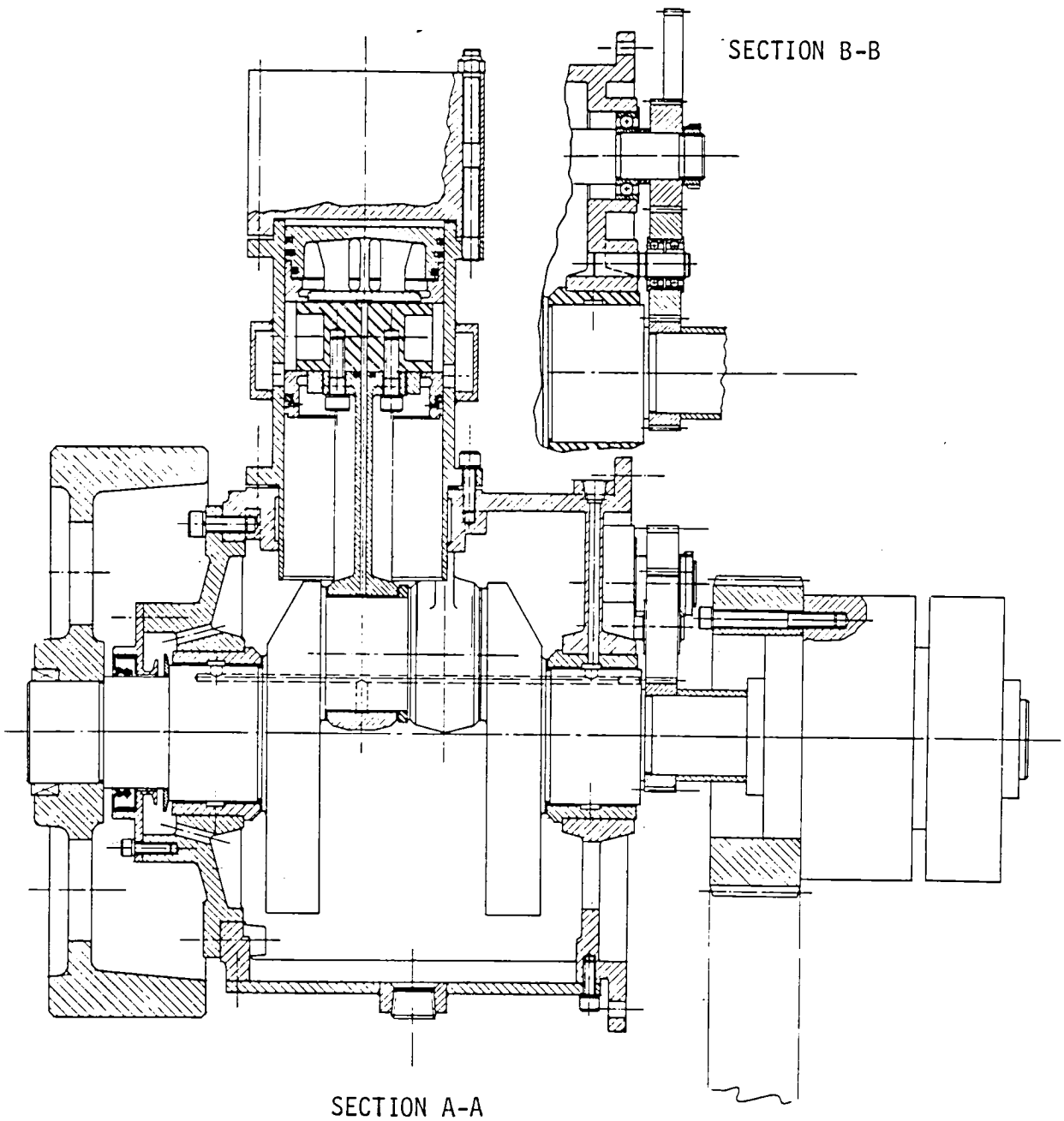

Figure 20b. - Baseline Steam Expander Section Views.

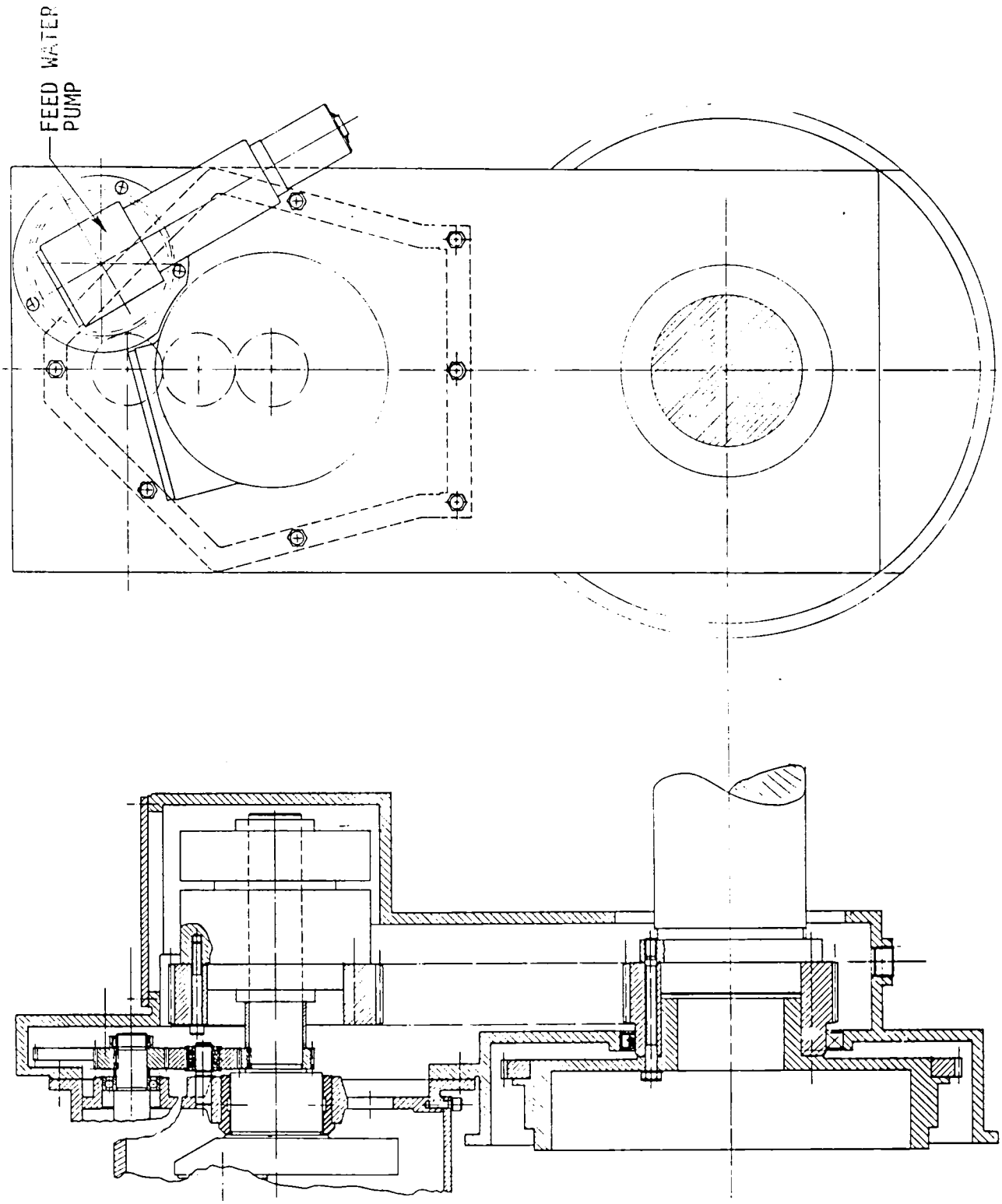

Figure 21. - Baseline power transmission configuration.

Since the general expander configuration is similar to that of other reciprocating engines, all components could be made with conventional tooling.

The baseline steam expander characteristics are summarized in Table 9.

TABLE 9. - BASELINE EXPANDER SPECIFICATIONS

90^{o} V-twin expander
Bore = 89 mm (3.5 in.)
Stroke = 89 mm (3.5 in.)
Total displacement = 1104 cm^3 (67.4 $in.^3$)
Expander speed = 199 rad/s (1900 rpm)
Piston speed = 5.6 m/s (1100 fpm)
Clearance = 0.066, fraction of stroke
Cut off = 0.100, fraction of stroke
Exhaust = 0.130, fraction of stroke
Approximate weight = 63 kg (140 lb)
Efficiency = 68.2 percent
Shaft output = 42.4 kW (56.8 hp)

Cooling Assembly Design

The baseline cooling assembly is illustrated in Figure 22. The assembly is composed of a condenser with shutters, fan, subcooler, and oil cooler. The condenser is a typical truck radiator design. The condenser core is a standard flattened tube, sheet fin assembly with a shallow bottom header. The fan and shutters are standard catalogue items, and the subcooler and oil cooler are simply specific lengths of readily available finned tubing arranged for cross flow cooling by means of the fan or ram air stream. Thus no extraordinary expenses are associated with the cooling system requirements for a steam bottoming cycle.

Condenser pressure (hence temperature) actuated shutters in front of the condenser control the cooling air flow. The high efficiency fan is driven through a thermostatic clutch by a pulley on the diesel. Since the condenser is designed for complete ram air cooling above 64.4 km/hr (40 mph) the fan normally free wheels while driving. The variable slip fan drive will provide for complete condensing of the steam even at full load at low vehicle speeds where the fan input could approach 3 kW (4 hp). A condensate subcooler and expander and diesel engine oil coolers are placed between the condenser core and the fan. The subcooler serves to insure noncondensible purging from the condenser and to protect the pump against cavitation.

Other cooling assembly operating characteristics and features are discussed in the report section titled Freeze Protection Research. Cooling assembly specifications are summarized in Table 10.

Feedwater Pump Design

The feedwater pump selected for the steam bottoming cycle system was a pump previously developed during the automotive steam engine program. The pump requirements for the steam bottoming cycle are identical to those established for the steam car system except for maximum flow rate. These requirements are:

- The ability to pump pure water (deionized - no lubricants).
- Maximum delivery pressure of 8.3 MPa (1200 psia).
- Maximum water temperature of 394^{o}K (250^{o}F).

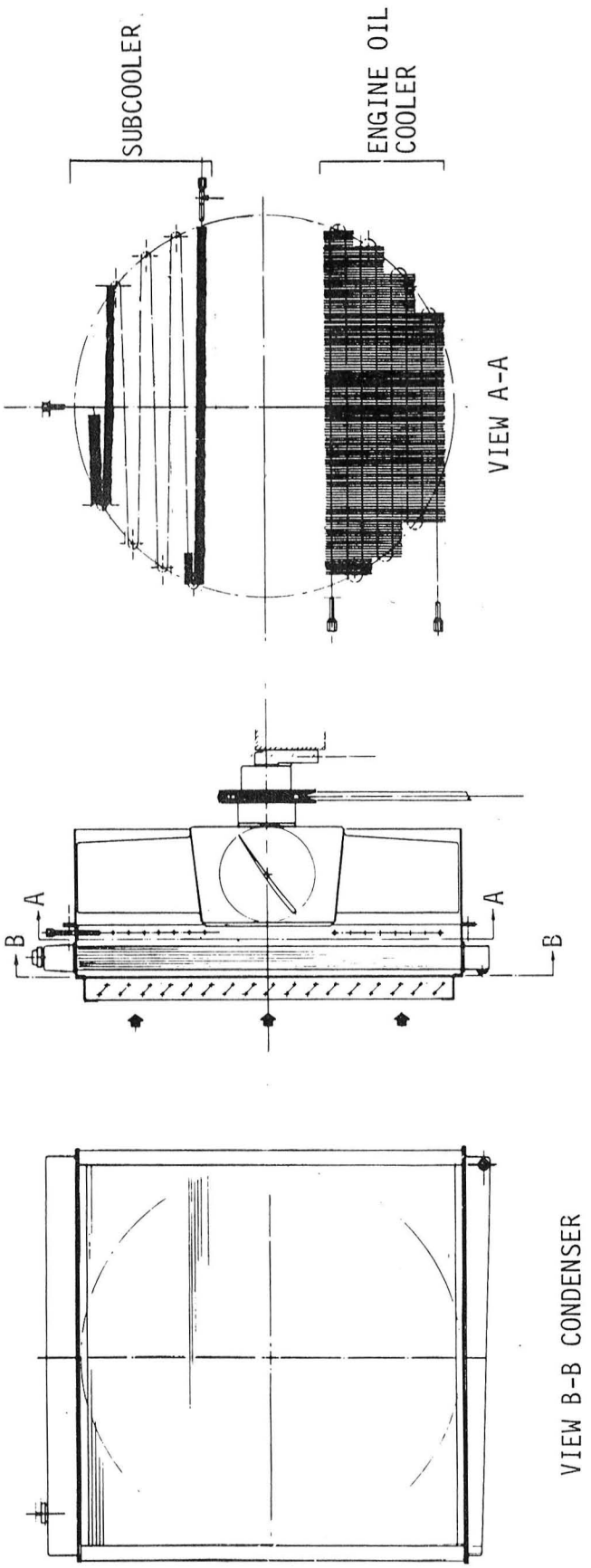

Figure 22. Baseline cooling assembly configuration.

TABLE 10. BASELINE COOLING ASSEMBLY SPECIFICATIONS

CONDENSER - STANDARD RADIATOR CORE		
Dimensions	=	1016x1016x38 mm (40x40x1.5 in.)
Frontal Area	=	0.79 m^2 (8.5ft^2)
Heat Transfer Area	=	23.2 m^2 (250 ft^2)
Weight	=	45 kg (100 lb)
SHUTTERS		
Dimensions	=	1016x1016x51 mm (40x40x2 in.)
FAN		
Diameter	=	0.91m (36 in.)
Peak Fan Power	=	3.4 kW (4.5 hp)
SUBCOOLER		
Tubing	=	9.5 mm (3/8 in) OD, 343 fins/m (8.72 fins/in.)
Length of Finned Tube	=	6.1m (20 ft)
Frontal Area	=	0.16 m^2 (1.75 ft^2)
Weight	=	2.7 kg (6 lb)
OIL COOLER		
Tubing	=	9.5 mm (3/8 in.) OD, 343 fins/m (8.72 fins/in.)
Length of Finned Tube	=	4.9m (16 ft)
Frontal Area	=	0.13 m^2 (1.4 ft^2)
Weight	=	2.3 kg (5 lb)
TOTAL ASSEMBLY		
Weight	=	79 kg (175 lb)

- Low NPSH capability.
- Size suitable for packaging in an automotive system.
- Self priming capability.
- Drainability for freeze protection.

During the automotive program, two commercial pumps were tested and found to be unsuitable as delivered. Several modifications, primarily of seals and valves, to the most promising unit were made until exceptional performance was obtained and all pump requirements were met. The pump development program and results are well documented in reference (8).

The baseline feedwater pump, modelled after the steam engine feed pump discussed above, is illustrated in Figure 23. It is a fixed positive-displacement two-piston in-line pump, with eccentric operated pistons and positive piston return (no springs). The pump weight is approximately 4.1 kg (9.0 lb) with overall dimensions of 76x257x277 mm (3.0x10.1x10.9 in.). Precision heavy-duty ball and roller bearings are on the driveshaft and eccentrics, and the entire piston actuating mechanism is oil immersed in a sealed case located above the pumping section. The inlet valves and passages to the pump were carefully designed to result in a very low NPSH capability, approximately 0.6m (2 ft) water head at maximum required water flow.

The feedwater pump is driven directly off the expander in a 1:2 speed ratio, as illustrated in Figure 23. Flow control is accomplished by unloading solenoids that keep the intake valves open. Each of the pump cylinders is separately controlled by modulating the fraction of time (pulse width modulation) during which its intake valve is unloaded, resulting in an efficient and smooth water flow modulation technique.

Baseline feedwater pump specifications are listed in Table 11. Pump features which protect against freeze damage are discussed in the Freeze Protection Research section of this report.

Miscellaneous Bottoming Cycle System Components

Other components in the bottoming cycle system include a shutdown drain and freeze proof sump system, make-up water demineralizer cartridge and a controls/diagnostics package based on the running control and trips and instrumentation schematics of Figures 24 and 25. The proposed control system is based on a digital microprocessor and will be a rugged

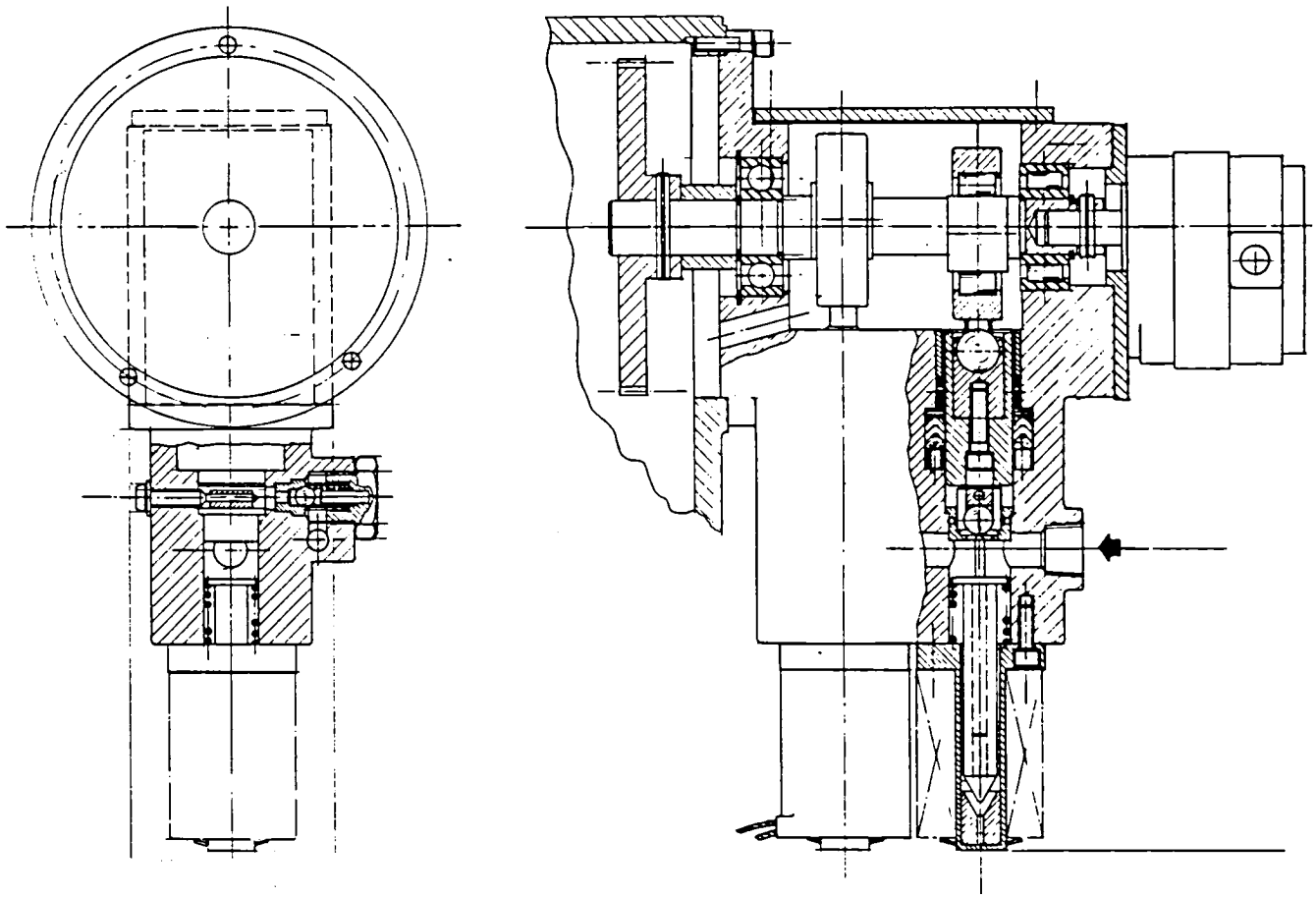

Figure 23. Baseline feedwater pump configuration.

TABLE 11. BASELINE FEEDWATER PUMP SPECIFICATIONS

Configuration - Fixed displacement, two cylinder in line
Bore - 25.4 mm (1.0 in.)
Stroke - 2.4 mm (0.095 in.)
Shaft Speed - 100 rad/s (950 rpm)
Output Pressure - 8.27 MPa (1200 psia)
Output Flow - 0.14 m^3/hr (0.6 gal/min)
Weight - 4.1 kg (9.0 lb)

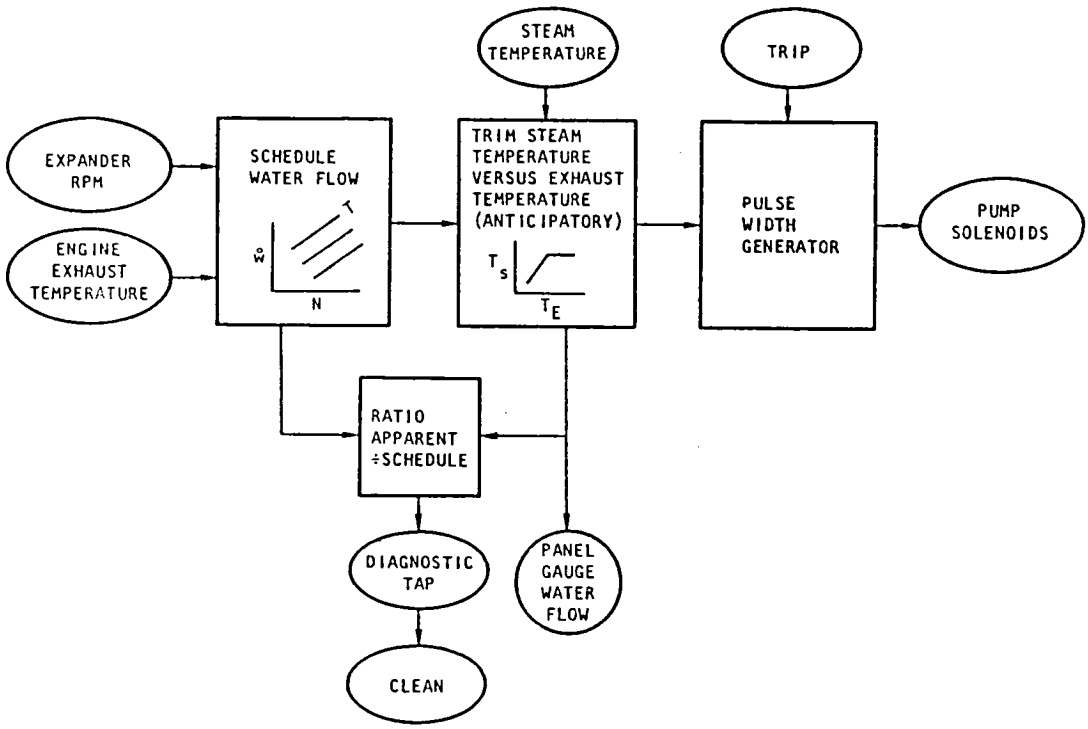

Figure 24. Running control system.

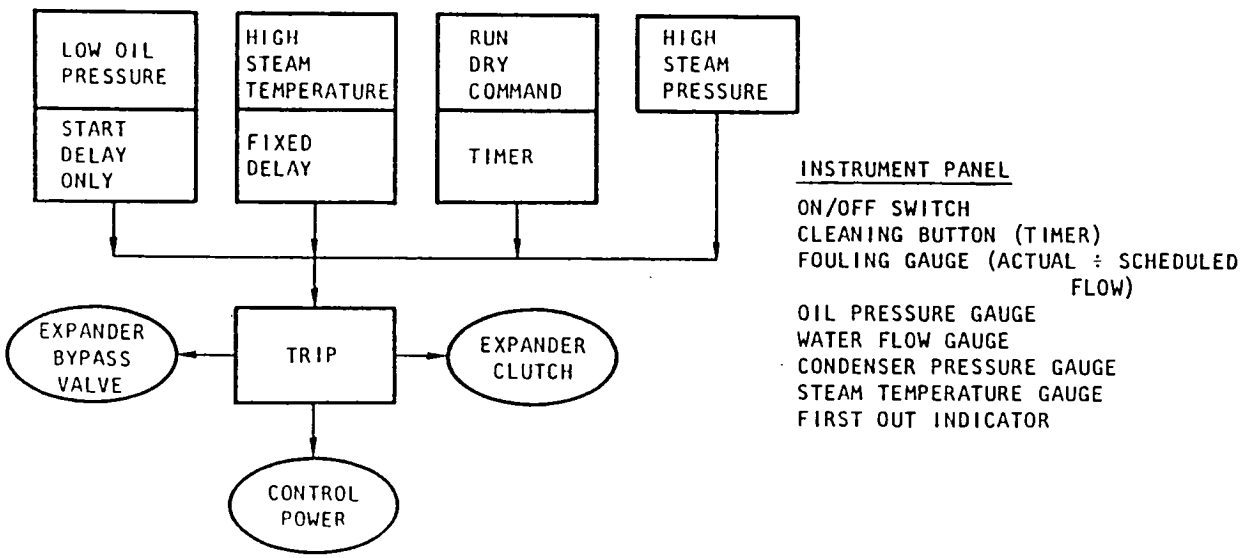

Figure 25. Trips and instrumentation schematic.

package to survive the road environment. Ceramic integrated circuits, quality connectors, double sealed package, isolated input/output and automotive grade sensors are typical components required.

The system is designed to be benign in that, if it fails, it would disconnect the expander drive clutch and the boiler would safely run dry. The cooling fan for the diesel engine oil cooler would still be driven by the diesel.

Advantages of the Steam Bottoming Cycle System

A major advantage of the steam Rankine bottoming cycle system is that its working fluid, water, will not decompose at diesel exhaust temperatures like various candidate organic fluids. An emergency boiler bypass or other overheating protection devices or strategies are not required. In fact, when water is used in the bottoming cycle, the boiler can be self-cleaned by running the diesel for a few minutes with no water flow.

There is a strong tendency for finned-tube boilers in exhaust gas streams to accumulate soot deposits. These deposits tend to decrease heat transfer and increase gas-side pressure drop. If allowed to accumulate for long periods they will cause serious tube degradation, and eventual failure.

In testing a finned tube boiler for similar service, Thermo Electron Corp. found that performance deteriorated by as much as 30 percent after only 100 hours of operation (9). In that case, an organic fluid, rather than steam, was used and run-dry cleaning was not possible due to potential decomposition of residue organic fluid in the tubes.

With a steam system, water flow can be halted, while the engine is running. The expected peak gas temperatures of 1200° to 1400°F will not harm the tube materials.

The ability of a boiler to be self cleaning is a function of the gas temperature and to a lesser extent gas velocity. In a study of gas side steam generator fouling prepared for the U.S. Navy, Solar Turbines International concluded that "the threshold temperature for self-cleaning lies between 670° to 785°F" or 628° to 692°K (10). The mechanisms by which cleaning occurred were:

- Some flaking off of loose soot formations, but predominantly
- Oxidation of the formations, which reduced the bonding strengths of the deposits.

Vaporization was not found to be a factor since tests run with inert gases showed no self-cleaning even at elevated temperatures. The time it takes to effect a complete cleaning of the tubes is difficult to quantify but is strongly a function of temperature. In one test raising the gas temperature from 700° to 747°K (800° to 885°F) decreased cleaning time from 6-1/2 to 1 hr. In another test, with a gas velocity of 50.3 m/s (165 ft/s), and a temperature of 739°K (870°F), the tubes were completely cleaned, and performance restored in 12 min. In the current application, with temperatures up to 922° to 1033°K (1200° to 1400°F), it is safe to assume that cleaning would occur fairly rapidly.

In addition to providing for the only simple boiler cleaning method, water is a safe cheap fluid. The steam system is non-hermetic and can easily be protected from damage by unclutching the system upon failure. Due to its standard component configurations the system can be serviced by a diesel mechanic. And finally good performance over typical speed and load ranges is expected .

The only potential drawback to a water-based bottoming cycle is possible damage to system components due to freezing. This concern is addressed as shown in the following report section.

FREEZE PROTECTION RESEARCH

Since water expands upon freezing, there is potential for steam bottoming system damage when the vehicle is left idle for a long period at ambient temperatures below 273°K (32°F). Prior testing of freeze management strategy for the earlier steam car program led to pump and sump designs which protected against freeze damage. These early tests also demonstrated that the feedwater pump selected for the bottoming system, even in a 244°K (-20°F) cold soaked system, would self-prime with 3.7m (12 ft) of lift and run if fed with 294°K (70°F) water. The layout for the original steam car freeze tests is represented in Figure 26.

Additional freeze protection tests were conducted for the current contract to identify boiler conditions which would result in freeze damage and to verify that a conventional truck radiator core would drain to prevent freeze damage and restart cold without ice plugging. A truck radiator shutter in front of the condenser was also tested in a refrigerated wind tunnel to demonstrate that the condenser could be protected from freezing and that the condenser temperature could easily be controlled.

The recent test procedures and results as well as the freeze management strategy recommendations for the baseline steam bottoming system are discussed in the following report sections.

Boiler Freeze Protection

Freezing is not expected to be a problem for the boiler during system startup or while running since the boiler is in the hot exhaust stream and it can be preheated before cold water from the sump is pumped through it. The only potential for freeze damage will result from ineffective purging of water from the boiler upon system shutdown. Water will be located in the first (top) four passes of the boiler and low quality steam in the next three passes during operation. Because of the spiral wound construction of the monotube boiler, gravity drain down is not feasible regardless of boiler orientation.

Boiler tube freeze tests. - The purpose of the boiler tube freeze tests was to determine the maximum amount of water that can be left in a boiler tube before freeze damage will occur. The test procedure consisted of freezing four sample boiler tubes, each containing a different amount of water. Diametral measurements were made on each tube before and after freezing.

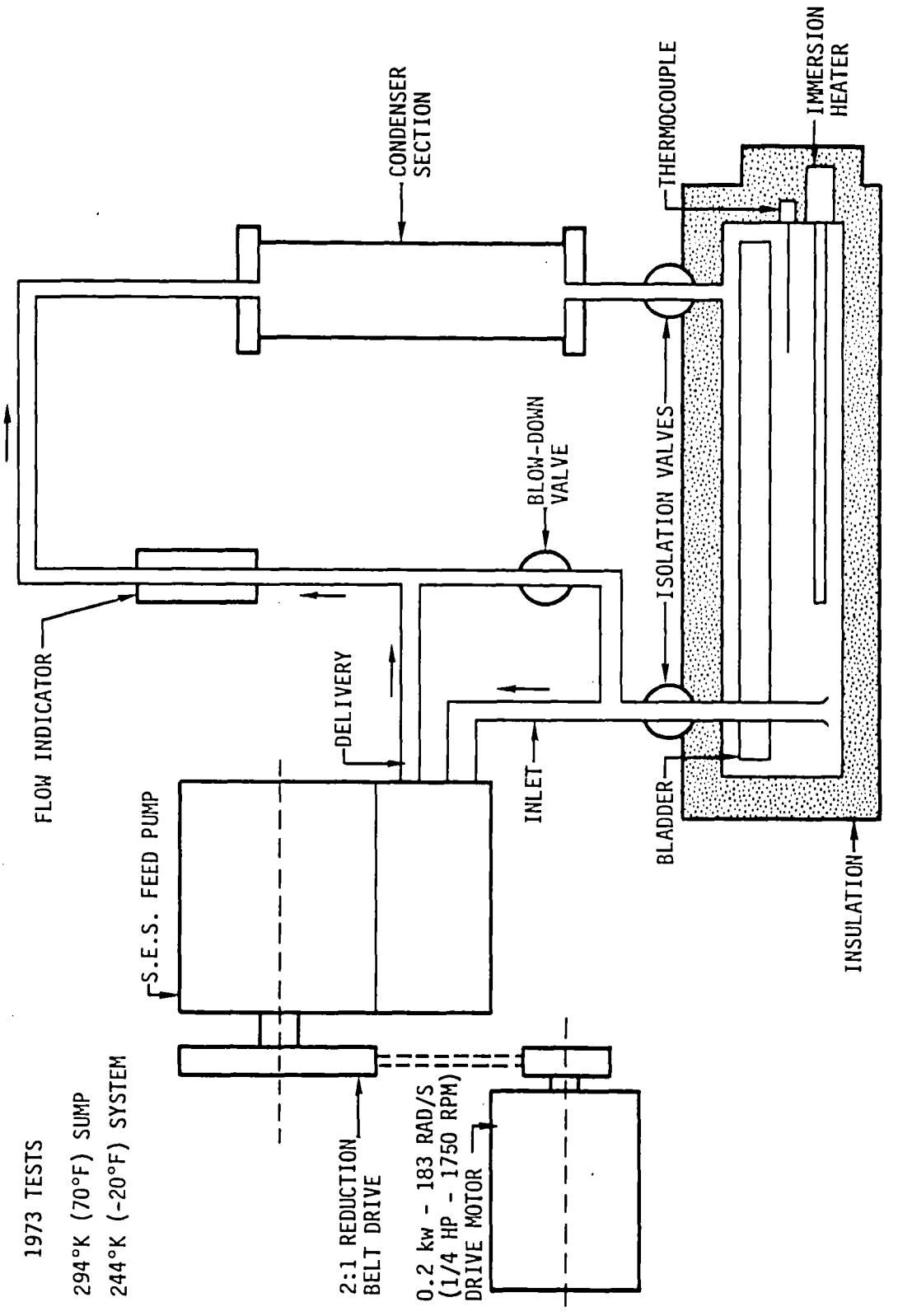

Figure 26. - Layout for steam car system freeze protection tests conducted in 1973.

The test was repeated for six freeze/thaw cycles. 12.7 mm (1/2 in.) diameter soft copper tubing was used. The tubing was bent into a U-shape with an inside diameter of 254 mm (10 in.) (similar to the coil diameter of the baseline system boiler). The tubes were filled with the following volumes of water:

Tube 1 - 3.62 cc (minimum amount of water needed to fill lower bend of U)

Tube 2 - 2.77 cc (3/4 of volume in Tube 1)

Tube 3 - 1.81 cc (1/2 of volume in Tube 2)

Tube 4 - 43.4 cc.

Tube 4 was purposely filled considerably higher than the other sample tubes to simulate boiler blowdown failure.

The test measurements from boiler tube freeze tests are presented in Table A-1, Appendix A.

Allowing for measurement error, etc., Tubes 1, 2, and 3 showed no effect from freeze/thaw cycling when they contained small amounts of water since adequate room for expansion existed. Tube 4 showed noticeable deformation after the second freeze cycle (date - 6/10). This deformation was severe enough to permanently set the tube at new dimensions. A second deformation was noted in subsequent freeze cycles suggesting eventual failure of the tube was likely. Tube 3 was filled with an equal amount of water as Tube 4 halfway through the test sequence (6/21 at 11:15 a.m.). A significant deformation was noted in Tube 3 in the next freeze cycle.

These freeze tests showed that tube deformation will only occur in tubes containing a large amount of water.

Boiler freeze protection strategy. - Although the thermal energy stored in the boiler mass is theoretically enough to boil the boiler dry, the recommended boiler shutdown approach is to open a bypass to the sump downstream of the pump and allow high pressure steam to blow water back through the boiler. In this fashion, only small amounts of water will be left in the boiler. This procedure is supported by prior experience. Hot but unfired boilers similar to the baseline boiler have been left apparently dry after being vented to the condenser. On occasion these boilers were subsequently frozen and refired without purging with no perceptible boiler damage.

Also in the event that some inappropriate operating procedure or control failure leaves the boiler full of water, cranking the expander will also pump out the water.

Expander Freeze Protection

The expander will not see a significant amount of water after shutdown of the system. Only superheated steam is contained in the expander during operation. Condensing of the contents of the expander will amount to only a small amount of liquid. Subsequent freezing should not pose a problem.

During cold startup, condensation of steam in the supply piping, accumulator, and expander cylinder may present a problem if the amount of liquid is enough to form a slug in the cylinder. Damage to valves, connecting rods, etc., is possible. Preheating of the supply piping, accumulator and cylinder heads with exhaust or engine oil may be advisable.

Condenser Freeze Protection

The greatest threat of freeze damage to the condenser exists while the bottoming cycle system is operating.

If condensing is left uncontrolled in cold weather, freezing of condensate within the tubes is possible. Because the condenser is oversized under these conditions, complete condensation occurs before the end of the condenser tubes. The condensate film provides little heat to the tube surface. Tube surface temperatures can approach air temperature. If air flow is uncontrolled, ice formation inside the tubes is possible.

Startup and shutdown freeze problems for the condenser are related. Water left in the condenser at shutdown can freeze and cause tube blockage. Surface tension effects inside the condenser tubes can contribute to the formation of a meniscus which alone may freeze and block the condenser tubes. If melting of this ice is not accomplished during startup, tubes can fill with condensate and freeze.

Cold chamber testing of an air-cooled condenser was conducted to evaluate the severity of the problems mentioned above. The test layout is illustrated in Figures 27 and 28. An automobile radiator was used as the test condenser. The radiator was placed in a box that was connected to a boiler. Air flow through the box was controlled by a shutter.

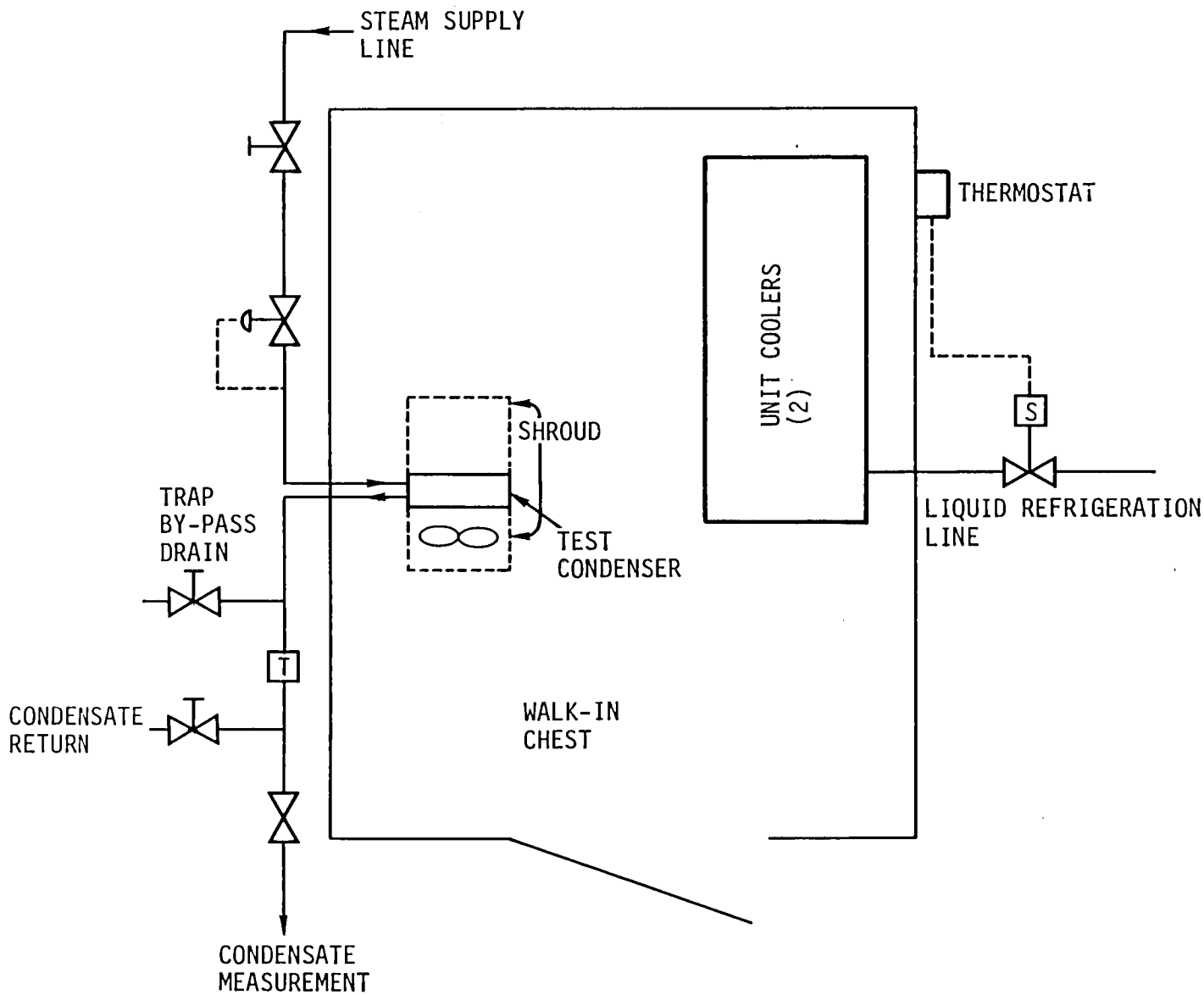

Figure 27. - Condenser freeze test layout.

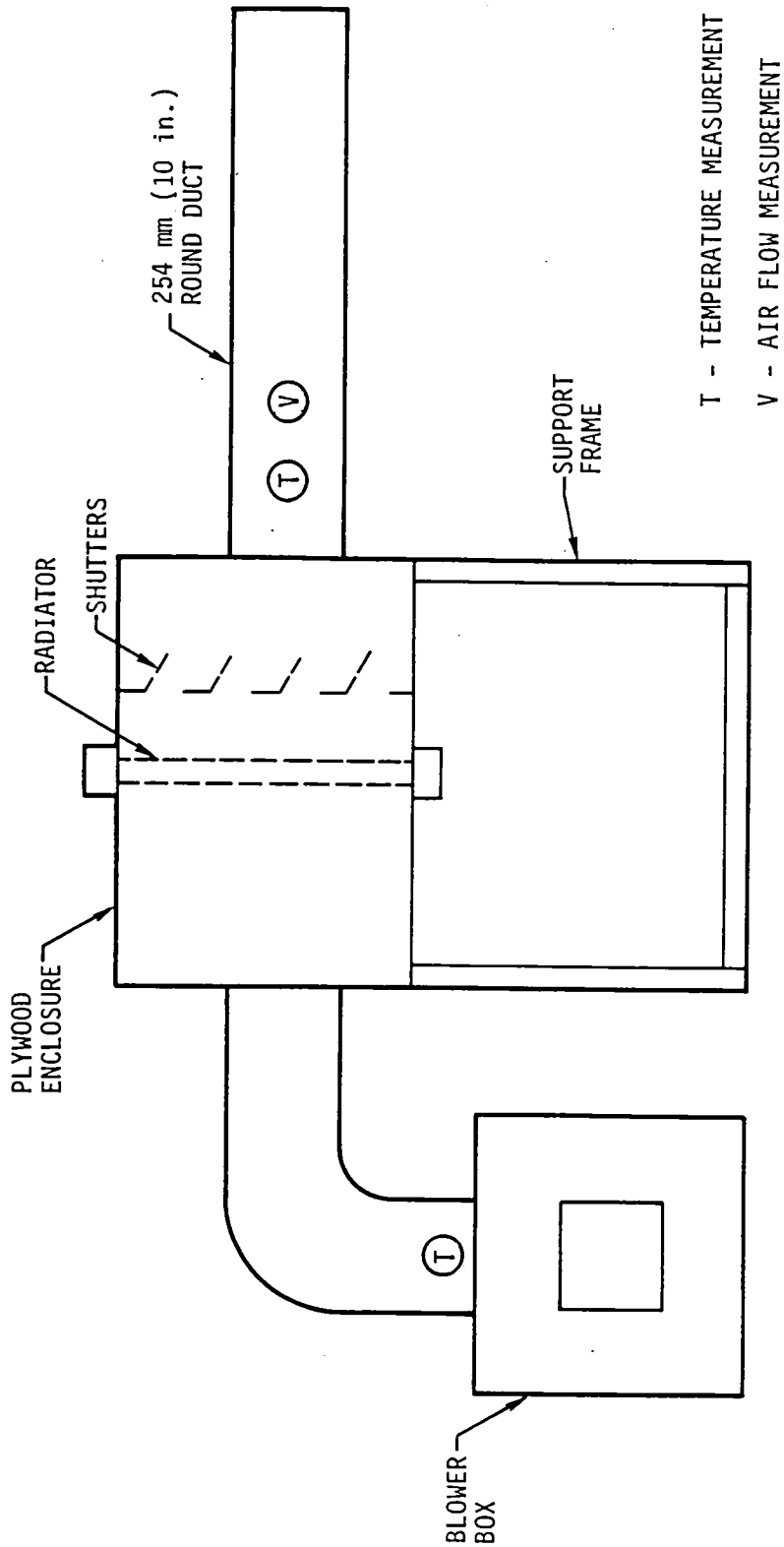

Figure 28. - Freeze protection condenser test rig.

Condensing tests were run in both the continuous mode to evaluate steam condensing control problems and startup/shutdown modes to determine whether meniscus formation was a significant freezing problem.

The test condenser was instrumented with thermocouples at the following locations as represented in Figure 29:

- The base of the tubes of the front row (4 tubes)
- Base of tubes, back row (1 tube)
- Outside surface temperature of front row tubes (three locations)
- Entering air temperature
- Leaving air temperature.

Continuous operation condenser freeze tests. - For the continuous operation tests, it was decided to set the flow rate such that the film thickness of the condensate would be less than or the same as that expected in the full size unit. A film thickness estimate for the full size unit was determined from:

$$t = \text{film thickness} = \sqrt[4]{\frac{4K\mu\Delta TL}{g\rho(\rho - \rho_v)h_{fg}}} \qquad (44)$$

where

K = thermal conductivity of the condensate

μ = viscosity of the condensate

ΔT = temperature difference $T_{condensate} - T_{wall}$

L = Length of the condenser tube

g = acceleration due to gravity

ρ = density of condensate

ρ_v = density of vapor

h_{fg} = latent heat of vaporization.

RADIATOR SPECIFICATIONS
432 x 673 x 33 mm (17 x 26.5 x 1.3 in.)
2 ROWS
30 TUBES
630 FINS/METER (16 FINS/in.)
OVAL TUBES, 11.9 x 2.3 mm (0.469 x 0.09 in.)
FIN LENGTH, 12.3 mm (0.484 in.)

x - THERMOCOUPLES
ADDITIONAL MEASUREMENTS
AIR INLET TEMPERATURE
AIR OUTLET TEMPERATURE
ROOM TEMPERATURE
WEIGHT OF CONDENSATE
AIR FLOW

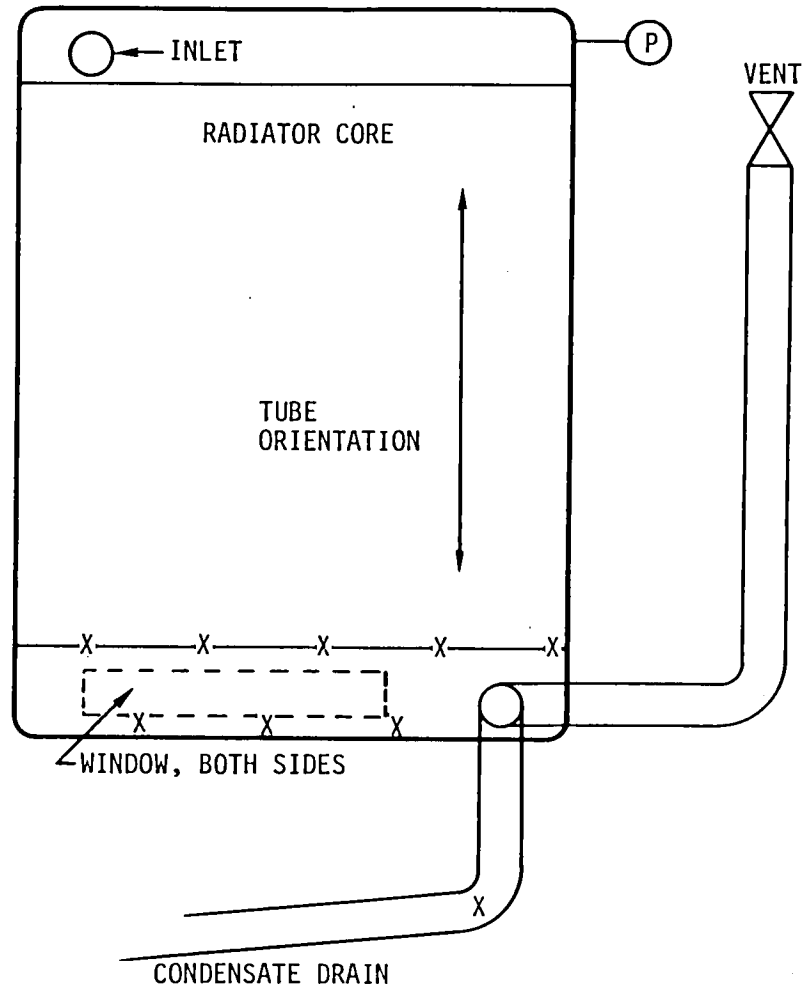

Figure 29. - Test condenser specifications.

For baseline design conditions:

t = 0.109 mm at 2.6 kg/hr/tube

= (0.0043 in. at 5.7 lb/hr/tube).

The test unit flow rate was scaled to the ratio of tube perimeters for test and full size units

$$\frac{P_{test}}{P_{full}} = 0.42$$

Test flow rate = (0.42)(2.6)

= 1.09 kg/hr/tube (2.39 lb/hr/tube)

Since 16 tubes are employed in the test radiator, the maximum test flow rate was 17.4 kg/hr (38.2 lb/hr).

The results of the continuous operation condenser tests, documented in Tables A-2 and A-3 of Appendix A, indicate that potential does exist for tube freezing during continuous operation if air flow rate through the condenser is not controlled during cold weather. It is also obvious that the lowest temperature at which a condenser can operate is a function of the steam flow rate. As flow rate is increased, minimum operating temperature decreases.

Condenser draindown tests. - Two tests were conducted to evaluate whether standard radiator cores drain sufficiently to prevent freeze damage under normal start-up and shutdown conditions and whether an appropriate start-up strategy could be devised.

For the first test, the condenser was run in the continuous mode with 11 kg/hr (25 lb/hr) steam flow for several minutes. The condenser was then shut down and allowed to drain. The meniscus of water remaining in the bottom of the tubes was removed from all the tubes in the back row. A total water volume of 1.2 cc (0.073 $in.^3$) or 0.15 cc/tube (0.001 $in.^3$/tube) was collected. Given a tube cross sectional area of 0.18 cm^2 (0.028 $in.^2$), the mean meniscus height was determined to be 0.84 cm (0.33 in.). The cold chamber temperature was then lowered so that the condenser would freeze. The system was then restarted and no problems

were encountered in running the condenser after having been frozen.

For the second condenser draindown test, the steam flow was increased to 20.9 kg/hr (46 lb/hr). The cooling air shutters were opened to maximize airflow and condensation with the test chamber temperature at about 283°K (50°F). The steam flow was then shut down and the room temperature was lowered to 258°K (+5°F) and allowed to remain this way overnight. The next morning, the tube ends were visually inspected. All meniscuses were frozen. At least two of the tubes appeared to have openings in the ice. The steam line was then preheated to remove condensate before the steam was fed to the condenser and the air fan was turned on with the shutters closed. Finally, the steam flow was started. The condenser defrosted instantly. The above test was repeated twice with the same results..

Freeze up of the condenser after draindown does not appear to be a problem. Standard radiators will drain enough to avoid damage. The meniscus height observed was not sufficient to damage the tubes. And in any case, the frozen meniscus will thaw out instantly. To further insure against freeze problems, the condenser could be tilted slightly to minimize meniscus formation or the tube ends could be scarfed at about a 30 deg angle for complete tube draindown.

Condenser freeze protection strategy. - To prevent condenser freeze up when the bottoming system is operating in cold weather, the use of airtight dampers to limit air flow through the condenser is required. Such a shutter would be thermostatically controlled to maintain a given condenser temperature. In addition, bypass of steam from the boiler to the condenser during low steam flow rate situations may be desirable.

The condenser freeze tests indicate that the only strategy required for condenser protection is the use of standard radiator cores and positive control of cooling air to the condenser during cold weather light load operation. Cooling air control is easily accomplished with off-the-shelf thermostatically controlled radiator shutters.

Boiler Feed Pump Freeze Protection

The baseline boiler feed pump design is based on the one developed for the steam car. The concept for protection developed and tested during the steam car program is based on the removal of water from those components which would be

damaged by ice formation and its transference to a container designed to tolerate ice.

Design development. - In the case of the steam car feed pump, the development evolved as follows: initial testing showed that although the major portion of water was drainable, so that no damage from ice formation would occur, enough water remained to block the smaller passages and prevent priming. The problem was a combination of mechanical design and physical orientation. For example, the original valve lifters were too stiff and the solenoids too weak to provide reliable operation. Also, a poorly located passageway prevented gravity drainage. The selection of new solenoids and rearrangement of the passageways provided satisfactory drainage.

The major development problem was to modify the pump so that it would prime itself and pump while in an initially frozen condition. In order to prime, the pump must be able to draw a vacuum, which requires the seals and valves to work properly when cold and/or frozen. After much evaluation, cotton-filled nitrile rubber high-pressure seals were found to give the best all-around performance. The valves were changed as follows: the formed-disc inlet valves were replaced by balls with appropriate seats which reduced the area of contact at the valve seat and, therefore, the degree of adhesion to the seats due to residual water/ice films. The springs for the outlet ball valves were retained but the spring load was reduced. Also the cylinder clearance volume was decreased to provide the necessary compression to drive the outlet valves off their seats for priming. New, stronger solenoids were provided to break the inlet valves from their seats reliably. (These solenoids are required also for the drainage sequence and to provide flow modulation during regular pump operation.)

The net result of the above modifications was the development of a pump which: 1) drained reliably; 2) turned over at 244°K (-20°F) while providing about 0.04 MPa (12 in. Hg) suction; 3) at this initially frozen condition, primed and began to pump water. In addition, subsequent testing through about a dozen freeze/thaw cycles showed that shearing of the ice film did not damage the high pressure seals, and more than 1,000 hr of pump operation have been completed with no loss of performance after the pump was subjected to freeze testing.

TECHNOLOGY REQUIREMENTS

The preliminary steam bottoming system design presented in the previous section of this report is conservatively based upon steam engine experience gained during low emission automobile projects of the 1970's.(12)

Experimental hardware demonstrated encouraging durability at steam temperatures of 800° to 900°K (1000 to 1100°F) and pressures to 13.8 MPa (2000 psia). The more efficient engines used piston type expanders lubricated by hydrocarbon base stock oils. Boilers were typically the once-through (no steam drums or recirculation) type, "mono-tube" or single circuit, and made of stainless steel tubes with gas side fins. Piston type water pumps and air cooled condensers were the norm.

Thus, while substantial performance benefits for long haul trucks are projected with the proposed baseline bottoming system without departing significantly from proven technology, certain system advances could improve hardware reliability and performance and reduce system cost and weight. Specifically, FMI has evaluated the advancement in the state of the art required to make it possible to design and fabricate reliable hardware for the following components:

- Dry lubricated expander.
- Compact small tube parallel flow boiler.
- Compact air to steam condenser with shutdown dryer system for the freeze protection subsystem.

The following discussions of the above components include an assessment of the labor hours required to complete an appropriate technology development program.

Expander Piston Ring Limitations

All current commercial piston type steam expanders use oil lubricated piston rings. FMI, under prior contracts, developed the current art in steam engine oils in cooperation with Exxon and Mobil. The additive package developed by Exxon provides de-emulsification, rust inhibition, and extreme pressure boundary lubricity. Combined with natural or synthetic hydrocarbon base stock, the resulting oil is a nonadherent, soft decomposition product when subjected to superheated steam in the boiler. Exxon now supplies this oil to the South African

Railway for use in the 722°K (840°F) Red Devil steam locomotive. The Mobil version using the single distillate fraction synthetic base stock (Mobil 1 H) has demonstrated even better performance in limited tests by FMI.

Given the opportunity for production development, oil lubricated steam expanders can be expected to be more durable than internal combustion piston engines even at high steam temperatures, 800-900°K (~1000-1100°F), as the environment is benign (no combustion acids, oxygen, soot or atmospheric dirt). However, oil lubrication has the drawbacks of system complexity and cylinder cooling performance losses. The following discussion outlines potential engine improvement methods for reducing or eliminating piston ring oil lubrication. Four tables summarize the possibilities ranging from current practice through unlubricated hard faced pressure balanced rings.

Table 12 outlines current practice with "splash lubricated" piston rings. The practical disadvantage is the need to separate oil from the condensate, and water from the crankcase. Long term scale formation in the boiler due to oil deposits has not been observed but it is still a possibility. Expander performance is undoubtedly reduced by oil lubrication. The cool oil is pumped into the hot end of the cylinder and then scraped, hot, back to the sump. The thermal efficiency penalty is difficult to assess. The expander oil cooler load has been measured and the oil heat rejection is roughly twice the measured mechanical friction loss, that is, the oil cooler load is comparable to 10 to 15 percent of the net shaft power.

The limited experience with Mobil 1 base stock indicates that the synthetic oil is a superior lubricant. The high, single boiling point of 644°K (700°F) requires much less oil circulation to keep the ring face damp. Unfortunately, little empirical work has been devoted to reducing the oil circulation and measuring the performance potential of Mobil 1.

Table 13 outlines potential lubrication improvement by using a counterflow expander (exhaust valve in head rather than exhaust ports at the bottom of the stroke). Classically, the counterflow expander has been less efficient than a uniflow type. Current high piston speed designs, crankcase splash lubrication rather than oil injection, and better analytical methods might result in comparable efficiencies for the two expander types. Unfortunately, similar expander designs of each type operating under the same steam cycle have not been tested and publicly documented. The lubrication advantage of a counterflow is that the oil-wet rings do not cross over exhaust ports and the rings are more effectively isolated from the

TABLE 12. - CHARACTERIZATION OF OIL-LUBRICATED EXPANDER PISTON RINGS - CURRENT PRACTICE

Method:

- Oil lubricated from bottom
- "Uniflow" (exhaust ports in liner)
- Hard coated conventional rings and liner
- Custom formulated but not exotic oil

Durability:

- Excellent

Performance:

- Excellent at high load with mechanical efficiencies over 90 percent
- Light load efficiency loss predominantly heat transfer related

System Disadvantages:

- Oil carryover into steam exhaust must be mostly recovered and returned to crankcase. Complicated oil separator and plumbing system
- Steam blowby into crankcase must be boiled off and vented to condenser. Potential for bearing failures if too much water accumulates in crankcase during cold starts

Potential Improvements:

- Limited experience with Mobil 1 (synthetic hydrocarbon) suggests that an order of magnitude reduction in oil consumption may be possible. The single, high boiling point reduces the quantity of oil needed to keep the rings wet
- Limited experience with hard coated (other than chrome plate) also suggests that substantial lubrication margin is available for reducing oil consumption

TABLE 13. - CHARACTERIZATION OF OIL-LUBRICATED EXPANDER PISTON RINGS WITH COUNTERFLOW EXHAUST

Method:

- Same as current uniflow
- Exhaust and intake valves in head
- Oil coated surfaces not swept by steam during exhaust process

Durability:

- Probably excellent

Performance:

- Historically efficiency of counterflow has been lower than uniflow
- Limited recent tests of modern counterflow types have been inconclusive

System Disadvantages:

- Some oil carryover into steam will still occur
- Steam blowby into crankcase will still occur

Potential Improvements:

- A crosshead design could provide separation of steam blowby before it could reach and condense in cold crankcase

steam. Potentially, the rings could be positioned well below the piston crown in a cooler region and hence need very little oil flow for cooling.

Table 14 outlines the possibilities when using graphite rings. High pressure oil-free air compressors at similar pressures and temperatures frequently use graphite rings. Graphite rings in steam engines were successfully used in Germany in the thirties but no detailed documentation can be found. Two brief experiments have been attempted in modern times. GE ran a 6.9 MPa, 811°K (1000 psi, 1000°F) steam expander for 150 hr with graphite rings. This EPA sponsored project resulted in an expander efficiency comparable to oil lubricated expanders. The ring wear rate was very high but not catastrophic. No significant graphite alloy or refinement of pressure balancing was attempted. FMI built a graphite piston ringed steam expander under a DOE program for solar power. Development cost problems curtailed this project before any significant data were obtained.

Graphite rings would appear to be only an interim solution. They must be expected to have a finite life due to wear and they are fragile.

Table 15 outlines the potential of unlubricated hard rings running against a hard cylinder bore. Several material pairs have a potential for infinite life and acceptable friction provided that the ring face pressure is low enough. Candidates like Tribaloy, silocon carbide and metal/ceramic alloys are used in severe environments. Their use as engine piston rings requires an unconventional design approach. Unlike 2480°K (4000°F) combustion engine gas, a small percentage of the steam can leak past the rings with little performance penalty and no structural problems. The technique for incorporating unlubricated hard rings in a piston steam expander would be to almost completely pressure balance the piston ring. The major problem anticipated would be in stabilizing the lightly loaded ring to maintain contact with the inevitable thermal bore distortions. The ring would be expected to have more blowby than a conventional oil lubricated ring.

One concept that may satisfy the demands of the steam expander is shown in Figure 30. This FMI proprietary concept is characterized as a ventilated band seal. The band is a split ring with almost complete pressure balancing. Ventilation between the inner and outer faces is provided. The length of the band is used to provide torsional rigidity and low tip contact pressure through the long "wheelbase." The small and pressure balanced backing ring of conventional cross section provides the preload on the band and the band to piston gas

TABLE 14. - CHARACTERIZATION OF UNLUBRICATED GRAPHITE EXPANDER PISTON RINGS

Method:

- Multi-step, pressure balanced graphite rings
- Similar pressure-velocity profiles as graphite rings for air compressors

Durability:

- Potentially good
- Graphite/binder/bore coating system undeveloped for these conditions
- Substantial trial and error development appears likely

Performance:

- Small increase in friction
- Probable improvement in thermodynamic performance without cooling effect of oil

System Disadvantages:

- Fragile rings may fail if frosted at cold start
- Performance will deteriorate with inevitable wear of rings

TABLE 15. - CHARACTERIZATION OF UNLUBRICATED HARD EXPANDER PISTON RINGS

Method:

- Very hard ring face, nearly floating pressure balancing
- Hard coated liner perhaps ceramic for low thermal expansion

Durability:

- Potentially infinite life if pressure balanced ring is stable
- Unlike I-C engine some leakage is acceptable hence seal need not be perfect
- Simpler system without oil contamination

Performance:

- Small increase in friction likely
- Some leakage likely
- Thermodynamic performance better without cooling effect of oil
- Applicable to both counterflow, uniflow and compound designs

System Disadvantages:

- Taller assembly since a crosshead piston, rod, and seal are needed to eliminate steam from oil
- First cost premium of expander likely to be offset by reduced cost of overall system without oil contamination

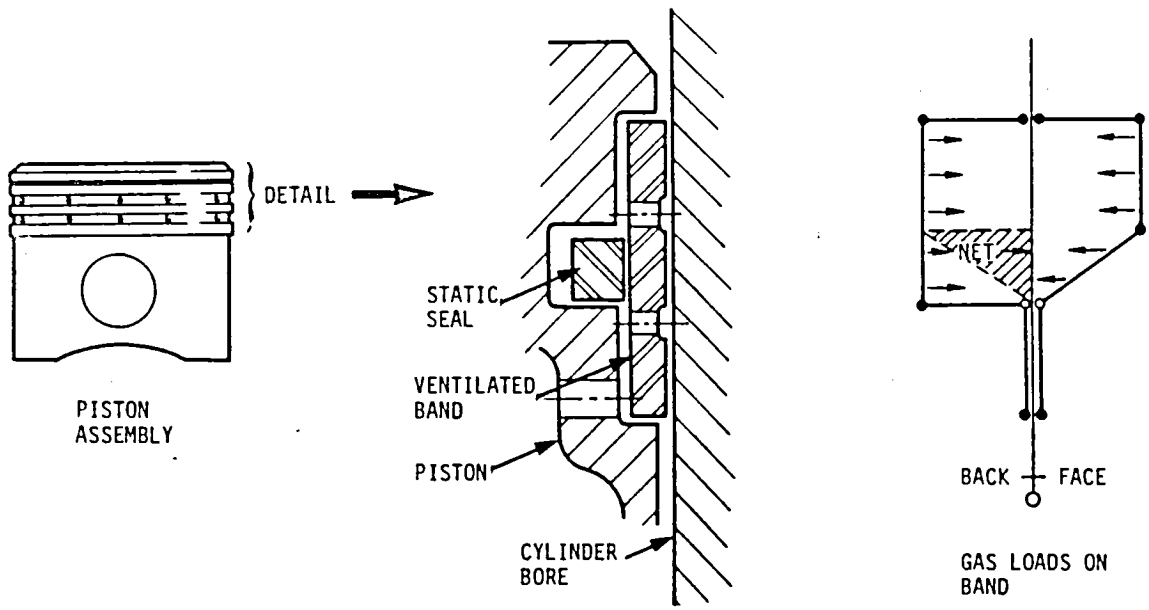

Figure 30. Foster-Miller ventilated band for unlubricated piston ring

seal. It would be likely to have pressure balancing relief on the piston sealing face as well to reduce parting friction as the seals travel over bore distortions.

An assessment of the development effort needed to prove this piston ring concept suggests that a two phase approach be taken. This unconventional design would benefit from fundamental analytical and experimental work. A 9-month to one year research phase could be conducted on a simple oscillating piston in a closed, unheated cylinder. Analysis and geometric variables could be correlated for confirmation of theory without the complexities and instrumentation difficulties of a live steam rig. Given a basic slide-crank-piston-cylinder rig (a diesel or steam engine with the valves sealed), one man year of analytical/experimental engineering and a supporting man year of technician time could provide the basic design tools and models.

A second phase of development on a running steam expander could develop the basic durability and performance data. Again a one year program should be adequate. This phase would necessarily be more expensive because of the test loop complexity, more difficult instrumentation environment and the need to accumulate significant running time on several ring modification stages. A 1 man year engineering effort is again adequate but perhaps 2 man-years of technician time and substantial hardware expenses would be needed to complete the second phase.

Compact Boiler Limitations

The baseline boiler design is a monotube design. The water passes through the boiler in a single tube with no parallel circuits. A more compact design was studied to determine the potential benefits of parallel circuiting of the water/steam flow.

Table 16 shows the comparison between single, three and nine parallel coil boiler designs. The parallel coil designs benefit from increased heat transfer coefficients due to smaller hydraulic radii with obviously diminishing benefits with increasing numbers of coils. The parallel circuit designs, however, were not as optimized as the single "monotube" design.

The multi-circuit boiler approach could save about one-third on the heat exchange weight or perhaps 16 kg (35 lb) for a 40 kW (50+ horsepower) bottoming cycle. The parallel coil approach does have development risks in that steam flow stability between coils, proportional gas flow distribution between coils and manufacturing and maintenance techniques would need to be developed. Any theoretical advantage in steam side pressure loss reduction would likely be lost when sufficiently stiff individual coil flow orifices were determined. Finally, as a practical matter, finned tubing in the small diameters and thin walls that would be optimum for the parallel coil designs is not commercially available.

Our recommendation at this point is to stay with the single circuit design for this power level. Should an application with a larger engine, say 750 kW (1000 hp), arise a 3 circuit design should be developed using commercially available 5/8 in. O.D. tubing.

TABLE 16. - COMPARISON OF 1, 3, AND 9 COIL BOILER DESIGNS

Parameter (Normalized to Optimized Single Coil Boiler)*	Number of Parallel Coils 1	3	9
Total Tube and Fin Weight	1.0	0.67	0.62
Metal Energy Content	1.0	0.82	0.81
Heat Transfer Area	1.0	0.68	0.67
Maximum Tube OD, (in.)	15.9 (5/8)	9.50 (3/8)	6.4 (1/4)
Tube Wall, (in.)	1.24 (.049)	0.89 (.035)	0.71 (.028)

$42^{o}K$ ($75^{o}F$) Pinch Point,
$811^{o}K$/6.9 MPa ($1000^{o}F$/1000 psia) Steam

*Single Coil Boiler
Tubing Weight 45 kg (99 lb)
Heat Transfer Area 15.8 m^2 (170 ft^2)

Condenser Drying For Freeze Protection

The results of freeze protection research conducted as a part of this contract and in previous programs were discussed in a section of this report titled Freeze Protection Research. Natural drainage, frosting and startup experiments on a representative condenser core and boiler tube coils were described. In summary, a conventionally constructed and proportioned (particularly condenser tube width) condenser was shown to drain without freeze-prone miniscus formation particularly if the ends of the tubes were scarfed at an angle in the sump or the core was tipped a few degrees.

The boiler coils were found to be structurally safe if the residual trapped water level was not significantly above the level of the inner bend. The boiler can be expected to be dry after the hot shutdown if a blowdown valve bypassing the expander is activated on shutdown. The thermal energy stored in the boiler tube metal approximately equal the heat required to vaporize the working water inventory. Further safety can be had if the bottoming cycle boiler charge is dumped to the

condenser shortly before the diesel is stopped. The idle exhaust energy of the diesel can boil the boiler dry in roughly one minute.

A potential system failure mode due to freezing is an unsuccessful attempt to start the diesel in freezing weather. In this case it is possible to have a liquid filled boiler with no heat source available to dry it out. A simple system approach to a cold start dryer, or for that matter a forced dryer for normal shutdowns, is to use the expander as an air pump.

By cranking the expander in the normal direction and venting the exhaust to ambient, the expander will pump air backward through the boiler. A vent from the condenser bottom header and a check valve between the expander air vent valve and the condenser inlet would complete the system. Given normally spring open positions on the two vents the system would automatically assume the air purge mode during startup and shutdown. The vent solenoids would close the vents only after some minimum exhaust time/temperature was reached. The solenoid controlled feedwater pump valves would be of the normally open type as well so that the boiler water would be pushed back to the condenser and ultimately the air pumped by the expander would purge the condenser core as well.

Development of this concept could be simply conducted on an ambient temperature rig. Existing expander, feedwater pump and boiler hardware could be set up with appropriate vent valves. Flooding the system with a known quantity of water would be followed by cranking the exhaust vented expander and measuring the purged water amount and rate for effectiveness. Some minimum successful cranking speed is anticipated as a very slow cranking speed would result in substantial blowby and poor expander performance as a compressor.

The labor requirements for such an experiment are estimated at 3 engineering man months and 6 technician man months. Hardware costs would be minimal for a company with existing small steam engine systems.

Short Term Technology Development Needs

Based on the previous component development discussions and FMI's extensive experience with steam engines and steam systems, the following short term development needs have been identified:

- Complete "Mobil 1"/Triballoy durability development for minimum oil carryover.
- Test a complete breadboard system for freeze protection.
- Test boiler fouling and self-cleaning on a diesel.
- Develop valve guides which reduce the high steam leakage and excessive wear which is characteristic of current cooled metal types.

These items are intended to produce the most significant advances with the least investment of time and capital. Justification for the first task can be found in the previous assessment of expander piston ring limitations. It is also apparent from the freeze protection research results and condenser drying discussion that freeze protection system events, expander cranking purge and boiler blowdown strategy require confirmation by overall system testing. And although boiler fouling and self-cleaning are well documented in gas turbine exhaust stream thermal energy recovery, some tests of boiler self-cleaning in a diesel exhaust stream with its lower excess air and larger particulate sizes, would be reassuring. Finally, ceramic bushings or condensing valve guides, which would allow high pressurized sealing of a liquid instead of hot vapor, might be effective in reducing steam leakage and increasing component life.

STEAM RANKINE BOTTOMING SYSTEM ECONOMICS

The cost and performance advantages of the steam Rankine bottoming system are best illustrated by comparing the proposed turbocharged engine/bottoming cycle system (TC/B) to an adiabatic engine without a bottoming system. The turbocharged turbocompound engine with aftercooling (TCPD/A) was selected as the reference for the following evaluations since, according to the NASA data presented in Table 17, it has the best performance of the four adiabatic engine configurations considered.

Equipment Costs

Cost estimates for major bottoming system components as well as technical assistance in component design and specification were provided by established manufacturers of the same or similar items. The condenser design was reviewed and priced by a truck radiator firm who also supplied sample cores for the freeze tests previously described. The expander and power transmission were priced by a major diesel engine firm on the basis of preliminary design drawings. The boiler cost was estimated by a boiler and finned tube manufacturer. The feedwater pump is a slightly modified version of a currently produced model and its price was therefore estimated with reference to the vendor prices for the standard model.

TABLE 17. NASA REFERENCE DIESEL DATA (PART 2)

Adiabatic diesel configuration	Power output*		Brake specific fuel consumption		Mission fuel economy		Selling price**
	kW	Bhp	kg/(kW-h)	lb/(Bhp-hr)	km/m^3	mpg	
TC	236	317	0.192	0.315	2410	5.66	$14,000
TC/A	239	320	0.189	0.310	2440	5.75	$14,500
TCPD	250	335	0.181	0.297	2550	6.00	$16,000
TCPD/A	254	340	0.178	0.293	2580	6.08	$16,500

*Full speed (199 rad/s, 1900 rpm), full throttle.

**Add $40 per kW ($30 per Bhp) for engine ratings above those listed.

Other system components are standard off-the-shelf items. The shutters, fan, and cartridge demineralizer are catalog items. The control subsystem cost was determined by FMI's production equipment division. The subsystem includes sensors, controls, displays, interfaces and power drivers, processor and support circuitry, a power supply, cables, connectors, and an enclosure. The subcooler, oil cooler, and system plumbing costs were also in-house estimates.

Original equipment manufacturer (OEM) costs were requested for all items for a production rate of 10,000 bottoming system units per year. Table 18 summarizes the bottoming system equipment costs on an OEM, manufacturing and selling basis.

TABLE 18. STEAM BOTTOMING CYCLE COMPONENT COSTS (production rate - 10,000 units/year)

Item	Manufacturing cost	OEM price	Selling price
Expander w/transmission	$1,030	$1,800	$2,060
Boiler	800	1,400	1,600
Control subsystem	440	765	880
Condenser	370	650	740
Boiler feed pump	85	150	170
Plumbing	75	130	150
Demineralizer	75	130	150
Shutters	60	100	120
Fan	35	60	70
Subcooler	35	60	70
Oil Cooler	30	50	60
Totals	$3,035	$5,295	$6,070

Manufacturing costs were obtained by dividing OEM prices by 1.75. Seventy-five percent was suggested to be a typical mark-up between the manufacturer and OEM. A selling price to manufacturing cost ratio of 2.0 was suggested by NASA. Again, this is an approximation of industry practice. Assuming that the prime manufacturer is a diesel firm, producing the expander and pump in-house, an installed selling price of $6,070 appeared reasonable. No credit has been taken in costing the steam bottoming for elimination of the muffler and the sharing of the cooling fan function with the diesel oil cooler.

Maintenance Costs

Maintenance costs were more difficult to quantify. The approach taken was to compare the relative maintenance requirements of the TC/B and TCPD/A system. Components or features of the TC/B system which would cause it to require more maintenance than the TCPD/A system were identified and the additional maintenance cost was estimated. Annual maintenance experience and cost guidelines for diesel truck engines and cooling systems, provided on a proprietary basis by a major engine manufacturer, formed the basis for the following analysis which is summarized in Table 19.

It was assumed that both the TC/B and the TCPD/A systems would have the same basic engine maintenance requirements as a standard heavy-duty diesel less the cooling system maintenance. The condensing subsystem of the bottoming cycle was assumed to have the same maintenance requirements as a current diesel cooling system for an annual cost of $220, while $110 was estimated for maintenance of the aftercooling components of the TCPD/A engine. The aftercooler maintenance cost estimate is lower since it is a gas-to-gas instead of a gas-to-liquid heat exchanger. The net maintenance charge to the TC/B for its cooling system was therefore $220 - 110 = $110/year.

The reciprocating steam expander of the TC/B and the high speed turbocharger turbine of the TCPD/A will both require maintenance above and beyond that required by the basic adiabatic engine. It was assumed that since these components are essentially equal in complexity no difference in maintenance cost exists between systems due to this hardware.

The boiler, control system, and feedwater pump of the TC/B system have no parallel components in the TCPD/A system. Maintenance of these items will therefore result in additional annual operating costs specific to the bottoming cycle. The boiler feed pump is a positive displacement piston device which may have to be replaced once a year. Assuming the replacement

TABLE 19. SUMMARY OF STEAM BOTTOMING SYSTEM MAINTENANCE COST ANALYSIS.

Objective: Determine maintenance cost of steam Rankine bottoming system by comparison of Adiabatic Turbocharged Diesel plus steam bottoming cycle (TC/B) to Adiabatic Turbocompound Diesel Engine with Aftercooling (TCPD/A)	
Current diesel maintenance costs:	
Total maintenance (engine, drive train, etc.)	$14,580/yr
Engine only (1 major overhaul @ 500,000 mi)	$ 5,300/yr
Cooling system only	$ 220/yr
Itemized maintenance items and differential costs:	Per Year
• Maintenance of basic adiabatic diesel engine is the same for TC/B and TCPD/A systems	$ 0
• Since TC/B condensing system maintenance is approximately the same as that for a standard diesel (+220/yr) and the less complex aftercooling system maintenance is approximately half that required for a standard diesel ($110/yr) the net annual maintenance charge due to the bottom cycle is $220 - 110 = $110.	$110
• Maintenance requirements for TC/B reciprocating steam expander and TCPD/A high speed turbocharger turbine are essentially equivalent.	$ 0
• Boiler feedwater pump will be replaced each year with rebuilt unit.	$120
• Demineralizer cartridge will be replaced annually.	$ 50
• Boiler will require acid wash once a year.	$ 50
• Control system will require $250/yr for labor and replacement parts.	$250
Total maintenance cost for steam bottoming system	$580

unit is a rebuilt pump, and requires 1 hr of labor for installation, an annual charge of $120 was assessed. Other annual maintenance charges include replacement of the demineralizer cartridge ($50.00) and a yearly acid wash cleaning of the inside (water side) of the boiler tubes ($50.00). Finally a sum of $250.00 for control system maintenance (parts and labor) was allowed.

The bottom line of the analysis was that the TC/B system would cost approximately $580 per year more to maintain than the competing TCPD/A system, and this maintenance charge is assumed to be attributable to the steam bottoming cycle system.

Performance and Cost Summary

The performance, capital cost and operating cost of the competing systems are reported in Table 20. The prices of both basic adiabatic diesel engine configurations were determined from the NASA-supplied data of Table 17. The TC/B compound system selling price is the sum of the TC engine price $14,000 and the bottoming system cost, $6,070. The TCPD/A system price is the cost of a 254 kW (340 hp) engine, $16,500, plus a premium of $40 per kW ($30 per hp) for an additional 24 kW (33 hp).

The bottoming cycle supplies an extra 42 kW (56 hp) to the TC engine or a 17.7 percent increase in output for a given fuel usage rate. The basic TC engine is rated at 2410 km/m^3 of fuel (5.66 mpg), so the TC/B configuration fuel economy will be 2830 km/m^3 fuel (6.66 mpg). At 160,930 km/yr (100,000 mi/yr) and $317/$m^3$ of fuel ($1.20/gal), the annual fuel bill for the TC/B system is $18,018. The annual fuel cost for the comparable TCPD/A system rated at 2580 km/m^3 (6.08 mpg) is $19,737. Thus the annual distance traveled and fuel cost specified by NASA imply a $1,719 annual fuel savings value for the TC/B system.

The additional maintenance required by the compound system is shown to absorb nearly one-third of the fuel savings.

Economic Analyses

Three measures of economic viability were considered in the steam Rankine bottoming system review: simple payback period, net present value (NPV), and return on investment (ROI).

TABLE 20. PERFORMANCE AND COSTS OF COMPETING SYSTEMS

	TCPD/A turbocompound adiabatic engine with aftercooling scaled to 278 kW (373 hp)	TC/B 236 kW (317 hp) turbocharged adiabatic engine with 42 kW (56 hp) steam bottoming cycle
Performance		
B.S.F.C., kg fuel/kW-hr (lb fuel/hp-hr)	0.178 (0.293)	0.163 (0.268)
Mission fuel economy, km/m^3 of fuel (mi/gal)	2580 (6.08)	2830 (6.66)
Capital Cost		
Total engile system price	$17,460	$20,070
Added price	-	$2,610
Operating Costs		
Annual fuel cost, @ $\$317/m^3$ fuel and 160,930 km/yr ($1.20/gal and 100,000 mi/yr)	$19,737/yr	$18,018/yr
Annual fuel savings	-	$1,719/yr
Added annual maintenance	-	$ 580/yr

Simple Payback Period

Simple payback period is defined as the length of time required for the cash proceeds produced by the investment to equal the original cash outlay required by the investment. For this application the cash outlay is the added cost of the TC/B versus the TCPD/A system and the cash proceeds are the relative fuel savings generated. Thus,

$$\text{payback period} = \frac{\$2610}{\$1719/\text{year}}$$

$$= 1.5 \text{ years}$$

A more conservative analysis includes the added maintenance costs of the compound engine (TC engine plus bottoming system) as a negative cash proceed so that

$$\text{payback period} = \frac{\$2610}{\$(1719 - 580)/\text{year}}$$

$$= 2.3 \text{ years}$$

Figure 31 illustrates the relation between payback period and the capital cost between the competing systems with and without maintenance charges.

Payback period analysis is widely used because it is an easy to understand measure of cash impairment and it requires no assumptions or detailed knowledge of economic parameters such as discount rates, taxes, and depreciation. On the other hand, it is not a true measure of profitability in that it ignores the timing of cash flows, the time value of money and cash flows after the payback period.

Net Present Value (NPV)

Net present value measures the value of an investment with all relevant after tax cash flows discounted at an appropriate rate. If the NPV is greater than zero, then the investment is acceptable.

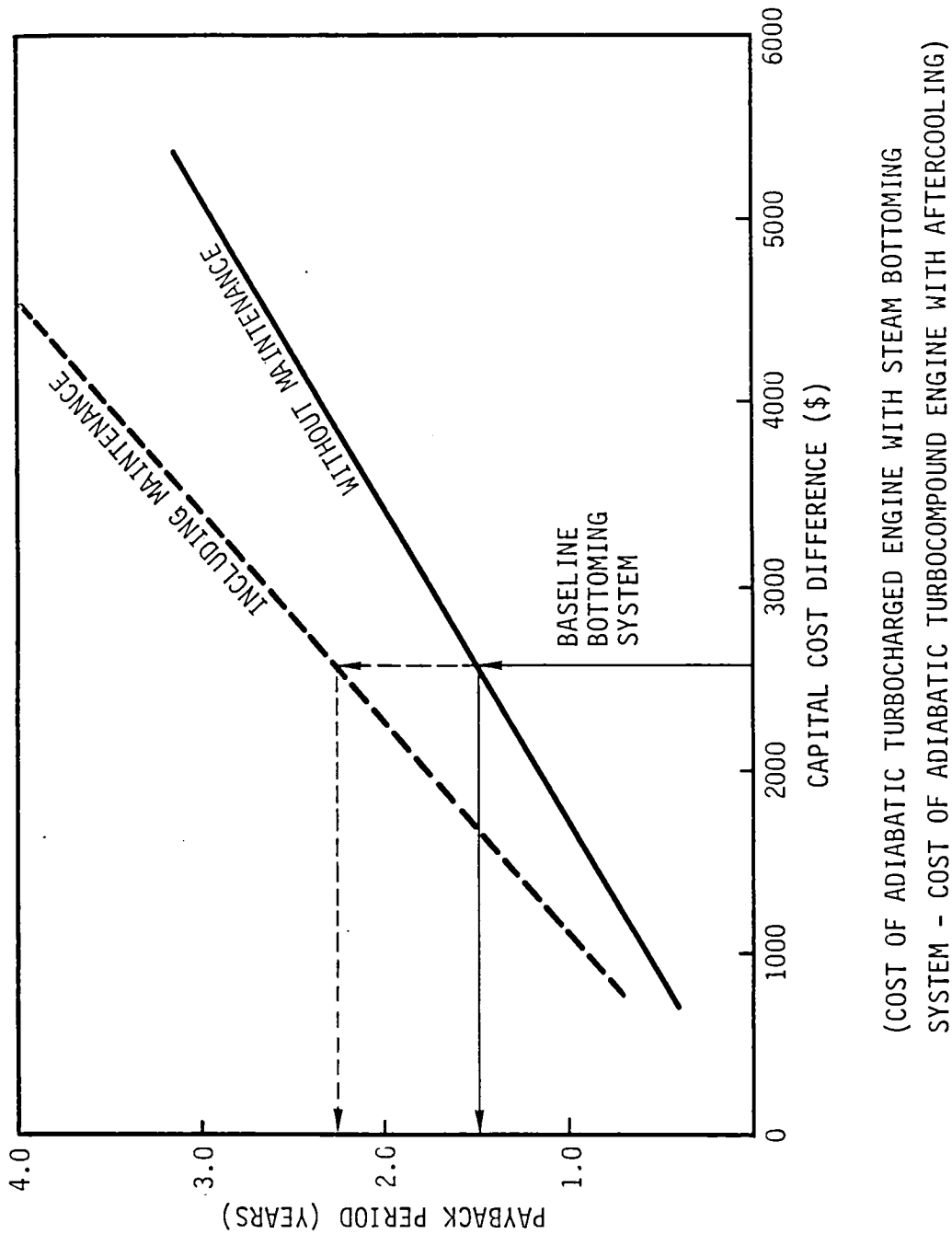

Figure 31 - Sensitivity of payback period to capital cost difference between turbocharged engine with bottoming system and turbocompound engine with aftercooling.

NPV is calculated using the following equation:

$$NPV = \sum_{n=o}^{N} \frac{C_n}{(1 + i)^n} \qquad (45)$$

where

N = useful life of the system, years

n = year index (= 0, 1, 2, ... 7)

C_n = total cash flow for year n

i = cost of capital (discount rate)

The initial and subsequent cash flows for the comparative cost analysis being considered were determined according to the following formulations:

for n=o

$$C_o = \text{initial capital investment} = -IC \qquad (46)$$

for n=1,..N

$$C_n = (1 - TR)(F_n^A - F_n^B + M_n^A - M_n^B) + TR(D_n^B - D_n^A) + M_n(TC)(IC) \qquad (47)$$

where

IC = added cost of system with bottoming cycle = $2610

TR = tax rate

F = fuel cost

M = maintenance cost

D = depreciation cost

TC = tax credit

M_n = 1, if n = 1

= 0, if n ≠ 1

superscript A = TCPD/A system
B = TC/B· system

The following economic parameters, recommended by NASA, were assumed for the NPV analysis:

N, useful equipment life - 7 years

TR, corporate tax rate - 46 percent

TC, investment tax credit - 7 percent

i, cost of capital - 12 percent

F, cost of fuel - \$317/m^3 fuel (\$1.20/gal)

Depreciation was calculated using the accelerated cost recovery system (ACRS) over a 5-yr period. The depreciation schedule was as follows:

Year	Percent of initial capital cost
1	15
2	22
3	21
4	21
5	21

The results of the NPV analysis are presented in Figure 32. Due to the uncertainties inherent in this type of analysis, the plots show not only baseline results, but also the sensitivity of the NPV to maintenance costs and added capital cost of the bottoming system. For the baseline case (\$580/yr maintenance cost, \$6070 bottoming cycle cost), the NPV is \$1232, so that the bottoming system appears to be a sound investment according to this measure.

A recommendation not to invest would be indicated for a capital cost difference greater than \$4,600 or almost twice the estimated value.

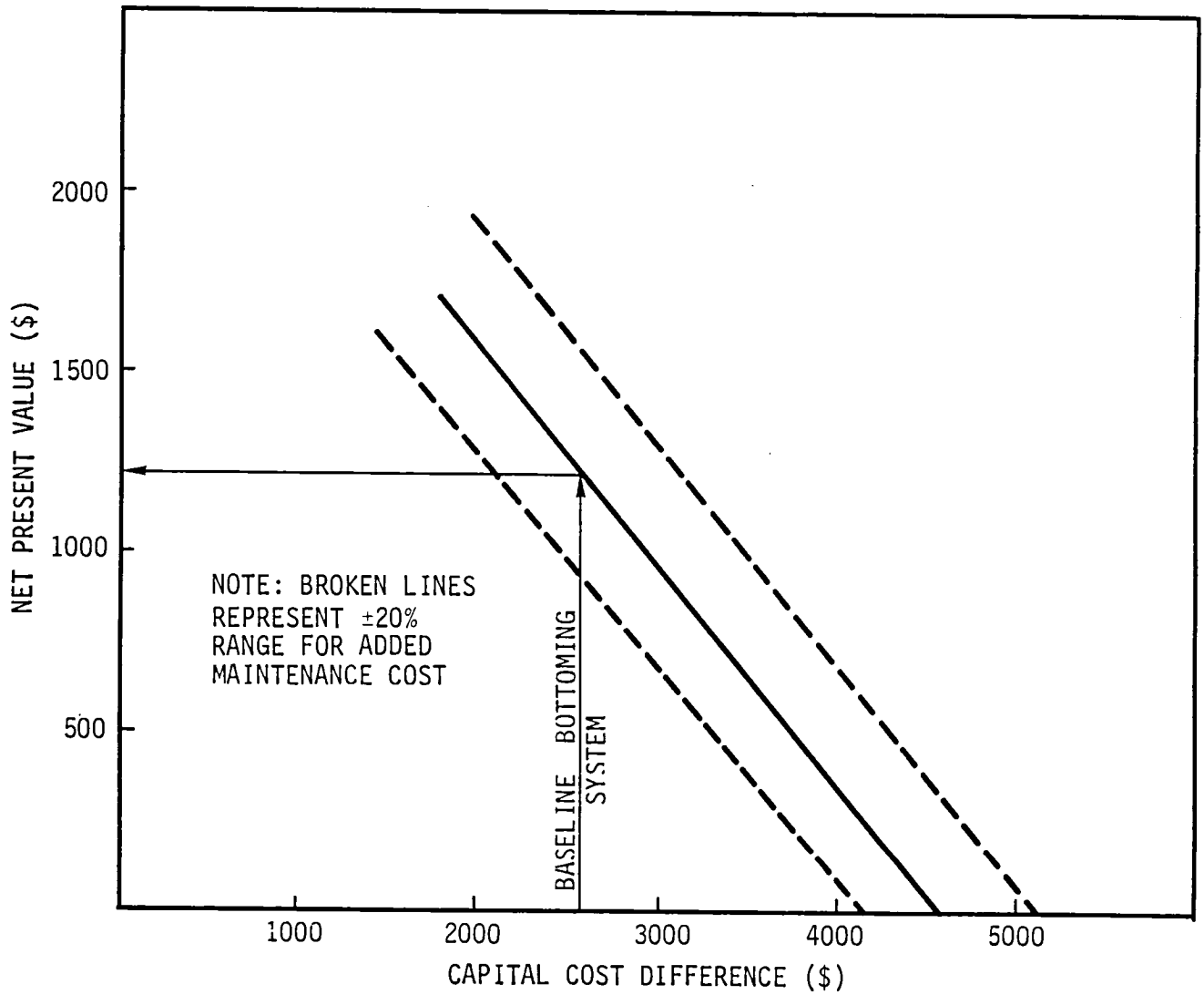

ASSUMPTIONS: 7 YR. LIFE
12% COST OF CAPITAL
46% TAX RATE
7% TAX CREDIT
$\$317/m^3$ ($1.20/GAL) FUEL COST
0% ESCALATION RATE

Figure 32. - Sensitivity of net present value to capital and maintenance cost differences between competing systems.

Net Present Value capital investment analysis is a better measure of investment profitability than payback period because it considers both the time value of money and the timing of all cash flows. Although it is theoretically sound and is increasingly popular in practice, it does have the drawback of being complicated to calculate. This economic measure also tends to favor large projects.

Return on Investment (ROI)

The final economic indicator considered in this review of bottoming cycle economics was Return on Investment (ROI). ROI was the primary economic evaluation technique used by top financial officers of 300 of Fortune 500 largest industrial firms according to a 1981 questionnaire. The ROI (also called the internal rate of return) is that discount rate which equates the project investment with the expected returns. ROI is found by varying the discount rate from Eq (45) until the NPV equals zero. Generally, if the ROI is greater than the current cost of capital, a project is economically acceptable.

The results of the ROI analysis, presented in Figure 33, show that even if the added system cost with a bottoming cycle was 25 percent more than estimated, or if the added maintenance cost was 40 percent higher, the ROI would still be greater than 20 percent and the investment would still be very attractive.

The results shown so far assume no escalation for labor or consummable materials costs. Many analysts, however, believe that the cost of fuel could escalate at 3 percent or more above the general rate of inflation. This, of course, would make bottoming cycle economics look even better. Figure 34 shows the effect of escalating fuel prices on ROI. With a 3 percent fuel escalation rate, the baseline ROI would improve from 27 percent to 30 percent.

Finally, the estimates presented so far have been based on conservative bottoming cycle technology. Figure 35 shows the effect of advanced steam expander technology on ROI. A 10 percent improvement in expander output would yield an ROI of 37 percent, all else being equal.

Thus, although the baseline design is technically sound and economically attractive to the end user, less conservative performance projections can be justified with very slight technical risk and significant economic gains. Viability analysis for a business venture must, of course, further account for production development, tooling, market penetration, and the future cost of fuel.

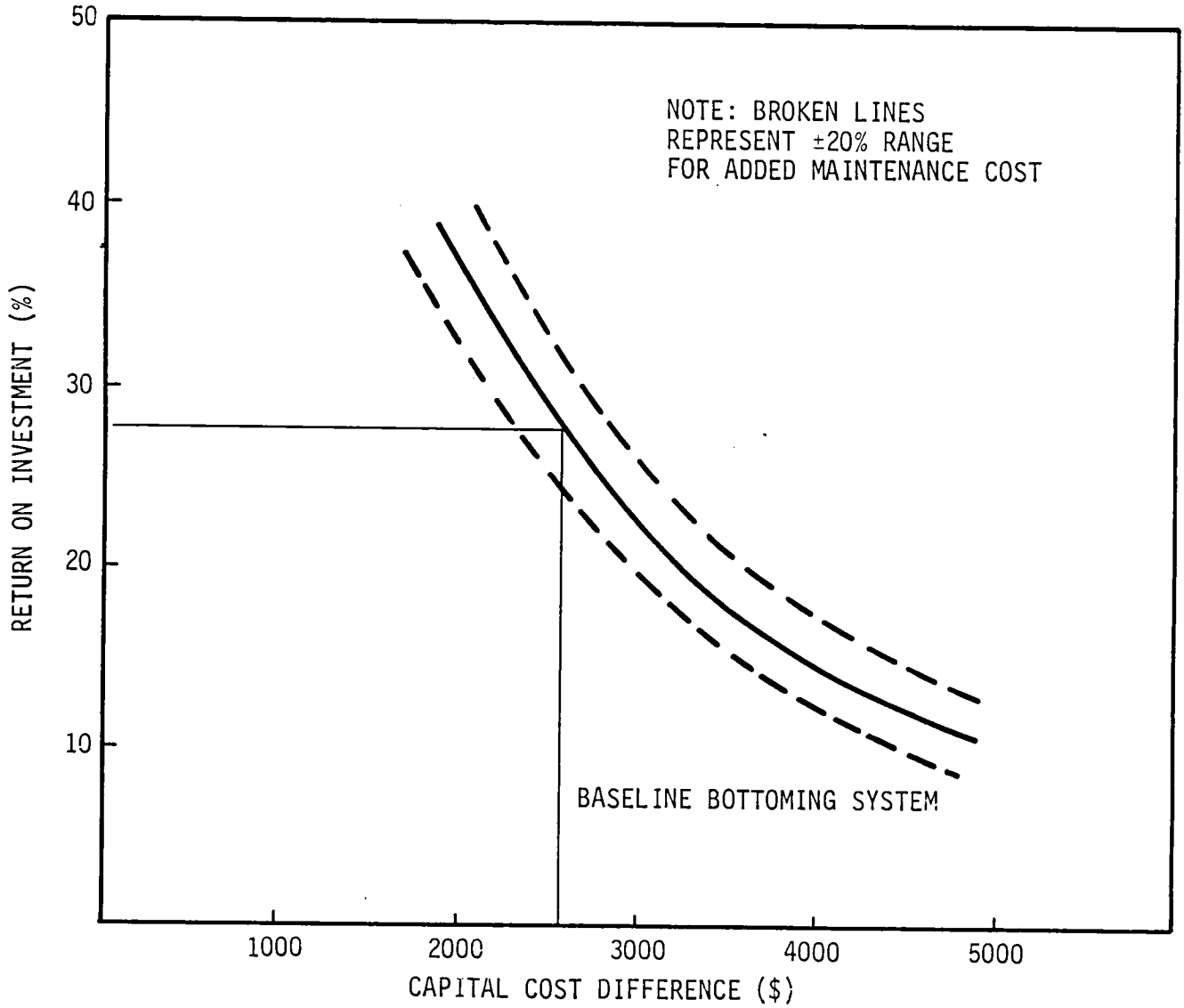

ASSUMPTIONS: 7 YEAR LIFE
46% TAX RATE
7% TAX CREDIT
$\$317/m^3$ ($1.20/GAL) FUEL COST
0% ESCALATION RATE

Figure 33. - Sensitivity of Return on Investment to capital and maintenance cost differences.

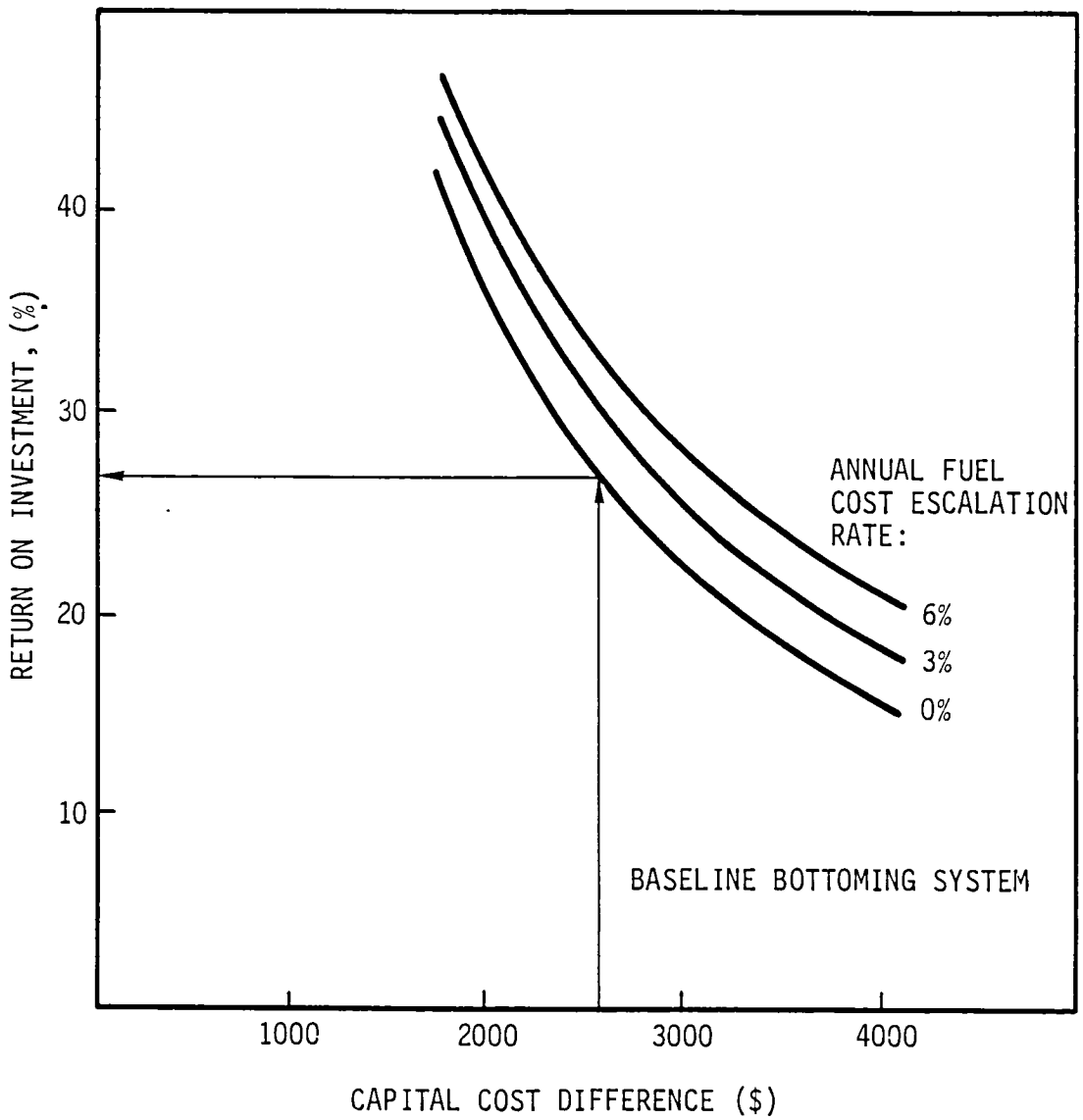

ASSUMPTIONS: 7 YEAR LIFE
46% TAX RATE
7% TAX CREDIT
$\$317/m^3$ ($1.20 GALLON) BASELINE FUEL COST

Figure 34. - Effect of fuel cost escalation rate on Return on Investment.

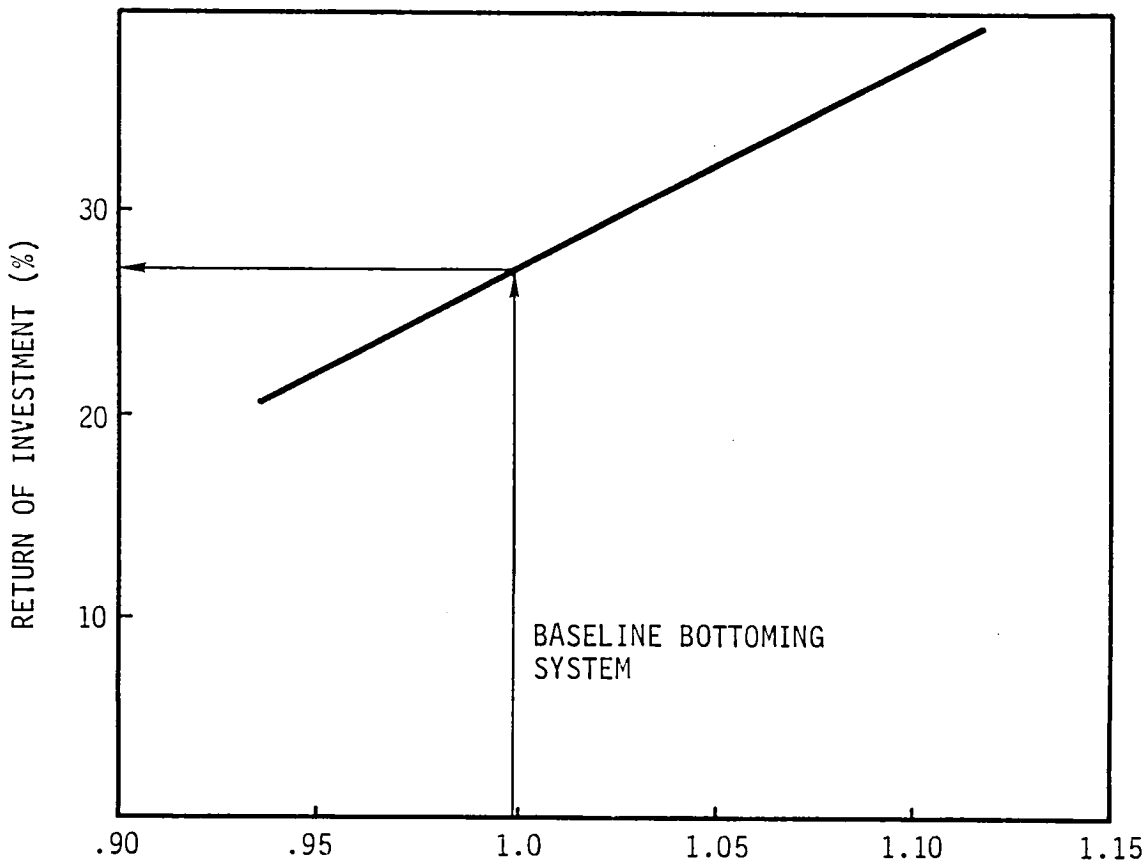

ASSUMPTIONS:
- $580/YR. MAINTENANCE COST DIFFERENCE
- $2580 CAPITAL COST DIFFERENCE
- 7 YEAR LIFE
- 46% TAX RATE
- 7% TAX CREDIT
- $317/$m^3$ ($1.20/GALLON) FUEL COST
- 0% ESCALATION RATES

Figure 35. - Effect of improved expander performance on Return on Investment.

ADVANCED STEAM BOTTOMING CYCLES

Two advanced steam bottoming cycles for application to heavy duty transport diesels were investigated. One assumed the baseline TC diesel exhaust temperature of 944°K (1240°F). The other assumed an arbitrarily higher diesel exhaust temperature of 1144°K (1600°F). Diesel exhaust flow rate and fuel-air ratio were assumed to be the same as for the baseline case. The condenser back pressure for the advanced cycles was decreased from the conservative baseline 0.138 MPa (20.0 psia) to 0.103 MPa (15.0 psia).

Improved Cycle for 944°K (1240°F) Diesel Exhaust

Three design variations are projected for this improved bottoming cycle system: a ceramic cylinder head, piston crown insulation and refined mechanical design for reduced friction. The use of nonstructural ceramics in the expander allows the steam temperature to be increased from 811° to 866°K (1000° to 1100°F), 55°K (100°F) higher than the bulk of our durability development experience. No other system materials changes are needed.

Due to these minor alterations, the expander efficiency was assumed to be improved to 75 percent as opposed to the measured performance of 68 percent used in the baseline design. The increased efficiency should be possible with the higher steam superheat (less cycle condensation loss) and reduced friction losses.

The boiler size was substantially increased for maximum energy recovery. The boiler tube bundle increased from 52 to 113 kg (114 to 250 lb). Energy available to the expander increased by increasing steam temperature 55°K (100°F) and increasing steam mass flow by 4 percent. The pinch point clearance was thus reduced to 22°K (40°F) and the stack temperature reduced from 485° to 453°K (413° to 355°F).

The increased steam volume flow of 11 percent (at higher temperature, same pressure, therefore, lower density) would still allow the expander to operate in the peak efficiency range so that expander displacement remained the same as for the baseline design.

Total bottoming cycle power increased 28 percent for this improved design due to the 10 percent increase in expander efficiency, 7 percent increase in energy recovery with the

larger boiler and a 7 percent Rankine cycle efficiency increase resulting from increasing steam temperature and decreasing condenser back pressure.

Advanced Cycle for 1144°K (1600°F) Diesel Exhaust

The more advanced bottoming system design is based upon maximum extraction of energy from the stack gas and utilization of a more efficient steam cycle made possible by the higher diesel exhaust gas temperature. An exhaust gas temperature of 1144°K (1600°F) and a stack gas temperature limit of 422°K (300°F) implies 41 percent more thermal energy is available in the diesel exhaust than for the baseline or improved baseline cases. In addition, the boiler design selected cools the exhaust below the 422°K (300°F) limit intended to protect against condensation of corrosive stack gas components. This design feature with its implied 105 percent boiler efficiency is judged to be reasonable due to the stainless steel tubes and nickel-chromium alloy tube and fin coating which protects against corrosion. Exhaust energy recovered by the boiler in the advanced system with the higher exhaust temperature is, therefore, 68 percent greater than that for the baseline design.

Boiler exit steam conditions of 950°K (1250°F) and 10.3 MPa (1500 psia) were chosen as the practical limit of ASME code conditions for 316 stainless steel boilers with relatively thin-walled tubing. The boiler was sized for a 22°K (40°F) pinch point, as in the previous improved design, resulting in a stack temperature of 380°K (225°F) and a tube bundle weight of only 125 kg (275 lb).

The expander was assumed to have a 70 percent expansion efficiency with ceramic insulation. The inlet steam volume flow increase of 19 percent and the higher expansion ratio needed at the higher pressure ratio would require an increase in displacement of 63 percent. Increasing the expander bore and stroke from 88.9 mm to 104.6 mm (3.5 in. to 4.12 in.) would provide this while maintaining the same speed (199 rad/s, 1900 rpm) as the diesel. Expander piston speed would increase to 6.60 m/s (1300 fpm), still within the range of our steam expander operating experience.

The net cycle efficiency or ratio of net power output to heat extracted from the exhaust steam is increased from 17 percent with the baseline cycle to 21 percent with this advanced cycle. The bottoming cycle power of the advanced cycle system with increased exhaust temperature is twice the baseline design output.

Performance and Economic Comparisons

Tables 21 and 22 list performance and cost elements for comparison of the three bottoming cycle systems. The improved cycle system for the baseline 944°K (1240°F) diesel exhaust generates 28 percent more power than the baseline design but at a marginally higher cost per unit power output. The advanced cycle with a 1144°K (1600°F) diesel exhaust produces twice the power as the baseline system at 15 percent lower cost per unit power output.

TABLE 21. - PERFORMANCE COMPARISON OF ADVANCED BOTTOMING CYCLES

Bottoming system	Baseline		Improved Cycle		Advanced Cycle	
Diesel exhaust flow rate, kg/s (lb/min)	0.364	(48.1)	0.364	(48.1)	0.364	(48.1)
Diesel exhaust temperature, ^{o}K (^{o}F)	944.0	(1240)	944.0	(1240)	1855.0	(1600)
Boiler						
Efficiency, percent*	88.0		94.0		105.0	
Steam pressure, MPa (psia)	6.9	(1000)	6.9	(1000)	10.3	(1500)
Steam temperature, ^{o}K (^{o}F)	811.0	(1000)	866.0	(1100)	950.0	(1250)
Stack temperature, ^{o}K (^{o}F)	485.0	(413)	453.0	(355)	380.0	(225)
Tubing weight, kg (lb)	52.0	(114)	113.0	(250)	125.0	(275)
Steam flow, kg/s (lb/hr)	0.0663	(526)	0.0680	(540)	0.0995	(790)
Expander						
Efficiency, percent	68.0		75.0		70.0	
Displacement, $m^3 \times 10^3$ ($in.^3$)	1.10	(67)	1.10	(67)	1.80	(110)
Speed, rad/s (rpm)	199.0	(1900)	199.0	(1900)	199.0	(1900)
Feedwater pump, kW (hp)	0.5	(0.7)	0.5	(0.7)	1.1	(1.5)
Condensing Load, kW (Btu/sec)	148.0	(140)	154.0	(146)	225.0	(213)
Net Bottoming Cycle Power, kW (hp)	42.0	(56)	54.0	(72)	84.0	(113)
Total Power, kW (hp)	278.0	(373)	290.0	(389)	320.0	(430)
BSFC, kg fuel/kW-hr (lb/hp-hr)	0.163	(0.268)	0.158	(0.259)	0.142	(0.234)
Reduction in specific fuel consumption relative to TC diesel, %	14.9		17.8		25.7	
Relative power	1.0		1.28		2.02	

*Based on extracting thermal energy from diesel exhaust to a stack temperature of $422^{o}K$ ($300^{o}F$)

**236 kW (317 hp) TC diesel engine plus bottoming system.

TABLE 22. ECONOMIC COMPARISON OF ADVANCED BOTTOMING CYCLES

Bottoming System	Baseline	Improved cycle	Advanced cycle
OEM Costs, $:			
Expander (scale by displacement)	1,800	1,800	2,935
Pump (scale by flow)	150	155	225 (3 cylinder)
Boiler (scale by weight)	1,400	3,070	3,375
Condenser (scale by load)	920	960	1,400
Controls & sensors (constant functions)	765	765	765
Other (scale by flow)	260	270	390
TOTAL OEM COST	$5,295	$7,020	$9,090
INSTALLED COST	$6,070	$8,047	$10,420
COST PER UNIT POWER OUTPUT, $/kW ($/hp)	145(108)	150(112)	123(92)

SUMMARY OF RESULTS

The United States Department of Energy (DOE), with NASA Lewis Research Center management, sponsored studies of exhaust energy recovery systems for advanced diesel truck engines. Four configurations of hypothetical "adiabatic" or uncooled diesels were specified.

Foster-Miller, Inc. (FMI) was contracted for the study on steam bottoming cycles. The basic concept is to run a small steam engine from a high pressure boiler heated by the diesel exhaust. The adiabatic diesel is of particular interest as the exhaust temperature is actually higher than a conventional, cooled diesel even though the efficiency is higher. A bottoming cycle in an adiabatic diesel thus benefits from two factors: the available exhaust energy is higher and the efficiency of the bottoming cycle is improved by running at a higher peak cycle temperature.

Bottoming System Analysis

The first phase was to perform a parametric study of a range of cycles and hardware sizes on candidate adiabatic diesel configurations and to conduct a diesel exhaust gas temperature sensitivity analysis. The important parameters were: diesel exhaust temperature and mass flow, boiler size, steam cycle (peak pressure and temperature) and expander efficiency as a function of the steam cycle.

The boiler sizing study was done by analyzing a series of specific heat exchanger configurations with a proprietary multi-nodal computer model. Boiler tube and fin weight required to recover exhaust energy down to specified stack temperature was determined as a function of process variables: steam pressure, steam outlet temperature and diesel gas temperature. The significant conclusion was that the diesel gas temperature is the dominant factor. A 110°K (200°F) higher gas temperature can reduce the final stack temperature by 28°K (50°F) at the same boiler weight. The total energy recovered with the higher stack temperature at constant boiler weight is one-third higher as the total temperature drop in the gas increases by 139°K (250°F). The steam pressure and temperature have little effect on the boiler weight required to recover a given energy from the diesel exhaust.

The power that can be produced from a given steam flow and steam cycle is determined by the expander efficiency. For a single expansion piston stage, expander exhaust or condenser pressures below about 0.10 MPa (15 psia) cannot be efficiently utilized because of the increased friction and heat transfer

losses associated with the increased piston displacement needed to produce the higher expansion ratios.

As one would expect, the most power is produced by the more efficient (high pressure and temperature) steam cycles. Increasing the system weight for a given cycle by increasing the boiler and hence expander sizes increases power but with diminishing returns as the boiler effectiveness increases.

Practical constraints imposed on the study included: ASME boiler code stress limits, maximum back pressure on the diesel of 0.0015 MPa (6 in. H_2O) ram air cooled at 64.4 km/hr (40 mph) and over with 50 percent ram recovery, a condenser of standard radiator core construction slightly tilted or with scarfed ends for freeze-proof draining and expander speed equal to the diesel speed of 199 rad/sec (1900 rpm).

Preliminary Design

A 811°K/6.90 MPa (1000°F/1000 psia) steam cycle was selected for the preliminary design. This represents the current proven durability and experimentally verified performance.

Prior testing of freeze management has shown that a 244°K (-20°F) cold soaked system could start up and run if fed with 294°K (70°F) water. Draining into a sump with a compliant member, e.g., a rubber ball, will allow freezing of the sump without damage. For a bottoming cycle, the hot oil line to the diesel oil cooler would be used to thaw out the sump. Additional tests were conducted for this study to verify that a conventional truck radiator core would drain to prevent freeze damage and restart cold without ice plugging. A truck radiator shutter in front of the condenser was also tested in a refrigerated wind tunnel to demonstrate that the condenser could be protected from freezing and that the condenser temperature could be controlled.

The adiabatic diesel selected for application of the bottoming system was the turbocharged version without an intercooler. A 0.14 MPa (20 psia) condenser pressure was selected so that non-condensable gases could be simply vented by a steam trap without a vacuum pump.

The net output, assuming ram cooling without fan power, is 42 kW (56 hp) added to the diesel's 236 kW (317 hp) or a 17.7 percent increase in power equivalent to a 15 percent reduction in specific fuel consumption.

The bottoming system layout has the expander output coupled to the diesel with a chain drive into the end of the transmission. A simpler arrangement, if chassis space is available, would have the expander coupled to the crank nose.

The boiler consists of ten conical passes of stainless steel tubes finned with carbon steel, ribbon brazed/coated with nickel-chromium alloy for corrosion protection. The tube and fin weight is 51.7 kg (114 lb). The maximum diesel back pressure is 0.001 MPa (4 in. H_2O) and the stack temperature is 485°K (413°F).

A major advantage of the steam cycle is that the water will not decompose like all other candidate fluids at diesel exhaust temperatures. An emergency boiler bypass is not needed. Soot fouling can be simply burned out by running the diesel for a few minutes with no water flow. Others have found that if not cleaned, power losses of 30 percent in 100 hr in a truck diesel exhaust boiler can be expected. No simple cleaning method besides running dry, possible only with steam, has been developed.

The expander is a two cylinder single expansion type with bore and stroke of 0.089m (3-1/2 in.). A cam and poppet valve train admits the steam near TDC while exhaust ports at the bottom exhaust the steam to the condenser. Oil lubricated plain bearings and hard coated piston rings follow prior practice. A hydraulic clutch would be used between the expander and the diesel for startup and as a disconnect should the bottoming cycle fail.

The condenser assembly includes shutter, fan, oil cooler and condensate subcooler. Condenser pressure (hence temperature) actuated shutters control the cooling air flow. The core is a flattened tube, sheet fin assembly with a shallow bottom header. A high efficiency fan is driven through a thermostatic clutch by a pulley on the diesel engine. The fan normally free wheels while driving but can be driven to provide complete condensing of the steam at full load at low vehicle speeds where the fan input could approach 3 kW (4 hp). A condensate subcooler and expander and diesel engine oil coolers are placed between the condenser core and the fan.

Other components include a piston type feedwater pump with electronic flow control of intake check valve unloader, shut down drain and freezeproof sump system, make-up water demineralizer cartridge and a controls/diagnostics package.

Total installed weight is estimated at 254 kg (560 lb) or 6 kg/kW (10 lb/hp). The boiler would replace the normal muffler function for some installed weight reduction.

The system is designed to be benign in that, if it fails, it would disconnect the expander drive clutch and the boiler would safely run dry. The cooling fan for the diesel engine oil cooler would still be driven by the diesel.

Economics

The reference diesel for economic comparison was the adiabatic turbocompound (blowdown turbine geared to the crankshaft) including an aftercooler.

We were most fortunate in receiving cost estimates as well as technical assistance on this project from established manufacturers of the same or similar major components. The condenser was technically reviewed and priced by a truck radiator firm who also supplied sample cores for the freeze testing. The expander was priced, part by part, by a major diesel engine firm.

The boiler was priced by a boiler and finned tube manufacturer. The feedwater pump could be a minor modification of a currently produced model. The shutters and fan are catalog items. FMI priced the controls and instrumentation system in our production equipment group.

A summary of component descriptions and costs is given in Table 23. These costs are OEM price estimates in annual volumes of 10,000. Assuming that the prime manufacturer is a diesel firm, producing the expander and pump in-house, the installed selling price is estimated at $6,070. No credit has been taken for elimination of the muffler and the sharing of the cooling fan function with the diesel oil cooler.

The economic comparison with the NASA specified turbocompound adiabatic diesel is given in Table 24. Fuel savings were calculated by simply ratioing the specific fuel consumptions at maximum power. The prices of both versions of the adiabatic diesels, the annual engine duty and the price of fuel were specified by NASA.

The simple payback of increased first cost is calculated to be 1.5 years. A maintenance cost estimate was made by comparison of similar truck engine component experience provided to FMI on a proprietary basis. The added maintenance cost is shown to absorb nearly one-third of the fuel savings.

TABLE 23. - SYSTEM COMPONENTS AND COSTS

Component	Description	OEM Price
Expander	V-twin, 0.089m (3-1/2 in.) bore and stroke, 199 rad/sec (1900 rpm). oil lubricated	$ 1,800
Feedwater Pump	Two cylinder, solenoids on intake valves for flow control	150
Boiler	Clad fins on stainless tubes, 52 kg (114 lb) bundle, 0.001 MPa (4 in. H_2O) gas side loss	1,400
Condenser	0.79 m^2 (8.5 ft^2) frontal area, typical truck core, ram cooled above 64.4 km/hr (40 mph) with shutters, fan, subcooler and oil cooler	920
Controls and Sensors		765
Other		260
	TOTAL OEM PRICE:	$ 5,295

resulting in a simple payback including maintenance of 2.3 years.

In our opinion, the baseline design is technically sound and economically attractive to the end user. Viability analysis for a business venture must, of course, further account for production development, tooling, market penetration, and the future cost of fuel.

An improved cycle and system for the baseline 944°K (1240°F) diesel exhaust was devised which generates 28 percent more power than the baseline design but at a marginally higher cost per unit power output. A more advanced cycle with a 1144°K (1600°F) diesel exhaust was conceptualized which produces twice the power as the baseline system at 15 percent lower cost per unit power output.

TABLE 24 - RELATIVE SYSTEM PERFORMANCE AND ECONOMICS

	Aftercooled turbocompound adiabatic engine scaled to 278 kW (373 hp)	42 kW (56 hp) steam bottoming cycle on 236 kW (317 hp) adiabatic turbocharged diesel
B.S.F.C., kg of fuel/kW·hr (lb fuel/hp·hr)	0.178 (0.293)	0.163 (0.268)
Total engine system price	$17,460	$20,070
Annual fuel cost @ $317/m^3 of fuel and 160,000 km/year ($1.20/gal and 100,000 mi/year)	$19,737	$18,018
Added price	-	$ 2,610
Annual fuel savings	-	$ 1,719
Simple payback (years)	-	1.5
Added annual maintenance	-	$ 580
Simple payback including maintenance (years)	-	2.3

REFERENCES

1. Bryzik, W., "TACOM/Cummins Adiabatic Engine Program," Proceedings of the Twentieth Automotive Technology Development Contractors' Coordination Meeting, Dearborn, Michigan, October 1982.

2. Hoagland, L.C., Demler, R.L., Gerstmann, J., "Design Features and Initial Performance Data on an Automotive Steam Engine, Part I - Overall Powerplant Description and Performance," SAE 740295, 1974.

3. Demler, R.L., "Demonstration of a Steam Powered Face Haulage Vehicle," FMA/DOE ET-75-C-01-9016. July 1979.

4. Krepchin, I.P., and Volkin, R.L., "Modeling Analysis and Inspection of Waste Heat Boiler DD965, USS Kincaid," Foster-Miller, Inc., Waltham, MA, February 1982.

5 Demler, R.L., "The Application of the Positive Displacement Reciprocating Steam Expander to the Passenger Car," SAE 760342. February 1976.

6. Taylor, C.F., and Taylor, E.S., The Internal Combustion Engine, Second edition, Scranton, Pennsylvania: International Textbook Company, 1961.

7. Kays, W.M., and London, A.L., Compact Heat Exchangers, Second Edition, McGraw-Hill, New York, 1964.

8. Demler, R.L., "Design and Development of an Automotive Propulsion System Utilizing a Rankine Cycle Engine (Water Based Fluid), Final Report" Prepared for the U.S. ERDA under contract No. EY-76-C-02-2701. *001, September 1977.

9. "Diesel-Organic Rankine-Cycle Compound Engine for Long-Haul Trucks," Thermo Electron Corp., DOE/CS/52832-4, December 1981.

10. Roberts, P.B. and Kubasco, A.J., "Combined Cycle Steam Generator Gas Side Fouling Evaluation" Solar Turbines International, SR79-R-4557,20, July 1979.

11. Luchter, S. and Renner, R.A., "An Assessment of the Technology of Rankine Engines for Automobiles," EKDA-77-54, April 1977.

APPENDIX A - FREEZE PROTECTION TEST RESULTS

TABLE A-1. - TUBE MEASUREMENTS THROUGH FREEZE/THAW CYCLING

Note: Each tube was measured at 2 diametral locations, D1 and D2

DATE		5/31	6/9	6/9	6/10	6/10	6/10	6/21	6/21	6/21	6/21	6/21	6/21
TIME		3:20 p.m.	11:30 a.m.	1:50 p.m.	9:30 a.m.	12:00 noon	9:30 a.m.	10:40 a.m.	11:15 a.m.	1:30 p.m.	2:10 p.m.	2:55 p.m.	
TUBE TEMP.(°F)		67	23	75	25	72	75	24	65	22	61	29	
1	D1	.5952	.5840	.5837	.5828	.5837	.5844	.5840	.5848	.5838	.5840	.5837	
	D2	.6564	.6569	.6567	.6560	.6570	.6563	.6562	.6566	.6568	.6566	.6566	
2	D1	.5952	.5843	.5843	.5834	.5836	.5834	.5834	.5841	.5834	.5838	.5825	
	D2	.6587	.6599	.6596	.6591	.6624	.6587	.6585	.6599	.6567	.6589	.6593	
3	D1	.5830	.5827	.5820	.5824	.5827	.5834	.5823	.5825*	.6378*	.6376	.6384	
	D2	.6550	.6552	.6552	.6551	.6553	.6552	.6550	.6557	.6476	.6456	.6450	
4	D1	.6308	.6316	.6318	.6482	.6488	.6488	.6484	.6482	.6523	.6510	.6514	
	D2	.6362	.6360	.6360	.6488	.6486	.6492	.6491	.6492	.6523	.6525	.6520	

* Water content of Tube 3 increased to 43.4 cc.

TABLE A-2. - CONTINUOUS OPERATION - CONDENSER TEST NO. 1

Initial Low Temperature Test - May 13, 1983

Steam Flow - 20 lb/hr (Atmos. steam)

Shutter Closed

Initial Time - 5:23 p.m. - Room set at 10°F

TIME	5:27	5:31	5:36	Test terminated possible freeze condition
Lower Tube Temperatures	81	72	55	
	82	70	51	
	95	82	68	
	117	107	98	
	93	77	67	
Outer Surface Temperatures	45	35	28	
	59	44	33	
	41	31	26	
Air In	22	14	9	
Air Out	116	98	89	

Note - Air flow measured with closed damper at 182 cfm (125 fpm coil face velocity).

TABLE A-3. - CONTINUOUS OPERATION - CONDENSER TEST NO. 2

May 18, 1983

Steam Flow - 26 lb/hr

Shutter Closed

Room Set at 10°F

TIME	11:17 a.m.	11:27	11:38	11:45	11:57	*1 12:00	*2 12:06	12:16	12:36	2:15	2:19 p.m.
Lower Tube Temperatures	144	135	92	77	61	71	67	56	58	62	64
	156	153	101	89	69	91	78	67	71	81	70
	157	146	102	96	79	96	80	68	76	100	81
	157	136	131	112	111	107	88	87	97	103	92
	195	170	117	105	78	110	88	78	95	115	88
Outer Surface Temperatures	120	104	75	63	43	63	47	41	47	51	34
	124	116	79	70	50	71	51	44	55	70	49
	116	92	69	59	40	56	45	39	41	39	31
Air In	45	43	27	23	19	18	11	5	3	9	2
Air Out	159	147	142	140	132	133	126	121	120	121	121

*1 - Increased Steam Flow to 33 lb/hr

*2 - Lowered Room Set Point to +4°F

APPENDIX B - LIST OF SYMBOLS

A - Surface area for heat transfer

A_p - Piston area

C - Cash flow

CO - Cut-off, admission valve timing

D - Depreciation cost

E - Exhaust valve timing

F - Correction factor for heat transfer equation or fuel cost as appropriate by context

IC - Added cost of diesel engine system with bottoming cycle

K - Thermal conductivity

L - Length

LMTD - Log mean temperature difference

M - Maintenance cost

N - Useful life of system

P - Power or pressure as appropriate by context

PP - Boiler pinch point

SP - Piston speed

T - Temperature

TC - Tax credit

TR - Tax rate

U - Overall heat transfer coefficient

W - Specific work

a,b,c - Variable coefficients

c_p - Specific heat

g - Acceleration due to gravity

h - Specific enthalpy

h_A, h_B, h_C, h_D - Enthalpy at state points A, B, C and D, respectively

h_B - Enthalpy at expander back pressure after isentropic expansion

h_{fg} - Latent heat of vaporization

i - Cost of capital, discount rate

$\dot{m}$ - Mass flow rate

n - Index

q - Heat transfer rate

t - Film thickness

$\alpha, \beta, \gamma,$ - Variable coefficients

Δ - Difference

∂ - Variable factor

η_B - Expander breathing efficiency

η_D - Expander diagram efficiency

η_{EX} - Overall expander efficiency

η_M - Expander mechanical efficiency

η_R - Rankine cycle efficiency

η_T - Expander thermal efficiency

μ - Viscosity

ρ - Density

Subscripts:

AD - Admission

CMP - Compression

EX - Expansion or expander

G - Diesel exhaust gas

GB - Diesel exhaust gas at boiler pinch point

I - Indicator or indicated

PM - Prime mover

SAT - Saturation

ST - Superheated steam

f - Saturated fluid

v - Vapor

w - Water

1 - Preheater section of boiler

23 - Vaporizer and superheater sections of boiler

Superscripts:
A - TCPD/A system
B - TC/B system

1. Report No.	2. Government Accession No.	3. Recipient's Catalog No.
NASA CR-168255		

4. Title and Subtitle	5. Report Date
Steam Bottoming Cycle for an Adiabatic Diesel Engine	March 1984
	6. Performing Organization Code

7. Author(s)	8. Performing Organization Report No.
E. Poulin, R. Demler, I. Krepchin, and D. Walker	FMI NAS-8273
	10. Work Unit No.

9. Performing Organization Name and Address	11. Contract or Grant No.
Foster-Miller, Inc. 350 Second Avenue Waltham, Massachusetts 02154	DEN 3-300
	13. Type of Report and Period Covered
12. Sponsoring Agency Name and Address	Contractor Report
U. S. Department of Energy Office of Vehicle and Engine R&D Washington, D.C. 20585	14. Sponsoring Agency Code Report No.
	DOE/NASA/0300-1

15. Supplementary Notes

Final Report. Prepared under Interagency Agreement DE-AI01-80CS50194. Project Manager, M. Bailey, Transportation Propulsion Division, NASA Lewis Research Center, Cleveland, Ohio 44135.

16. Abstract

A study of steam bottoming cycles using adiabatic diesel engine exhaust heat projected substantial performance and economic benefits for long haul trucks. A parametric analysis of steam cycle and system component variables, system cost, size and performance was conducted. An 811 K/6.90 MPa state-of-the-art reciprocating expander steam system with a monotube boiler and radiator core condenser was selected for preliminary design. When applied to a NASA specified turbocharged adiabatic diesel the bottoming system increased the diesel output by almost 18 percent. In a comparison of the costs of the diesel with bottoming system (TC/B) and a NASA specified turbocompound adiabatic diesel with aftercooling with the same total output, the annual fuel savings less the added maintenance cost was determined to cover the increased initial cost of the TC/B system in a payback period of 2.3 years. Also during this program steam bottoming system freeze protection strategies were developed, technological advances required for improved system reliability were considered and the cost and performance of advanced systems were evaluated. Related reports in the area of alternative power cycles for waste heat recovery from the exhaust of "adiabatic" diesel engines are as follows:

NASA CR-168256 (Organic Rankine) NASA CR-168257 (Brayton)

17. Key Words (Suggested by Author(s))	18. Distribution Statement
Waste heat recovery Steam Rankine cycle Bottoming system Preliminary design Economics	Unclassified - unlimited STAR Category 85 DOE Category UC-96

19. Security Classif. (of this report)	20. Security Classif. (of this page)	21. No. of pages	22. Price*
Unclassified	Unclassified	134	A07

*For sale by the National Technical Information Service, Springfield, Virginia 22161